EXAMINATION OF ENDOPLASMIC RETICULUM STRESS, THE UNFOLDED PROTEIN RESPONSE AND AUTOPHAGY IN IRON OVERLOAD-INDUCED INSULIN RESISTANCE

KHANG NGUYEN

A THESIS SUMIBTED TO THE FACULTY OF GRADUATE STUDIES IN PARTIAL FULFILMENT OF THE REQUIREMENTS OF THE DEGREE OF

Master of Science

GRADUATE PROGRAM IN BIOLOGY

YORK UNIVERSITY

TORONTO, ONTARIO

DECEMBER 2022

ABSTRACT

In this study, an in vitro model of L6 cells was first employed, followed by translation of iron overload administration in mice. In both, a compromise of insulin sensitivity was observed, and salubrinal could effectively attenuate this defect. More notably, I found that the insulin sensitizing effects of salubrinal were not observed in autophagy-deficient cell lines. Collectively, these observations suggested that autophagy produced protective effects against insulin resistance, and that its precise regulation was the key factor in mediating metabolic disorders. This led to the importance of targeting autophagy as the means to restore both ER stress and insulin sensitivity. In insulin resistant models, a downregulation of adiponectin is closely related to impaired autophagy. My study suggested that pre-treating L6 cells with the adiponectin receptor agonist ALY688 could prevent IO-induced insulin resistance and ER stress, which was consistent with the significance of adiponectin in T2D patients in clinical settings.

Overall, the studies described above highlight the significance of autophagy in skeletal muscles in iron overload- associated insulin resistance. IO is coupled with impaired mitochondrial dysfunctions, and my study has confirmed that these defects also lead to other organelles' dysfunctions, including the endoplasmic reticulum. My findings indicated for the first time that salubrinal elicited an eIF2α-autophagy which effectively suppressed ER stress and exhibited insulin sensitizing benefits. Additionally, the second study of my thesis unveiled a critical role of adiponectin as the key mediator in autophagy regulation under impaired metabolic syndrome conditions. Collectively, these findings implicated the potential benefits of using either salubrinal or ALY688 as pharmacological approaches in clinical studies regarding insulin resistance.

ACKNOWLEDGEMENTS

The thesis duration I had at the Sweeney lab was a good opportunity for me to obtain invaluable knowledge and experience. First and foremost, I would like to express my gratitude to my advisor, Dr. Gary Sweeney, for his support and thoughtful guidance during my thesis. It has been intellectually enriching to work with an enthusiastic professor who is willing to provide thorough advice for my work and challenge me to work harder as a researcher. Next, I would like to express my gratitude for Dr. Chun Peng for offering her support and constructive feedback during my master program. Thank you, Dr. Michael Scheid, Dr. Terrance Kubiseski, and Dr. Ali Abdul-Sater for devoting their precious time to my thesis examination. I would also like to express my appreciation for Dr. Kostas Pantopoulos, Dr. Ali Abdul-Sater, and Dr. Jon Schertzer for opportunities of collaboration with their projects, that culminated in potential co-authored publications. This journey would not have been possible without Dr. Hyekyoung Sung's conscientious support and guidance during my master journey. A very special thank to all members of the Sweeney lab for their support and encouragement. I was fortunate to have had a chance to work and share such memorable times with you all. Also, a sincere thank you to my best friend Nhu Dinh, who has always been supporting me all steps of the way. Last but not least, I owe the success of this thesis to my family, especially my beloved sisters An Thuy Nguyen, Jessica Nguyen and Mimi Nguyen. Thank you for loving me unconditionally and giving me the best opportunity to pursue my educational career. This thesis experience has been an opportunity of a lifetime that has both provided me with new knowledge and guided me towards the right direction on the path to my future career.

TABLE OF CONTENTS

LIST OF FIGURES

CHAPTER 1: LITERATURE REVIEW

1.1 Metabolic syndrome

1.1.1 Definition

Metabolic syndrome (MetS) is a condition of metabolic comorbidities which accelerate the progression of chronic diseases such as stroke, cardiovascular disease, and diabetes. These comorbidities are characterized based on clinical interpretations of elevated blood pressure, abdominal obesity, and aberrant cholesterol or triglyceride levels [1]. Each criterion represents a risk factor for chronic diseases [2]. A combination of more than one factor, however, will contribute to a higher risk of developing diabetes or heart diseases, the leading cause of death worldwide [3]. The underlying causes of MetS are closely linked to overweight or obesity, physical inactivity, aging and genetic factors [4]. Understanding and developing awareness for MetS etiology can help relieve the epidemiological and economic burden for the healthcare system.

Atherosclerotic cardiovascular disease is among the consequential complications of MetS. Cardiovascular disease is predominantly caused by an imbalance of high triglycerides and low High Density Lipoprotein Cholesterol (HDL-c) levels, leading to the buildup of plaque in the arteries with consequent myocardial ischemia [5]. Hypertension, another MetS factor, contributes to cardiac remodeling, including fibrosis, inflammation and ultimately heart failure [6]. In a clinical setting, hyperinsulinemia is known to increase the incidence of heart diseases through blood pressure elevation and enhanced renal sodium retention [7].

1.1.2 Iron overload in metabolic syndrome

Iron is an essential element for multiple cellular and metabolic processes. The body iron level is normally controlled by efficient homeostatic mechanisms, yet defects in this regulatory

system can lead to various complications such as insulin resistance and cardiovascular diseases [8]. When iron levels exceed the acceptable range, formation of NTBIs (non-transferrin bound labile iron) will occur and is accompanied with damages in the peripheral tissues [9]. Furthermore, substantial studies have disclosed that increased serum ferritin levels are strongly correlated with MetS. These include an increased prevalence of hypertension, elevated plasma glucose and triglycerides and enhanced abdominal adiposity. For example, the presence of MetS and hypertriglyceridemia increase the probability of having iron overload by up to 2.1 and 1.88 times, respectively [10]. Several studies also indicated that the prevalence of iron overload was significantly higher in metabolic syndrome subjects than in control subjects, suggesting the consequential relationships between iron-overloading conditions and metabolic syndrome [11][12].

1.2 Diabetes

1.2.1 Definition

Diabetes is a chronic metabolic disease which refers to the dysregulation of serum glucose levels. Type 1 diabetes (T1D), is associated with the inability to produce insulin due to diminished pancreatic beta-cells function and Type 2 diabetes (T2D), referred to overt insulin resistance in peripheral tissues such as liver, muscle and adipose [13]. T2D is a fast-growing epidemic affecting over 425 million people globally, making up a total of 90-95% of diabetes cases, according to the World Health Organization in 2020 [14]. Moreover, it is a hallmark leading to prevalence of other medical conditions such as stroke, neurodegenerative and heart disease, and cancers, among others [15-18]. Individuals with MetS are defined as having pre-

diabetes and their risks of developing full-blown T2D prevailed to up to 70%, if not intervened [19].

1.2.2 Obesity as a cause of diabetes

Obesity is a commonly occurred medical condition in both young people and adults, with approximately 25% observed in Canadian populations 18 and older [20]. It is defined as the accumulation of aberrant and excessive fat, impairing health and social well-being. BMI (Body Mass Index, calculated by weight over square of height) is used to define obesity where an individual having a value of greater than 30 kg/m2 is considered as obese [21]. Obesity is primarily caused by overnutrition, sedentary lifestyles and physical inactivity [22]. An imbalance in nutrient uptake and energy expenditure in obese patients will lead to excessive storage of body fat, a hallmark of MetS [23]. Indeed, obesity poses major global health issues as it is coupled with economic burden, decreased mental health and most importantly, increased risks for other medical complications such as T2D, cardiovascular disease and cancer. The increase in obesity prevalence is obvious, with its rates tripled worldwide, since 1975 [24]. In particular, approximately 700 million people were diagnosed with obesity in 2017 and an estimated 1 to 4 people would be living with this disease by 2045 [25]. The correlation of obesity and diabetes is inevitable as T2D incidences is six-fold for individuals with obesity [26]. This trend suggests that obesity in general and T2D in particular will continue to grow in severity, posing detrimental health concerns.

In the past, diabetes had been poorly understood, with treatment mainly involving exercise. As humans gained more understanding, they began to incorporate monitored diets and lifestyles into efforts to treat diabetes. For instance, doctors would suggest that patients eat whole grains, low carb and easily digested food [27]. These ways of managing diabetes did not

prove to be completely effective, and people with this condition still experienced severe health problems. The introduction of insulin in 1921 as a treatment completely changed this [28]. For over 100 years, studies on the regulation of insulin secretion and signaling have been at the forefront of the fields of cellular and molecular biology [29]. To this day, insulin remains the most effective treatment for type 1 diabetes while other non-insulin drugs like metformin, which helps reduce blood glucose, is the main treatment for type 2 diabetes [30]. Drugs, however, do not always work for all individuals due to their side effects. Therefore, understanding the pathophysiology of diabetes – specifically insulin resistance as one of the condition's early onset markers, is crucial.

1.3 Insulin resistance

1.3.1 Insulin action

Insulin is a peptide hormone produced by beta cells of the pancreatic islets and encoded by the INS gene in humans [31]. Arguably the most studied hormone in history, research involving insulin is embedded within most major cell biology discoveries, ranging from pro-hormone production and trafficking, membrane biology, exocytosis [32], receptor tyrosine kinases [33], Src homology 2 (SH2) domains [34], GLUT4 trafficking [35], to the regulation of carbohydrate, lipid, and protein metabolism [36]. More recently, studies about mitochondrial functions, mitophagy, autophagy or organelle- specific impairment have significantly improved our understanding how these organelles or cellular processes communicate with each other to regulate insulin sensitivity [37][38][39]. The first description of insulin resistance is dated back to 1936, when Harold Himsworth started measuring insulin action in the body [40]. He detected two types of diabetes being classified: type 1 is associated with disrupted insulin secretion, while impaired insulin action defines the hallmark of type 2 diabetes. This major finding in the

history of insulin resistance was subsequently followed by the discovery of the insulin receptor and the observation that insulin defects could be associated with insulin resistance in rodent and human models in 1973 and 1976, respectively. Since then, an increasing number of studies have focused on the insulin signaling pathway and its contributions to the etiology of insulin resistance- associated diabetes [41].

1.3.2 Insulin signaling pathway

Insulin performs its functions upon binding to the insulin receptor (INSR), initiating a complex cascade of downstream signaling events. Initially, phosphorylation of insulin receptor substrates (IRS) is induced by the receptor to allow for their binding to the src-homology-2 (SH2) domain within the p85 regulatory subunit of phosphatidylinositol 3-kinase (PI3K). Upon activation, PI3K phosphorylates phosphatidylinositol (4,5)-bisphosphate (PIP2) into phosphatidylinositol (3,4,5)-trisphosphate (PIP3), which recruits PDK1 and AKT adjacent to the cell membrane, upon build up. Here, PDK1 phosphorylates Akt at threonine 308 while phosphorylation of Akt at serine 473 is induced by mTORC2. Following these signaling pathways, Akt substrate AS160 is inhibited, and glucose transporters GLUT4 are translocated and integrated into the plasma membrane, facilitating glucose uptake into target tissues. Growth stimulation also takes place during the insulin signaling events via an alternative pathway Grb2-SOS-Ras-RafMEK1/2 to phosphorylate ERK1/2 [42]. Insulin performs both positive and negative feedback mechanisms. In the negative feedback, there is activation of S6K1 which serves to phosphorylate and inhibit expression of IRS1 [43].

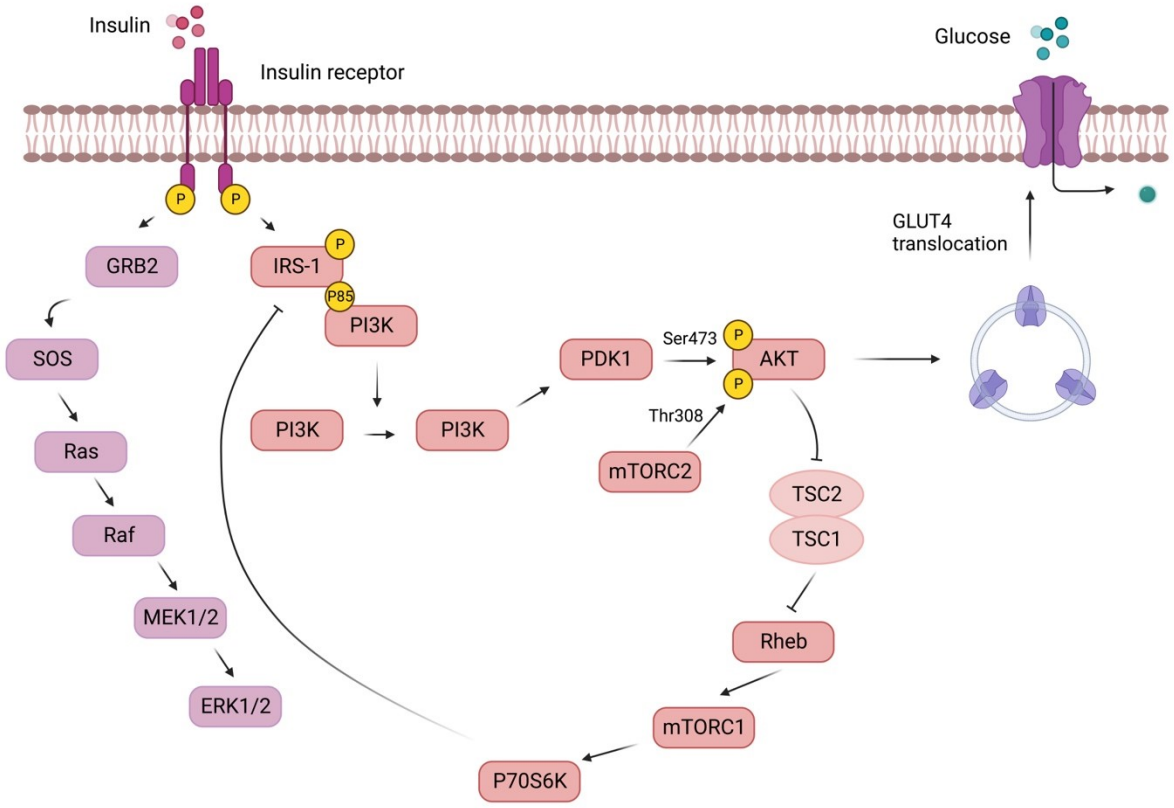

Figure 1. Insulin signaling pathway (Adapted from [44])

1.3.3 Insulin resistance and progression to diabetes

Insulin resistance occurs when cells do not respond well to insulin, leading to elevated blood glucose accumulation [31]. Insulin resistance is a characteristic of heart failure, cardiovascular disease, and T2D [45]. Insulin resistance in skeletal muscle, which is responsible for over three-fourths of insulin-initiated glucose disposal, is especially important [46]. Better comprehension of how skeletal muscle generates resistance to insulin can allow researchers to devise appropriate targets for interventions that are necessary to mitigate this problem. The pathophysiology underlying insulin resistance progression to diabetes is not well established,

yet emerging studies regarding c-Jun N-terminal kinase 1 (JNK1) proposed this kinase to be the main regulator driving glucose intolerance in diabetic states [47]. JNK is activated through inflammation, endoplasmic reticulum stress, oxidative stress, and mitochondrial dysfunction, while blockage of JNK has also been shown to prevent insulin resistance development to diabetes [48]. This finding is indicative of the causal relationship between insulin resistance and diabetes through other cellular stress events.

1.3.4 Iron overload, insulin resistance and diabetes

Among the leading etiological factors in the pathogenesis of insulin resistance are the effects of iron overload (IO). Additionally, cellular nutrient stress, such as the effect of the endoplasmic reticulum (ER), mitochondrial dynamics and energetics, and oxidative stress, are also emerging areas of investigation [49][50][51]. The first evidence for a relation between iron and human diabetes came from clinical observations of individuals with pathologic iron overload [52]. Hemochromatosis is characterized by mutation in the iron regulator gene, which subsequently leads to reduced expression of hepcidin and increased iron overload. Research shows that there is up to 23 % chance of developing diabetes in haemochromatosis patients [53]. Another condition that links iron overload and diabetes is thalassemia, which is characterized by deficient production of the beta globin subunit of hemoglobin. Thalassemia patients therefore require frequent blood transfusion which leads to iron overload. Prevalence of diabetes is observed in up to 30% of thalassemia patients [54]. The molecular mechanisms linking iron overload (IO) to T2D, however, are not fully understood. Cellular labile iron, which contains chelatable redox-active Fe2+/Fe3+, has been implicated in iron-mediated cellular toxicity by increasing oxidative stresses [55]. Excess accumulation of intracellular iron leads to

the generation of reactive oxygen species (ROS) and tissue damage, which is subsequently followed by the redox imbalance in various organelles [56].

ROS production is also a well-known source of impaired autophagy, cardiomyopathy, and insulin resistance [57]. Interventions to reduce iron have been proposed to enhance insulin sensitivity and prevent the onset of type 2 diabetes. These include the use of chelators, bloodletting, and iron restriction diet [58]. Dietary iron restriction and iron chelation significantly enhanced insulin sensitivity, β-cell function and prevented diabetes development in ob/ob mice [59]. In T2D, levels of serum ferritin and adiponectin are inversely correlated. Mice subjected to high-iron diet also showed adiponectin transcription downregulation via FOXO1-mediated repression with consequent glucose intolerance and insulin resistance [60]. Replenishment of adiponectin upon iron overload conditions effectively prevented the defects, suggesting that adiponectin was a potential mediator in IO-associated metabolic disorders [61].

1.4 Adiponectin

1.4.1 Adipose tissues and obesity

Studies highlighting the pathophysiology linking obesity and its progression to diabetes have been at the forefront in the field of cellular and molecular biology, with emphasis on adipocytes and their corresponding secretory molecules [62]. Accumulation of visceral adipose tissues, a characteristic of obese states, is tightly associated with insulin resistance, hyperglycemia, hypertension, and pro-inflammatory conditions, all of which contribute to T2D. Adipose tissues are connective tissues comprising mainly of fat cells called adipocytes. Their main roles are to serve as sites for energy storage, thermal insulation, and regulation of certain immune and endocrine secretory pathways [63]. In obese states, adipose tissues are coupled with secretion of adipokines that play main roles in the regulation and management of obesity.

These include production of leptins, TNF-α (Tumor Necrosis Factor Alpha), Monocyte Chemoattractant Protein1 (MCP-1) and Interleukin-6 (IL-6), and most importantly, adiponectin. Studies on the role of adipose tissues in diabetes began in 1994 with the successful positional cloning of the obese (ob) gene in mouse, encoding leptin, and the recognition that mutations in the ob gene leads to morbid obesity in human [64]. Leptin binds to and activates its cognate leptin receptor (LEP-R) in the hypothalamus, facilitating food intake and body mass. Leptin resistance is observed in patients of obesity and T2D, marking the importance in studies revolving adipocytes in general and their secretory molecules in particular [65]. The discovery of leptin and its functional role in facilitating obesity was subsequently followed by studies on other adipocytes- derived secretory molecules that play detrimental effects in obese patients. These include the pro- inflammatory cytokine TNFα, and its role in suppressing insulin action in liver and skeletal muscles in 1993 [66]. Contributions of other inflammatory mediators such as MCP-1, IL-6 and Vaspin (visceral adipose tissue-derived serpin; serpinA12) in inducing diabetes were also reported in animals and human models [67][68][69].

1.4.2 Effects of adiponectin

Adiponectin, a hormone secreted into the bloodstream by adipocytes, is the most abundantly produced adipokine in the circulation [70]. During obesity, an increase in adipose tissues is accompanied with elevated production of proinflammatory factor called hypoxia inducible factor 1α (HIF1α). This increase of HIF1α in turn induced downregulation of adiponectin, leading to inflammation, as observed in diabetes patients [71]. Numerous studies have indicated that the levels of serum adiponectin are inversely correlated with abdominal adiposity, a characteristic of obesity [72]. Obesity is accompanied by an increased risk of cardiovascular disease (CVD). Indeed, high levels of circulating adiponectin is known to exert

cardioprotective effects in clinical settings [73]. High adiponectin level is also implicated in reduced risks of myocardial infarction and coronary heart disease incidents in patients with T2D [74]. Additionally, pharmacological, and genetic approaches to elevate plasma adiponectin results in ameliorated obesity- induced endothelial dysfunctions and hypertension and preventive atherosclerotic disease [75][76]. Evidently, clinical studies indicated that higher plasma adiponectin is linked with T2D risks in many populations, and it is also employed as an effective diagnostic marker of T2D [77][78].

The identification of adiponectin was dated in 1995, as a protein of 224 amino acids long and located on the 3q27 chromosome. The protein is comprised of three spherical domains including an N-terminal sequence, a collagen like fibrous domain, and a globular domain with a C-terminal end [79]. Adiponectin undergoes oligomerization, resulting in three isoforms: trimer, hexamer, and high molecular weight (HMW) multimer. The combination of these isoforms is referred to as full length adiponectin (fAd), which can also be cleaved by proteolysis to form globular adiponectin (gAd) [80]. Of these three adiponectin isoforms, the HMW oligomer is the main adipokine facilitating insulin sensitivity and cardioprotective effects. As such, disruptions of HMW adiponectin were recorded in adipose tissues of obese individuals [81][82].

1.4.3 Adiponectin signaling

1.4.3.1 Adiponectin receptors and adaptors

The main adiponectin receptors identified are AdipoR1 and AdipoR2 which are integral membrane proteins with seven transmembrane domains belonging to the PAQR (Progesterone and Adiponectin Q Receptor) family [83]. AdipoR1 has high affinity binding for gAd and is

expressed mainly in skeletal muscle. On the other hand, AdipoR2 is abundantly expressed in liver with stronger affinity binding for fAd [84]. Adiponectin's protective effects require both forms of receptors. AdipoR1 induces phosphorylation and activation of the 5'-AMP-activated protein kinase (AMPK) pathway, leading to elevated glucose uptake, fatty-acid oxidation, and mitochondrial functions [85]. Meanwhile, AdipoR2 exerts its effects via promoting PPARα activity, resulting in improved lipid metabolism in primary cultured hepatocytes [86]. Studies have shown that overexpression of both receptors led to enhancement of AMPK and PPARα activities and abrogation of diabetic conditions in db/db mice. Simultaneous knockout of AdipoR1 and AdipoR2, on the other hand, resulted in impaired glucose and lipid metabolism, with consequent insulin resistance, a hallmark of T2D [87].

Two types of adiponectin receptor adaptors have been studied including APPL1 (Adaptor protein, Phospho-tyrosine interacting with pH domain Leucine zipper 1) and APPL2. APPL1, upon binding to AdipoR1, exerts its effects in elevating glucose uptake, metabolism, and insulin sensitivity through activation of AMPK and p38 MAPK (Mitogen Activated Protein Kinase). Overexpression of APPL1 enhanced phosphorylation levels of AMPK and p38 MAPK in C2C12 myocytes and GLUT4 (glucose transporter 4) membrane translocation in L6 cells [88]. APPL2 is inversely correlated with APPL1 in inducing adiponectin signaling pathway. It forms a dimer with

APPL1, resulting in the APPL1-APPL2 structures which compete for interaction with the AdipoR1-APPL1 complex. APPL2 overexpression, as such, resulted in disrupted adiponectin signaling in C2C12 myotubes, while its deletion by RNAi (RNA interference) significantly ameliorated adiponectin-induced glucose uptake [89].

1.4.3.2 Adiponectin signaling pathway

PPARα and AMPK are the major signaling pathways activated by adiponectin. PPARα is a nuclear receptor protein that is responsible for regulating cellular homeostasis through enhancing insulin sensitivity, glucose, and lipid metabolism [90]. In clinical trials, use of synthetic PPAR α agonists has proved to lower triglycerides and effectively treat atherogenic dyslipidemia [91]. Adiponectin stimulates activation of PPARα and its target genes such as ACO (Acetyl CoA oxidase), CPT1 (carnitine palmitoyl transferase 1), and UCP (uncoupling protein). Upregulation of these genes induces fatty acid catabolism and mitochondrial fatty acid β-oxidation [92].

Another mechanism through which adiponectin exerts its effects is via the AMPK signaling pathway. AMPK is a sensor molecule crucial for maintaining energy homeostasis. When energy is depleted, ATP levels decrease, leading to activation of AMPK. Upon activation, AMPK prevents the catabolism of ATP while promoting its production to create energy source. A cascade of downstream effectors is initiated upon binding of adiponectin to AdipoR1. AMPK phosphorylation at T172 is induced via promoting APPL1-dependent LKB1 (liver kinase B1) translocation from the nucleus to the cytosol [93]. Upon activation, phosphorylated AMPK suppresses acetyl-CoA carboxylase (ACC) activity to increase rates of myocardial fatty acid oxidation (FAO) and promote ATP production [94]. AMPK also induces expression of p38 MAPK, which subsequently enhances GLUT4 translocation and glucose uptake [95]. Production of nitric oxide through endothelial nitric-oxide synthase (eNOS) in endothelial cells is another downstream effector of AMPK activation, resulting decreased inflammation and promoted vasodilation at vessels [96]. Adiponectin- depleted mice exhibited downregulation of

AMPK phosphorylation and insulin resistance, which is indicative of adiponectin's role in conferring metabolic enhancement [97].

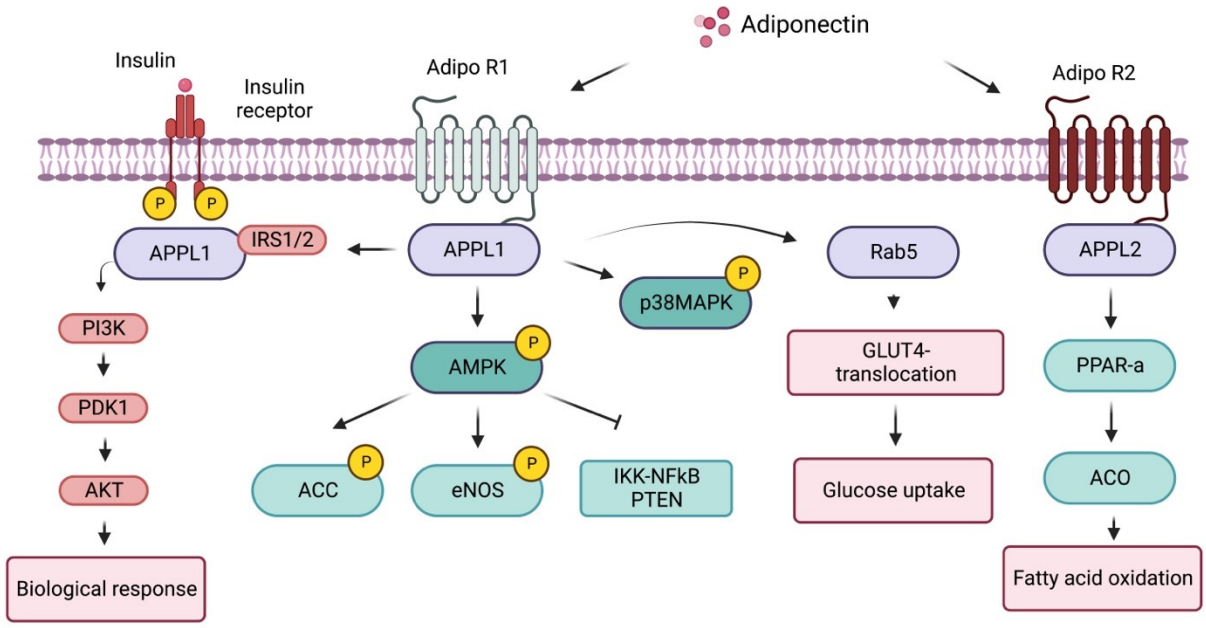

Figure 2. Adiponectin signaling pathway (Adapted from [98])

1.4.4 Adiponectin as a therapeutic target

Adiponectin exerts multifaceted effects in diabetic states, including managing glucose levels, lipid metabolism and insulin sensitivity through its anti-inflammatory and antioxidant benefits [99]. Adiponectin stimulation is known to diminish key pro-inflammatory molecules including TNF-α-stimulated expression of vascular cell adhesion molecule-1 (VCAM-1), E-selectin, intracellular adhesion molecule-1 and IL-8 in human aortic endothelial cells [100,101].

Expression levels of human monocyte- derived macrophages were promoted through induction of interleukin-10 (IL-10) by adiponectin, which is indicative of its effective prevention against vascular inflammation [102]. In human neutrophils, adiponectin significantly downregulated production of reactive oxygen species, key derivatives of inflammation, through regulation of NADPH oxidase [103]. Due to its clear correlation with certain metabolic conditions, targeting adiponectin as a prospective therapeutic treatment is of potential benefits.

Adiponectin's anti-diabetic effects are well established. High plasma adiponectin is closely associated with decreased risks of both T1D and T2D. Adiponectin facilitated glucose clearance and insulin sensitivity in high- fat diet mice via activation of AMPK [104,105]. In parallel with inducing AMPK phosphorylation, it inhibits the enzyme phosphoenolpyruvate carboxylase leading to prevention of gluconeogenesis [106]. In addition, adiponectin promoted insulin sensitivity through upregulating hepatic IRS-2 expression via an IL-6 dependent pathway [107]. Adiponectin-KO mice have shown to develop impaired glucose transport, insulin resistance, inflammation, and subsequent diabetes [108-111], while adiponectin replenishment could reverse insulin resistance and metabolic syndrome in models of T2D [112,113]. These observations further demonstrated the beneficial effects of adiponectin as an anti-diabetic factor.

Low levels of plasma adiponectin are closely related with diabetes [114]. This gave rise to an increasing interest of replacing the body's loss of adiponectin with its mimetic compounds. Studies suggested that the use of adiponectin mimetics has proved to exert similar effects to adiponectin including insulin-sensitizing, enhanced glucose oxidation, glucose uptake and fatty acid catabolism, via the AMPK-dependent pathway [115-117]. In particular, a peptide-based

adiponectin mimetic compound that was proposed to confer anti-diabetic effects is ALY688, developed by Allysta Pharmaceuticals. By binding to both AdipoR1 and AdipoR2, ALY688 initiates the adiponectin signaling pathway [118]. This peptide also provides great potency and specificity over small molecule mimetics. Using adiponectin-mimetic compound in general and ALY688 in particular is therefore of great potential benefit in diabetes studies.

1.5 Endoplasmic reticulum (ER) stress

1.5.1 Description of ER stress

Endoplasmic reticulum (ER) is structurally and functionally highly dynamic and adaptive, consisting of membrane sheets and tubules. The ER structure is regulated by scaffolding proteins. Disturbances of the structural apparatus is reported to contribute to the onset of insulin resistance and obesity. From the functional perspective, the ER is an undeniably important organelle that is responsible for protein synthesis, modification, and transport. As such, disturbances in the ER, both structurally and functionally would contribute to metabolic disorders in general and insulin resistance in particular [119].

ER stress, characterized by accumulated protein aggregates, is initiated upon compromised protein folding and ER functions [120]. Drivers of ER stress consist of nutrient starvation, hypoxia, calcium imbalance and sustained oxidative stress, among others [121-124]. Three cellular quality control mechanisms that ensured successful folding of the polypeptide chain upon ER stress have been well established including: endoplasmic reticulum-associated degradation (ERAD), the unfolded protein response (UPR) and autophagy. ERAD is a protective mechanism that can initiate the elimination of misfolded proteins through to prevent ER stress [125]. The complex series of signaling that lead ERAD from the ER into the cytoplasm includes: (1) unfolded/misfolded proteins are recognized by lectins and chaperones;

(2) ERAD substrates experience active retro translocation across the lipid bilayer through adaptor-dislocon complexes like SEL1L and HRD1; and (3) the VCP, or p97 moves substrates out of the ER membrane while simultaneously "breaking up their tertiary structure" and into the cytosol. ERAD, ER stress, and metabolism are also linked by the ER-localized protein SDF2L1, the suppression of which in the liver can similarly lead to ER stress, steatosis, and insulin resistance [126,127].

1.5.2 ER stress and the unfolded protein response (UPR)

Concurrent with ERAD, the unfolded protein response (UPR) is activated to cope with the effects of ER stress. This activation encompasses a signaling cascade with downstream targets functioning to alleviate ER stress by increasing the ER's folding capacity, reducing the protein folding load and activating ERAD. The UPR is mediated through three ER membrane sensors: protein kinase-like ER kinase (PERK), inositol-requiring enzyme-1 (IRE1) and activating transcription factor 6 (ATF6). These signaling cascades ultimately regulate ER chaperones, folding enzymes, antioxidants, lipid synthesis, protein degradation and translational attenuation [128]. The UPR was first discovered in 1986 by Munro and team. He found that GRP78 (Binding immunoglobulin protein) was the promoter of the UPR, the activation of which would generate three transmembrane sensors [129]. First, dissociation of GRP78 from PERK induces its serine/threonine kinase activity through dimerization and autophosphorylation [130]. Phosphorylated PERK then stimulates the activation of eukaryotic translation initiation factor 2 (eIF2α), which inhibits general translation to reduce the protein folding load [131]. Meanwhile, translation of activating transcription factor 4 (ATF4) is also activated, bringing about the expression of UPR target genes: chaperones and folding enzymes [132]. Activation of IRE1, the second arm of the UPR, promotes its RNase activity cleaving X-

box binding protein 1 (XBP1) mRNA. This enables the translation of an active transcription factor that acts on several UPR target genes [133]. Activation of IRE1 also leads to phosphorylation and activation of JNK via TNF receptor-associated protein factor 2 (TRAF2), as well as apoptosis signal-regulating kinase 1
(ASK1) [134]. Together, these help to degrade mRNA and reduce the protein folding load of the ER. The final arm of the UPR, ATF6, is activated by translocation to Golgi where it is cleaved by site-1 protease (S1P) and site-2 protease (S2P) to form a 50kDa active transcription factor [135]. This then translocates to the nucleus to active UPR target genes such as chaperones and those involved in lipid synthesis [136].

1.5.3 ER stress and the UPR in insulin resistance and diabetes

Some pioneering studies have illuminated this relationship between endoplasmic reticulum and insulin resistance. For example, it was found that overexpression of oxygen-regulated protein 150 (ORP150), a molecular chaperone that protects cells from ER stress, markedly improved insulin resistance and ameliorated glucose tolerance in obese mice [137]. To this end, mice that were deficient in X-box–binding protein–1 (XBP-1), a transcription factor modulating the ER stress response, were more prone to developing insulin resistance compared to wild type ones. Significantly, the UPR is specifically crucial in regulating protein aggregates formed in patients with Alzheimer's and Parkinson disease, conditions that are closely related with T2D [138].

1.6 Autophagy

1.6.1 Autophagy definition and function

To alleviate ER stress and restore optimal homeostasis, another endogenous cellular response is via induction of autophagy. Autophagy or self-eating is an evolutionarily conserved mechanism for bulk degradation of protein aggregates or organelles by transporting them to lysosomes [139]. Autophagy is both crucial in proteostasis and connected to ER function and stress, as autolysosomes can help regulate energy levels and eliminate "protein waste" potentially associated with human metabolic derangements [140]. It is also implicated in a broad range of diseases and is essential for cellular homeostasis [141-144].

1.6.2 Autophagy process

The concept of autophagy was initially established in the 1990s by Christian de Duve following his study of lysosomes in yeasts [145]. The morphology and key genes involved in autophagy were then characterized by Dr. Yoshinori Oshumi [146]. This work of autophagy mechanisms led to his 2016 Nobel Prize win in Physiology or Medicine. With the advancement of microscopy techniques, classification of autophagy was established including Macroautophagy, Microautophagy and Chaperone Mediated Autophagy (CMA), depending on delivery

methodologies [147]. Among these types, macroautophagy remains the most prominently studied. In particular, macroautophagy initiates with the formation of double lipid layers membranes called phagophores from the ER [148,149]. These structures then get separated from their sources and elongated until they are enclosed to become a ring-like structure called an autophagosomes. In the stage of phagophore elongation, autophagosomes recognize the target by adaptor proteins, and the term of autophagy is named differently depending on targets

such as mitophagy for mitochondria, lipophagy for lipid, or ERphagy for ER [150]. Once autophagosomes are loaded, they fuse with lysosomes, becoming autophago-lysosomes, transient single membraned structures that degrade targets with lysosomal proteolytic enzymes [151]. Once degraded, products or amino acids are released and used as cellular building blocks. Since these important findings, the significance of autophagy has been implicated in many studies. For instance, it is an important factor in anti-aging as a decrease in autophagic activity is indicative of aging in diverse organisms [152].

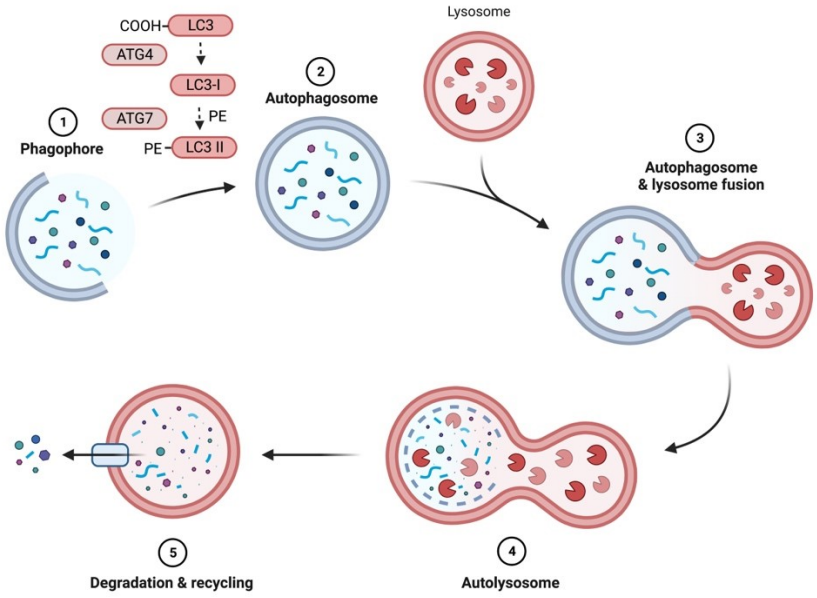

Figure 3. Process of autophagy

1.6.3 Autophagy in insulin action and diabetes

Autophagy is an important regulator in insulin resistance and T2D. Its mechanisms are not fully elucidated, yet impairment in the autophagic pathway constitutes development of T2D. β cell-specific deletion of Atg7 in mice led to decreased insulin secretion, abated β cell mass and amplified cell death [153]. Autophagy-knockout mice also exhibited disrupted glucose

tolerance and impaired insulin sensitivity [154]. Loss of autophagy diminishes mitochondrial functions via the PINK1/PARKIN pathway with resultant insulin resistance [155]. Induction of anti-inflammatory response is another mechanism through which autophagy mediates oxidative stress and insulin sensitivity [156]. Conversely, upregulation of autophagy through Atg5 genetic overexpression prevented mice from obesity and insulin resistance [157]. Correspondingly, liver targeted overexpression of Atg7 was proposed to alleviate obesity-associated ER stress and insulin resistance [158]. Gain of function of autophagy by pharmacological activation of rapamycin or carbamazepine exerts similar effects as observed in genetic approaches [159,160]. However, it should be noted that too much of autophagy can also place detrimental consequences in regulating metabolic diseases, specifically T2D through apoptosis. Collectively, these observations suggested that autophagy confers protective effects against obesity, insulin resistance and T2D and its precise regulation is the key factor in mediating metabolic disorders.

CHAPTER 2: STUDY 1

"Salubrinal promotes phospho-eIF2alpha-dependent activation of UPR leading to autophagy-mediated attenuation of iron-induced insulin resistance"

2.1 Abstract

Identification of new mechanisms mediating insulin sensitivity is important to allow validation of corresponding therapeutic targets. In this study, I first used a cellular model of skeletal muscle cell iron overload and found endoplasmic reticulum (ER) stress and insulin resistance occurred after iron treatment. Insulin sensitivity was assessed using cells engineered to express an Akt biosensor, based on nuclear Foxo localization, as well as western blotting for insulin signaling proteins. Use of salubrinal to elevate eIF2α phosphorylation and promote the unfolded protein response (UPR) attenuated iron-induced insulin resistance. Salubrinal induced autophagy flux and its beneficial effects on insulin sensitivity were not observed in autophagy-deficient cells generated by overexpressing a dominant-negative Atg5 mutant or via knockout of ATG7. This indicated the beneficial effect of salubrinal-induced UPR activation was autophagy-dependent. I translated these observations to an animal model of systemic iron overload-induced skeletal muscle insulin resistance. Administration of salubrinal as pre-treatment enhanced eIF2α phosphorylation and induced autophagy in skeletal muscle. This attenuated insulin resistance upon systemic iron administration. Together, my results show that salubrinal elicited an eIF2α-autophagy axis leading to improved skeletal muscle insulin sensitivity both in vitro and in mice.

2.2 Introduction

Iron is an essential element that is involved in many biological processes and sustaining balanced iron levels are essential for preventing the onset of a number of diseases [161]. Existing studies on iron deficiency and iron overload have bolstered our understanding of the importance of iron homeostasis and its regulation [162]. From a clinical perspective, iron overload is also pathologically important in primary hemochromatosis and secondary iron-loading anemias including thalassemia and myelodysplastic syndromes [163-165]. Furthermore, iron overload is the culprit underlying some forms of cancer, inflammation, neurodegenerative diseases and, most significantly, cardiometabolic diseases [166-169].

Insulin resistance remains the most notable and consequential metabolic dysfunction [170]. Under this condition, cells and tissues do not respond well to insulin [171], with associated consequences of type 2 diabetes and heart failure [172-174]. The molecular mechanisms underlying insulin resistance are widespread, with autophagy and endoplasmic reticulum (ER) stress both known to be important [175-177]. Autophagy is a well conserved process of 'self eating' involving degradation of cellular components such as damaged organelles and protein aggregates, thus playing important roles in maintaining cellular homeostasis [178]. Previous studies have established the significance of autophagy in regulating insulin signaling as well as metabolism in skeletal muscles [179]. By utilizing skeletal muscle cells, we previously showed that chronic iron overload leads to a profound autophagy defect via mTORC1-UVRAG inhibition that led to inhibition of autophagosome-lysosome reformation (ALR), with consequent insulin resistance [175].

In the endoplasmic reticulum, proteins are synthesized, modified, and transported to destined compartments. Perturbations in these processes can manifest as protein aggregation [180]. To survive a series of cellular stressors such as nutrient deficiency, Ca^{2+} imbalance, toxin and sustained oxidative stress [181-184] the unfolded protein response (UPR) will be engaged [185]. This can involve the activation of three transmembrane proteins: inositol-requiring protein 1 (IRE1), protein kinase RNA-like ER kinase (PERK) and activating transcription factor 6 (ATF6) [186]. These sensors aid in improving cellular homeostasis by expanding the ER protein-folding capacity, decreasing global mRNA translation, and increasing ER-associated degradation (ERAD), among others [187]. Upon activation, PERK will phosphorylate the downstream eukaryotic translation initiation factor (eIF2α) at Ser51, which enhances translation of a subset of mRNAs, including that encoding the activating transcription factor 4 (ATF4) [188-190]. This enhances cellular homeostasis by inhibiting translation, facilitating amino acid synthesis, inducing antioxidative stress response genes and increasing expression of autophagy genes. However, connections between iron, ER stress, UPR induction and autophagy in the regulation of insulin resistance are not clearly understood.

In this study, I hypothesized that ER stress upon iron overload leads to insulin resistance in skeletal muscle cells and that strategies to promote its downstream including UPR and autophagy are beneficial. In order to test my central hypothesis, three main questions were investigated. These include effects of iron on ER stress, insulin sensitivity and whether alleviating ER stress helps attenuate iron overload- induced insulin resistance. After establishing this model, the mechanisms were tested by using salubrinal- an inhibitor of eIF2α phosphatase and ALY688- an adiponectin receptor agonist as the main pharmacological

approaches to induce UPR/autophagy activation and clarify the relationship between iron overload and insulin sensitivity through ER stress.

2.3 Materials and methods

Cell culture and maintenance of L6 skeletal muscle cells

L6 rat skeletal muscle cell line was grown in alpha-minimum essential medium (AMEM) (Wisent; #210-010) supplemented with 10% fetal bovine serum (FBS) (Wisent; #080-150) and 1% antibiotic/antimycotic (Gibco; #15240062) at 37°C with 95% air and 5% CO_2. Cells were maintained in 75 cm^2 flasks and passed at 70% confluency. 3 mL of trypsin was first added to detach the cells from the flasks following by neutralization with 7 mL of 10% FBS AMEM. Cells were then centrifuged at 2000 RPM for 5 mins. 5 mL of 10% FBS AMEM was added in the cells for resuspension, with 10% of total cell and media mix being used for further plating in the new flask. For iron treatment, iron (II) sulfate heptahydrate (Sigma-Aldrich; #215422) was prepared by dissolving in sterile distilled water with the stock concentration of 100 mM.

Atg5K130R mutant cell line. A stable L6 Atg5K130R (Atg5K) dominant negative mutant cell line was generated as a cellular model of autophagy inhibition, as previously described [176]. This point mutation prevents conjugation to ATG12 and blocks LC3II incorporation and elongation of the autophagosome membrane.

Western blotting

L6 cells were seeded on 6- well plates until having 80-90% confluency. Cells were subjected to treatments of $FeSO_4$ 250 μM for 24-h followed by insulin 100 nM (Lilly; Humulin-R U-100) for

10 min. Control cells were starved in AMEM 0% FBS for 24-h. For salubrinal treatment, the drug (Sigma Aldrich; SML0951) was firstly made by dissolving salubrinal powder in DMSO to make the stock concentration of 0.04M. Cells were then treated with salubrinal for 24-h at the working concentration of 30μM. For salubrinal- iron groups, cells were pretreated with salubrinal 30μM for 30 min prior to iron treatment 24-h. Samples were washed with PBS (Wisent; 311-010-CL) and prepared using lysis buffer. Cells were also syringed to ensure further lysis, followed by collection and centrifugation at 10,000 RPM for 5 min at 4°C before being denatured at 95°C for 5 min. Cell lysates were run on 8% SDS-PAGE gels conducted at 90 V for 2 h. The gels were transferred to a polyvinylidene difluoride (PVDF) membrane at 120 V for 1.5 h. Membranes were submerged in 3% bovine serum albumin (BSA) blocking buffer for 1 h, followed by overnight incubation in 1:1000 dilution of primary antibodies: phospho-Akt s473 (Cell Signaling; #9271) and phospho-ERK (Cell Signaling; #9106L) at 4°C. Membranes were then washed with TBS-T three times before 1-h of secondary antibody incubation at room temperature. The secondary antibodies used was an anti-rabbit immunoglobulin G horseradish peroxidase-conjugated antibody
(Cell Signaling; #7074) and anti-mouse antibody (Cell Signaling; #7076) at 1:5000 dilution. Membranes were then quickly washed with Clarity Western ECL Substrate solution (BioRad; #1705061) and visualized using X-ray film development techniques. Western blot band intensity was quantified using ImageJ software, normalized to glyceraldehyde 3-phosphate dehydrogenase (GAPDH) (Cell Signaling; #2118) or total Akt (Cell Signaling; #9272).

To examine the role of iron and salubrinal in activating UPR, L6 cells were seeded on 6 well plates until having 80-90% confluency. 4 groups of treatment were performed for the salubrinal

experiment including control, salubrinal, iron, salubrinal iron. For control samples, cells were starved in AMEM media 0% FBS for 24 h. For iron- treated samples, cells were subjected to treatments of $FeSO_4$ 250 μM for 24 h. For salubrinal-iron groups, cells were treated with salubrinal

30 μM for 30 min prior to iron treatment 24-h. Western blot analysis was performed according to protocol aforementioned. 2 primary antibodies were used in this assay including p- eIF2α (Cell Signaling; #9721) and ATF4 (Cell Signaling; #11815).

To assess the effects of iron and salubrinal treatments on autophagic flux, L6 skeletal muscle cells were seeded on 6 well plates until having 80-90% confluency. 4 groups of treatment were performed including control, salubrinal, iron, salubrinal iron. For iron- treated samples, cells were subjected to treatments of $FeSO_4$ 250 μM in AMEM supplemented with 0.5 % FBS for 16 h. For salubrinal-iron groups, cells were pretreated with salubrinal 30 μM for 30 min prior to iron treatment 16-h. Western blot analysis was performed according to protocol aforementioned. 2 primary antibodies were used in this assay including LC3B (Cell Signaling; #2775) and SQSTM1/p62 (Cell Signaling; #5114).

Stable L6 Atg5K130R (Atg5K) dominant negative mutant and ATG7- knock out cell lines were used as molecular models to assess the role of autophagy in beneficial effects of salubrinal. Empty vector (EV) cells containing no foreign DNA were used as control with ATG5K cells and wild-type L6 cells were used as control with ATG7- knock out cell lines. Cells were seeded on 6 well plates until having 80-90% confluency. 4 treatment groups were determined including insulin, iron insulin, salubrinal insulin and salubrinal iron insulin. Cells were subjected to

treatments of $FeSO_4$ 250 μM in AMEM 0% FBS for 24-h followed by insulin 100 nM for 10 min. For salubrinal groups, cells were pre-treated with salubrinal 30 μM for 30 min prior to iron treatment. Western blot analysis was performed according to protocol aforementioned with 2 primary antibodies being used were phospho-Akt s473 (Cell Signaling; #9271) and phospho-ERK (Cell Signaling; #9106L).

Transforming Escherichia coli DH5α cells with SB100X and FoxO1 biosensor plasmids

50ng circular DNA of FoxO1 (AddGene; #106278) and SB100X (AddGene; #34879) plasmids were thawed, added to competent *E.coli* DH5α cells and gently mixed. The tube with DNA and competent cells was placed in 42°C water bath for 1 min and transferred onto ice for 2 min to reduce damage to cells. 800 μL of Luria-Bertani (LB) broth (Invitrogen; #12795027) was prepared and added to the tube, then incubated for 1-h at 37°C with 250 RPM shaking. Resulting bacterial cultures were spread on LB agar plates containing ampicillin and chloramphenicol (Sigma) for FoxO1 and SB100X plasmids, respectively. Plates were incubated inverted overnight at 37°C. A colony was then selected after 12-h to be propagated further in LB broth with antibiotics for overnight shaking at 250 RPM and 37°C.

Plasmid purification

125 mL of transformed bacterial culture was centrifuged for 20 min at 4,000 x g. Pellets were resuspended using the buffers provided by the Invitrogen PureLink Fast Low-Endotoxin Midi Plasmid Purification Kit (Invitrogen; #A35892). All purification steps were performed according to the protocol provided in the kit to elute plasmid products. DNA concentrations were determined, and the purified plasmids were stored at -80°C for future use.

Sleeping Beauty transfection of FoxO1 and biosensor plasmids into L6 skeletal muscle cells

Prior to transfection, low passage WT-L6 cells were cultured in a T75 flask to 90% confluency. 2 transfection mixtures were prepared. An integrase/DNA/OptiMEM mix was first created by adding FoxO1 Biosensor and SB100X plasmids at a 10:1 ratio respectively to OptiMEM (Thermo Fisher; #31985062) for a total volume of 150 µL. The first mixture was then combined with the second tube containing 3.6 µL of Lipofectamine 2000 (Invitrogen; #11668019) and 146.4 µL of OptiMEM. The mixture was then vortexed for 2 sec, spun down on tabletop centrifuge and incubated for 15 min at room temperature. On the other hand, L6 cells were trypsinized at room temperature for 15 min for the cells to detach from the bottom. The cells were then neutralized by adding AMEM media containing 10% FBS and antibiotics. 900 µL of cell and media mixture was seeded into 1-3 wells of a 6-well plate per plasmid. 100 µL of DNA and lipofectamine mix was then added in each well. Plate was gently shook to mix followed by incubation at 37ºC for 24-h. On day 2 of transfection, cells were split into a T25 flask and selected for successful transfection with 2 µg/µL of puromycin (Thermo Fisher Scientific; #A113803) the next day. After 24-h, AMEM media with 10% FBS was changed to the flask to maintain cell proliferation. Cells were subjected to a second time of puromycin selection 7 days later.

Real-time imaging of insulin signaling using fluorescent microscopy

L6 cells transfected with FoxO1 biosensor were seeded onto a 96-well plate for treatment. When cells reached 50-60% confluency, they were subjected to 6 groups of treatment including

control, insulin, iron, iron insulin, salubrinal iron and salubrinal iron insulin. For the iron treatment wells, cells were treated with $FeSO_4$ 250 μM overnight. For the salubrinal iron treatment groups, cells were subjected to salubrinal 30 μM for 30 min prior to overnight iron treatment. All treatments were performed using AMEM 0% FBS media. After incubation time, cells in all treatment groups were washed and starved in 0% FBS AMEM for 90 min, then treated with 100 nM insulin and imaged on EVOS FL Auto 2 for green fluorescence over a span of 30 min to observe fluorescent translocation. Nuclear fluorescence signal was traced from the nucleus to the cytosol in all treatments with number of cells being 10 for each treatment. Data quantitation was performed using Celleste software.

Insulin sensitivity measured by glucose uptake assay

A stable L6 cell line overexpressing GLUT4 with a myc epitope was used to examine insulin stimulated glucose uptake in L6 myoblasts. Glucose uptake assay was carried out based on the detection of 2-deoxyglucose-6-phosphate (2DG6P). L6-GLUT4myc cells (a kind gift from Dr Amira Klip, The Hospital for Sick Children, Toronto) were seeded on 96-well plate at 10,000 cells/ well before treatment. Cells were then treated with different conditions including control, iron, salubrinal, salubrinal iron (all stimulated with and without insulin 100nM). Treatment was performed as aforementioned. After 24 h treatment, insulin (100 nM) was stimulated for 15 min. 2DG (2-deoxyglucose) was added and incubated for 30 min, followed by addition of stop buffer and neutralization buffer according to the protocol from the Glucose Uptake-Glo Assay kit by

Promega. Finally, 2DG6P detection reagent was added and luminescence was recorded with 0.3–1 second integration using VarioSkan LUX.

ThT staining assay

L6 skeletal muscle cells were seeded at 70% confluency on a µ-slide 4-well chambered polymer coverslip (Ibidi), and the growth medium was then replaced with 0% FBS AMEM (Phenol-red free), iron treatment (250 µM) for 4 h. After treatment, Tht solution (Sigma- Aldrich; #T3516, 2.5 µM) was prepared in phenol-red free DMEM media 0% FBS and cells were stained for 30 min. After staining time, cells were imaged with HCS NuclearMask™ Blue Stain (Thermo Fisher; # H10325, 1:2000). Imaging was performed at 20x objective (Nikon A1 confocal microscope) in a 5% CO_2 live-cell chamber. Results were quantified using ImageJ software with at least 40 cells/ treatment/ field of views.

GRP-78 mCherry reporter

Cells stably expressing a GRP78 promoter driver mCherry reporter, which was generated previously [191], were seeded on 4-well chamber and subjected to iron treatment (250 µM) for 24 h. Imaging was performed at 20x objective (Nikon A1 confocal microscope) and 1 h intervals up to 24 h in a 5% CO_2 live-cell chamber.

Gene expression analysis

Total RNA was extracted with RNEasy Mini Kit (Qiagen, Toronto, Canada) and then converted to cDNA using the RevertAid RT Kit (Thermo Scientific; #K1691). qPCR was performed with Sso Advanced SYBR Green Master Mix (Bio-Rad; #1725270) starting with an initial activation at 95°C for 15 min, followed by 40 cycles of 94°C for 15 sec, 55°C for 30 sec and 70°C for 30

sec on a Bio-Rad CFX384 Touch Real-Time PCR Detection System. Relative gene expression levels were normalized to 18S rRNA. Primers used in this study are summarized in Table 1.

Name	Kind	Sequences (5'-3')
ATG5	Forward	CCTGAAGACGGAGAGAAGAAGAG
	Reverse	CGGGAAGCAAGGGTGTCAT
ATG10	Forward	CCTGTTTGCTTGGGATAGTGG
	Reverse	ACTTCCCCATCAATCTCCAC
ATG12	Forward	CATTCTTACCTGGCGTTGAG
	Reverse	CACTTCAAACCCTGTAATCC
ATG16	Forward	CACATCTTTACCCAGCATCAC
	Reverse	CAGGACAGAGGGTGCTTTC
LC3	Forward	TGTTAGGCTTGCTCTTTTGG
	Reverse	GCAGAGGAAATGACCACAGAT
s-XBP1	Forward	AAACAGAGTAGCAGCACAGACTGC
	Reverse	GGATCTCTAAGACTAGAGGCTTGGTG

Table 1. List of Primers used

Mouse model of iron overload-induced insulin resistance

Animals were fed ad libitum on regular chow diet and kept in temperature and humidity control rooms with a daily 12:12-h light–dark cycle. 20 8-weeks-old C57/BL6J male mice were categorized into four groups including control, iron, salubrinal and salubrinal iron. Iron dextran (Sigma Aldrich; #D8517) was delivered intravenously at 15 mg/kg in iron group mice while PBS was used as control. Intraperitoneal injection was performed in salubrinal groups (1mg/kg) on day 1, day 2 and day 3. For salubrinal iron groups, salubrinal was also injected at 1mg/kg on day 1, day 2 and day 3. On day 3, iron dextran was delivered intravenously at 15 mg/kg after 30 min of salubrinal injection. For phosphorylation of insulin signaling analysis, all mice were injected via tail vein with insulin (4 units per kg) 5 min before sacrifice. Skeletal muscles were

collected and lysed in tissue lysis buffer as described in table 2. BCA assay was performed to determine protein concentration and lysates were loaded on the gels with a concentration of 30 µg per well to run western blotting.

Lysis Buffer	**1ml**
30mM Hepes, pH 7.4	60µl/0.5M stock
2.5mM EGTA	10µl/0.25M stock
3mM EDTA	12µl/0.25M stock
70mM KCl	70µl/1M stock
20mM β-glycerolphosphate	10µl/2M stock
20mM NaF	40µl/0.5M stock
1mM Na3VO4	1µl/1M stock
200µM PMSF	1µl/0.2M stock
1µM Pepstatin A	1µl/1mM stock
10µM Et64	1µl/10mM stock
1µM Leupeptin	1µl/1mM stock
0.1% NP40	5µl/20% stock
0.01mM Okadaic acid	1ul/0.1mM stock
ddH2O	788µl

Table 2. Components of lysis buffer for skeletal muscle tissues

Measuring protein concentration using BCA assay

Cell lysates were collected using the same protocol as western blotting assay, in a working lysis buffer lacking bromophenol blue. 10 µL of crude lysates were aliquoted into 96- well plate and treated with 10 µL of the working BCA reagent (Thermo Fisher; #23225). A series of dilutions of Bovine Serum Albumin (BSA) were prepared from the kit and assayed alongside the unknowns to generate a protein standard curve. Samples were incubated for 30 min and the absorbance was measured at 562 nm using VarioSkan LUX. Results were then used to determine respective protein concentrations based on the standard curve generated.

Statistical analysis

One-way ANOVA test with turkey's multiple comparisons was carried out on GraphPad Prism to determine statistical significance in which p values < 0.05 were considered significant.

2.4 Results

Iron elevates ER stress and UPR induction in L6 skeletal muscle cells

To investigate the effects of iron on ER stress, I first employed the Tht assay to detect protein aggregates, an established marker of ER Stress. In this experiment, L6 skeletal muscle cells were treated with or without 250 μM $FeSO_4$ for 4 h, and Thioflavin T used as a probe to monitor misfolded protein accumulation. My results show fluorescence was significantly enhanced, indicative of protein aggregates, in iron treated L6 skeletal muscle cells (Fig 4A). Next, I examined the effects of iron overload on the unfolded protein response (UPR). To do so I generated L6 skeletal muscle cells stably expressing a GRP78 promoter-driven mCherry reporter. Time lapse imaging indicated a rapid increase in response to iron compared with control cells, which was apparent after 4 h and maintained up to 24 h treatment (Fig 4B). To verify the effectiveness of salubrinal, I then used western blotting (Fig 4C&D) to demonstrate that it induces a significant increase in phosphorylation of p- eIF2α and ATF4 level. This confirms salubrinal caused an increase in UPR activation, specifically via the eIF2α-ATF4 pathway. There was no significant effect of iron alone on p- eIF2α and ATF4 level, although an apparent small increase of p- eIF2α was observed (Fig 4C&D).

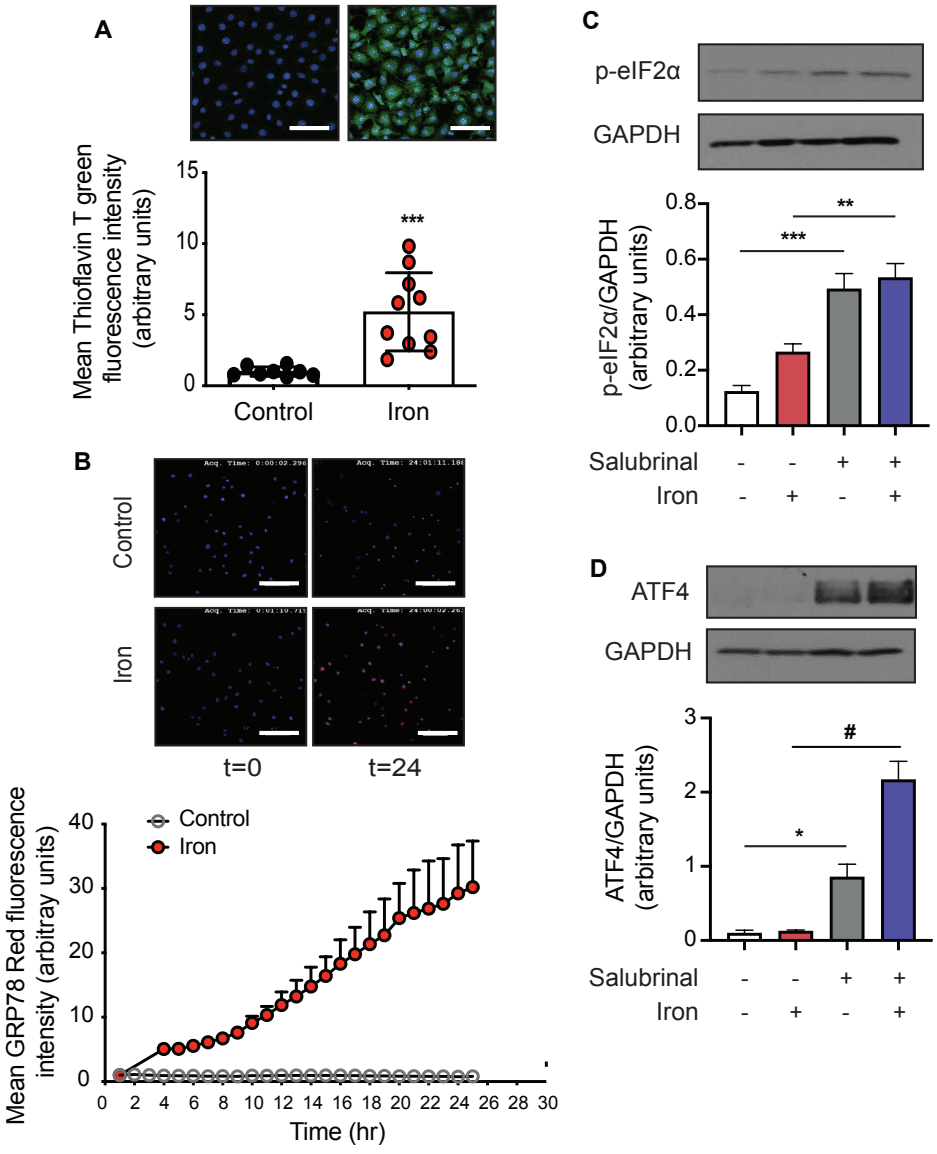
A
Mean Thioflavin T green fluorescence intensity (arbitrary units)
15
10
5
0
***
Control
Iron
B
Control
Iron
t=0
t=24
Mean GRP78 Red fluorescence intensity (arbitray units)
40
30
20
10
0
Control
Iron
0 2 4 6 8 10 12 14 16 18 20 22 24 26 28 30
Time (hr)
C
p-eIF2α
GAPDH
p-eIF2α/GAPDH (arbitrary units)
0.8
0.6
0.4
0.2
0.0
***
**
Salubrinal - - + +
Iron - + - +
D
ATF4
GAPDH
ATF4/GAPDH (arbitrary units)
3
2
1
0
*
#
Salubrinal - - + +
Iron - + - +

Figure 4. Effect of iron overload and salubrinal on ER stress and UPR activation **A.** Representative confocal images and quantification of Tht assay measuring protein aggregates in L6 skeletal muscle cells after iron injections ($FeSO_4$, 250 μM, 4 h) compared to control. **B.** Representative confocal images and quantification of L6 GRP78- mCherry reporter and quantification of mean red fluorescence for 24 h iron treatment compared to control. **C.** Representative Western blot images and quantification of phospho- eIF2α over GAPDH after iron treatment (250 μM, 24 h), with and without salubrinal treatment (30 μM , 30 min). Values are mean ± s.e.m (n=3) **P < 0.005 ***P < 0.0005 (one-way ANOVA with multiple comparisons). **D.** Representative Western blot images and quantification of ATF4 over GAPDH with after iron treatment (250 μM, 24 h), with and without salubrinal pre-treatment (30 μM, 30 min). Values are mean ± s.e.m (n=3) *P < 0.05 #P < 0.0001 (one-way ANOVA with multiple comparisons).

Iron impairs insulin sensitivity in L6 skeletal muscle cells; an effect prevented upon salubrinal treatment

Kinetics of insulin sensitivity was analyzed by generating L6 cell clones overexpressing an Akt biosensor combined with real-time analysis of fluorescence. This biosensor is based upon measure of phosphorylated FoxO1 translocation from the nucleus to cytosol. My representative images (Fig 5A) visually reflected the difference in nuclear fluorescence intensity over a timespan of 20 min. Quantification indicated that insulin stimulated Akt activity was significantly reduced in cells treated with insulin compared to control cells (Figs 5B&C). Both

temporal analysis (Fig 5B) and quantitation after 20 min (Fig 5C) showed that iron caused insulin-resistance and that salubrinal pre-treatment attenuated this effect of iron. Insulin sensitivity was also assessed by western blot analysis and results show that there was a significant decrease in insulin-stimulated phosphorylation of Akt s473 (Fig 5D) as well as ERK (Fig 5E) upon iron treatment. Upon salubrinal pre-treatment, improved insulin stimulated Akt s473 and ERK was observed, confirming the ability of salubrinal in rescuing insulin sensitivity upon iron overload.

Insulin resistance in skeletal muscle is manifested by decreased insulin-stimulated glucose uptake and to test the functional significance of my previous observations I next examined glucose uptake. A significant reduction in insulin-stimulated glucose uptake was found upon iron pre-treatment for 24-h (Fig 5F). Salubrinal pre-treatment elicited a significantly elevated insulin response in the presence of iron. Together, these results demonstrate the detrimental consequence of iron overload on skeletal muscle cell insulin sensitivity and the beneficial effect of salubrinal in attenuating insulin resistance.

Figure 5

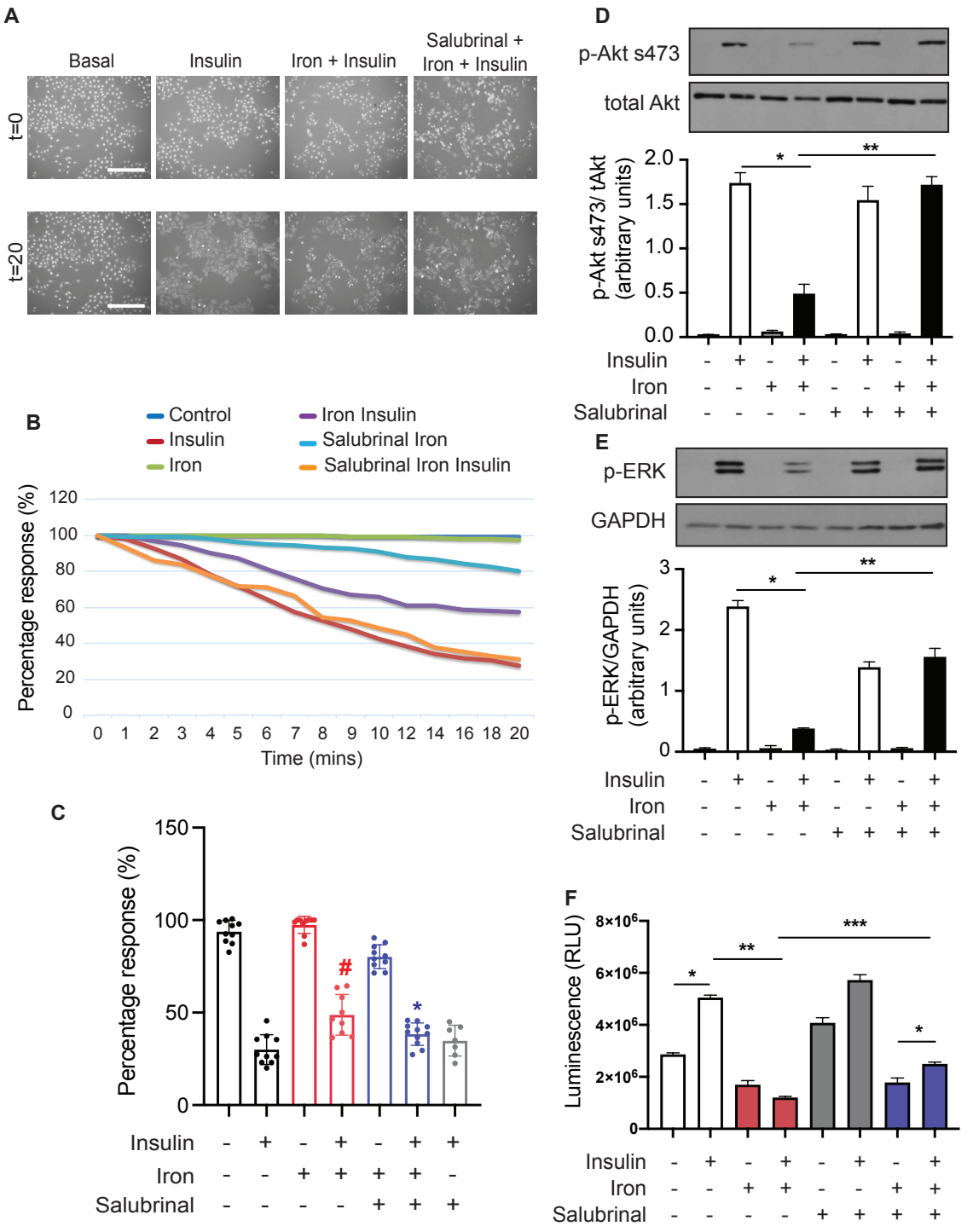
A
Basal
Insulin
Iron + Insulin
Salubrinal + Iron + Insulin
t=0
t=20
B
Control
Insulin
Iron
Iron Insulin
Salubrinal Iron
Salubrinal Iron Insulin
Percentage response (%)
Time (mins)
C
Percentage response (%)
Insulin
Iron
Salubrinal
D
p-Akt s473
total Akt
p-Akt s473/ tAkt (arbitrary units)
Insulin
Iron
Salubrinal
E
p-ERK
GAPDH
p-ERK/GAPDH (arbitrary units)
Insulin
Iron
Salubrinal
F
Luminescence (RLU)
Insulin
Iron
Salubrinal

Figure 5. Effect of iron and salubrinal on insulin sensitivity

A. Representative microscope images of biosensor cells recorded at timepoints t=0 and t=20 (min) with insulin stimulation (100 nM, 10 min) after iron treatment (250 μM, 24 h) with and without salubrinal pre-treatment (30 μM, 30 min) All experiments were repeated three times. Scale bar = 100 μm. **B.** Percentage change of green nuclear fluorescent signal in biosensor cells (n=10) recorded for a time course of 20 min with insulin stimulation (100 nM, 10 min) after iron treatment (250 μM, 24 h) with and without salubrinal pre-treatment (30 μM, 30 min). Percentage change was recorded as mean values. **C.** Percentage response (%) of green fluorescent signal in biosensor cells (n=10) recorded for a time course of 20 min with insulin stimulation (100 nM) after iron treatment (250 μM, 24 h) with and without salubrinal pre-treatment (30 μM, 30 min). Values are mean ± s.e.m *P < 0.05 #P < 0.0001 (one-way ANOVA with multiple comparisons). **D.** Representative Western blot images and quantification of phospho-Akt (s473) over total Akt with insulin stimulation (100 nM, 10 min) after iron treatment (250 μM, 24 h) with and without salubrinal pre-treatment (30 μM, 30 min). Values are mean ± s.e.m (n=3) *P < 0.05 (one-way ANOVA with multiple comparisons). **E.** Representative Western blot images and quantification of phospho-ERK over GAPDH with insulin stimulation (100 nM, 10 min) after iron treatment (250 μM, 24 h) with and without salubrinal pre-treatment (30 μM, 30 min). Values are mean ± s.e.m (n=3) *P < 0.05 (one-way ANOVA with multiple comparisons). **F.** Glucose uptake of L6 skeletal muscle cells with insulin stimulation (100 nM, 20 min) after iron treatment (250 μM, 24 h) with

and without salubrinal pre-treatment (30 μM, 30 min). Values are mean ± s.e.m. *P < 0.05 (one-way ANOVA with multiple comparisons).

Autophagy initiation and flux is upregulated in L6 skeletal muscle cells upon salubrinal treatment

I then used qPCR to examine changes in level of autophagy-related gene 5 (ATG5), autophagy related gene 10 (ATG10), autophagy-related gene 12 (ATG12), autophagy-related gene 16 (ATG16) and unc-51 like autophagy activating kinase 1 (ULK1). Heat map of scaled data (Fig 6A) shows that salubrinal alone most strongly increased the expression of ATG5, ATG12 and ATG10 compared to basal, while iron plus salubrinal had highest effect on ATG16 and ULK1 mRNA expression level. The effect of iron and salubrinal on autophagic flux was also investigated by measuring LC3 and p62 by western blot (Fig 6B&C). Data shows that both iron and salubrinal significantly increased formation of autophagosomes, as indicated by increased LC3-II detection (Fig 6B). However, a significant increase in p62 was observed only upon iron treatment, indicating a block of autophagic flux (Fig 6C). This iron-induced accumulation of p62 was significantly downregulated upon pre-treatment with salubrinal.

Figure 6

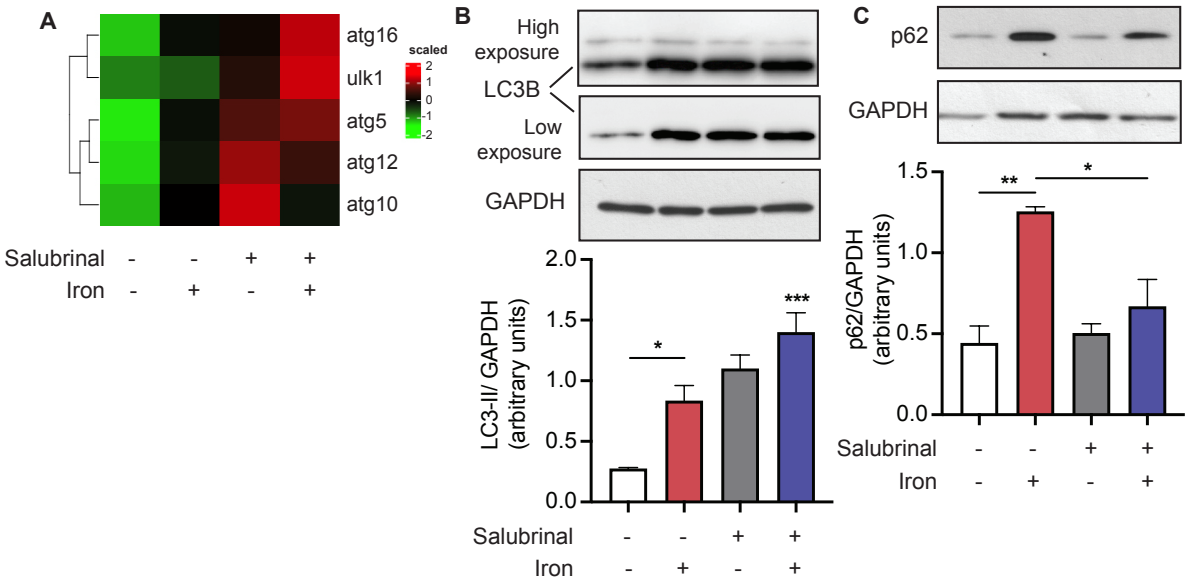
A
atg16
ulk1
atg5
atg12
atg10
scaled
2
1
0
-1
-2
Salubrinal - - + +
Iron - + - +
B
High exposure
LC3B
Low exposure
GAPDH
LC3-II/ GAPDH (arbitrary units)
2.0
1.5
1.0
0.5
0.0
*
***
Salubrinal - - + +
Iron - + - +
C
p62
GAPDH
p62/GAPDH (arbitrary units)
1.5
1.0
0.5
0.0
**
*
Salubrinal - - + +
Iron - + - +

Figure 6. Effect of iron and salubrinal on autophagy

A. Relative gene expressions— autophagy-related gene 5 (ATG5), autophagy-related gene 10 (ATG10), autophagy-related gene 12 (ATG12), autophagy-related gene 16 (ATG16) and unc-51 like autophagy activating kinase 1 (ULK1)- normalized to 18S rRNA expression with iron treatment (250 μM, 24 h), with and without salubrinal pre-treatment (30 μM, 30 min). **B.** Representative Western blot images and quantification of LC3B-II over GAPDH in L6 skeletal muscle cells after iron treatment (250 μM, 16 h), with and without salubrinal pre-treatment (30 μM, 30 min). Values are mean ± s.e.m (n=3) *P < 0.05 ***P < 0.0005 (one-way ANOVA with multiple comparisons). **C.** Representative Western blot images and quantification of p62 over GAPDH in L6 skeletal muscle cells after iron treatment (250 μM, 16 h), with and without salubrinal pre-treatment (30 μM, 30 min). Values are mean ± s.e.m (n=3) *P < 0.05 **P < 0.005 (one-way ANOVA with multiple comparisons).

Salubrinal promotes UPR activation thus alleviating IO-induced insulin resistance in mice

Mice with or without subcutaneous salubrinal pre-treatment and with or without systemic iron administration were injected with insulin (4 units per kg), 5 min before sacrifice as depicted in Fig 7A. Results showed that iron reduced insulin-stimulated phosphorylation of Akt s473 and ERK (Fig 7B-D), while salubrinal pre-treatment attenuated this development of insulin resistance, recapitulating the results of studies in L6 skeletal muscle cells reported above. Results also showed that there was an increase in both phosphorylation of eIF2α and ATF4 levels (Fig 7E-G) upon salubrinal or iron treatment.

Figure 7

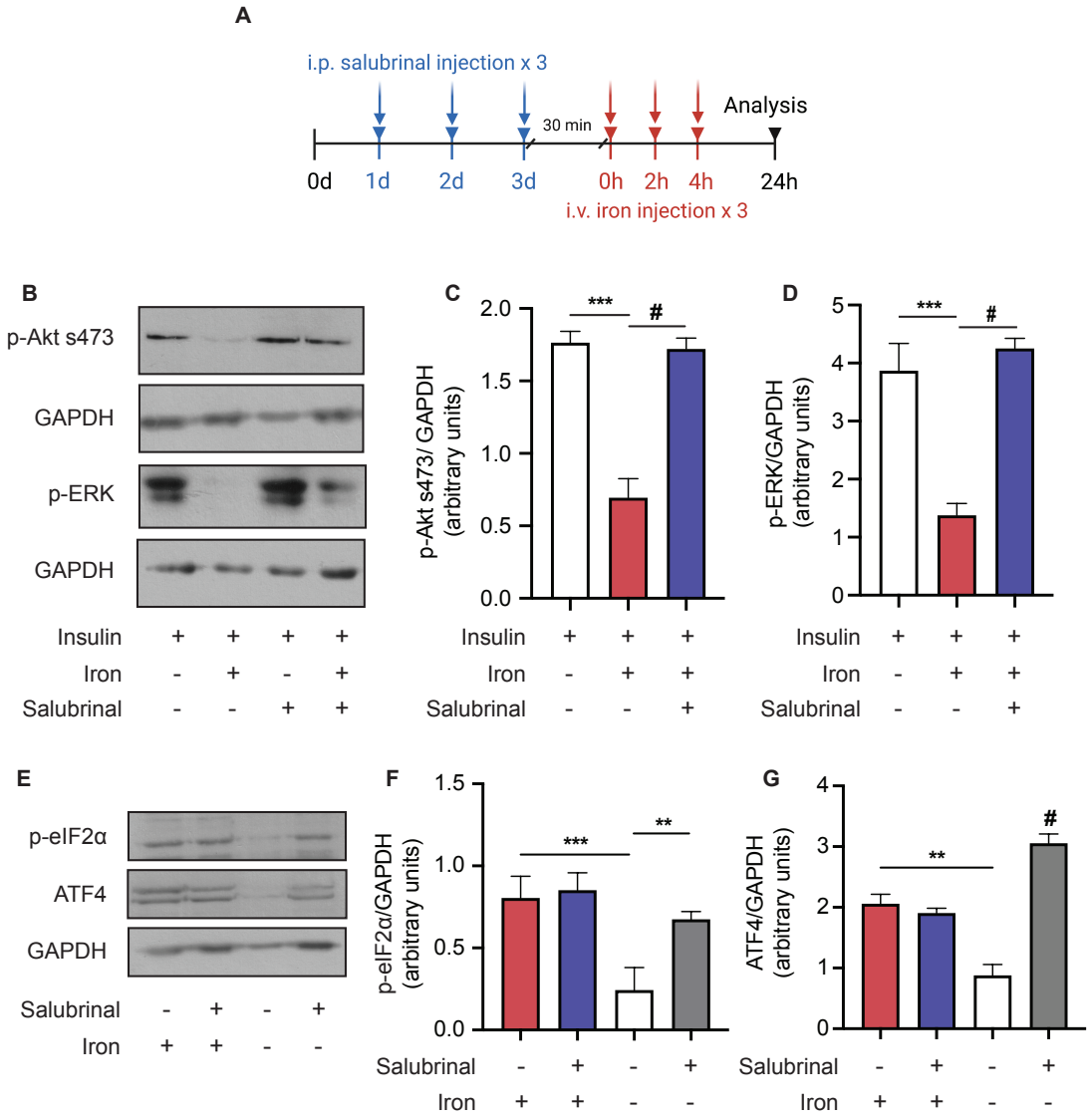
A
i.p. salubrinal injection x 3
30 min
Analysis
0d
1d
2d
3d
0h
2h
4h
24h
i.v. iron injection x 3
B
p-Akt s473
GAPDH
p-ERK
GAPDH
Insulin + + + +
Iron - + - +
Salubrinal - - + +
C
p-Akt s473/ GAPDH (arbitrary units)
2.0
1.5
1.0
0.5
0.0
***
#
Insulin + + +
Iron - + +
Salubrinal - - +
D
p-ERK/GAPDH (arbitrary units)
5
4
3
2
1
0
***
#
Insulin + + +
Iron - + +
Salubrinal - - +
E
p-eIF2α
ATF4
GAPDH
Salubrinal - + - +
Iron + + - -
F
p-eIF2α/GAPDH (arbitrary units)
1.5
1.0
0.5
0.0
***
**
Salubrinal - + - +
Iron + + - -
G
ATF4/GAPDH (arbitrary units)
4
3
2
1
0
**
#
Salubrinal - + - +
Iron + + - -

Figure 7. In vivo model of mice skeletal muscles with IO

A. Schematic diagram of salubrinal-iron injections' experimental plan. **B.** Representative Western blot images of phospho-Akt (S473) and phospho-ERK over GAPDH in skeletal muscles after iron injection followed by i.p. insulin injection with and without salubrinal injection. **C.** Quantification of phospho-Akt (S473) over GAPDH in skeletal muscles after iron injection followed by i.p. insulin injection with and without salubrinal injection. Values are mean ± s.e.m (n=5) ***P < 0.0005 #P < 0.0001 (one-way ANOVA with multiple comparisons). **D.** Quantification of phosphor ERK over GAPDH in skeletal muscles after iron injection followed by i.p. insulin injection with and without salubrinal injection. Values are mean ± s.e.m (n=5) ***P < 0.0005 #P < 0.0001 (oneway ANOVA with multiple comparisons). **E.** Representative Western blot images of phospho-eIF2α and ATF4 over GAPDH in skeletal muscles after iron injection followed by i.p. insulin injection with and without salubrinal injection. **F.** Quantification of phospho- eIF2α over GAPDH in skeletal muscles after iron injection followed by i.p. insulin injection with and without salubrinal injection. Values are mean ± s.e.m (n=5) **P < 0.005 ***P < 0.0005 (one-way ANOVA with multiple comparisons). **G.** Quantification of ATF4 over GAPDH in skeletal muscles after iron injection followed by i.p. insulin injection with and without salubrinal injection. Values are mean ± s.e.m (n=5) **P < 0.005 #P < 0.0001 (one-way ANOVA with multiple comparisons).

Autophagy plays a key role in mediating the beneficial effect of salubrinal on insulin sensitivity

To test whether autophagy is critical for the beneficial effect of salubrinal in alleviating insulin sensitivity, the loss of function approach was used by generating two autophagy- deficient

cellular models: overexpression of a dominant-negative ATG5K130R mutant and knockout of ATG7.

Analysis of insulin sensitivity by western blotting (Fig 8) demonstrated that iron-impaired insulin sensitivity could be attenuated by salubrinal in cells transfected with empty vector but not in autophagy-deficient ATG5K130R overexpressing cells (Fig 8 A&B). Similarly, knockout of ATG7 effectively blocked the capacity of salubrinal to rescue insulin sensitivity (Fig 8 C&D). Taken together, my results suggest that induction of autophagy flux by salubrinal is essential to alleviate IO-induced ER stress and insulin resistance in L6 skeletal muscle cells.

Figure 8. Role of autophagy in beneficial effect of salubrinal

A. Representative Western blot images and quantification of phospho-Akt (S473) over total Akt in EV and ATG5 cells with insulin stimulation (100 nM, 10 min) after iron treatment (250 μM, 24 h) with and without salubrinal pretreatment (30 μM, 30 min). Values are mean ± s.e.m (n=3) *P < 0.05 ***P < 0.0005 (one-way ANOVA with multiple comparisons). **B.** Representative Western blot images and quantification of phospho-ERK over GAPDH in EV and ATG5 cells with insulin stimulation (100 nM, 10 min) after iron treatment (250 μM, 24 h) with and without salubrinal pretreatment (30 μM, 30 min). Values are mean ± s.e.m (n=3) *P < 0.05 (one-way ANOVA with multiple comparisons). **C.** Representative Western blot images and quantification of phospho-Akt (S473) over total Akt in L6 and ATG7 cells with insulin stimulation (100 nM, 10 min) after iron treatment (250 μM, 24 h) with and without salubrinal pretreatment (30 μM, 30 min). Values are mean ± s.e.m (n=3) *P < 0.05 (one-way ANOVA with multiple comparisons). **D.** Representative Western blot images and quantification of phospho-ERK over GAPDH in L6 and ATG7 cells with

insulin stimulation (100 nM, 10 min) after iron treatment (250 μM, 24 h) with and without salubrinal pretreatment (30 μM, 30 min). Values are mean ± s.e.m (n=3) *P < 0.05 **P < 0.005 (one-way ANOVA with multiple comparisons).

Figure 8

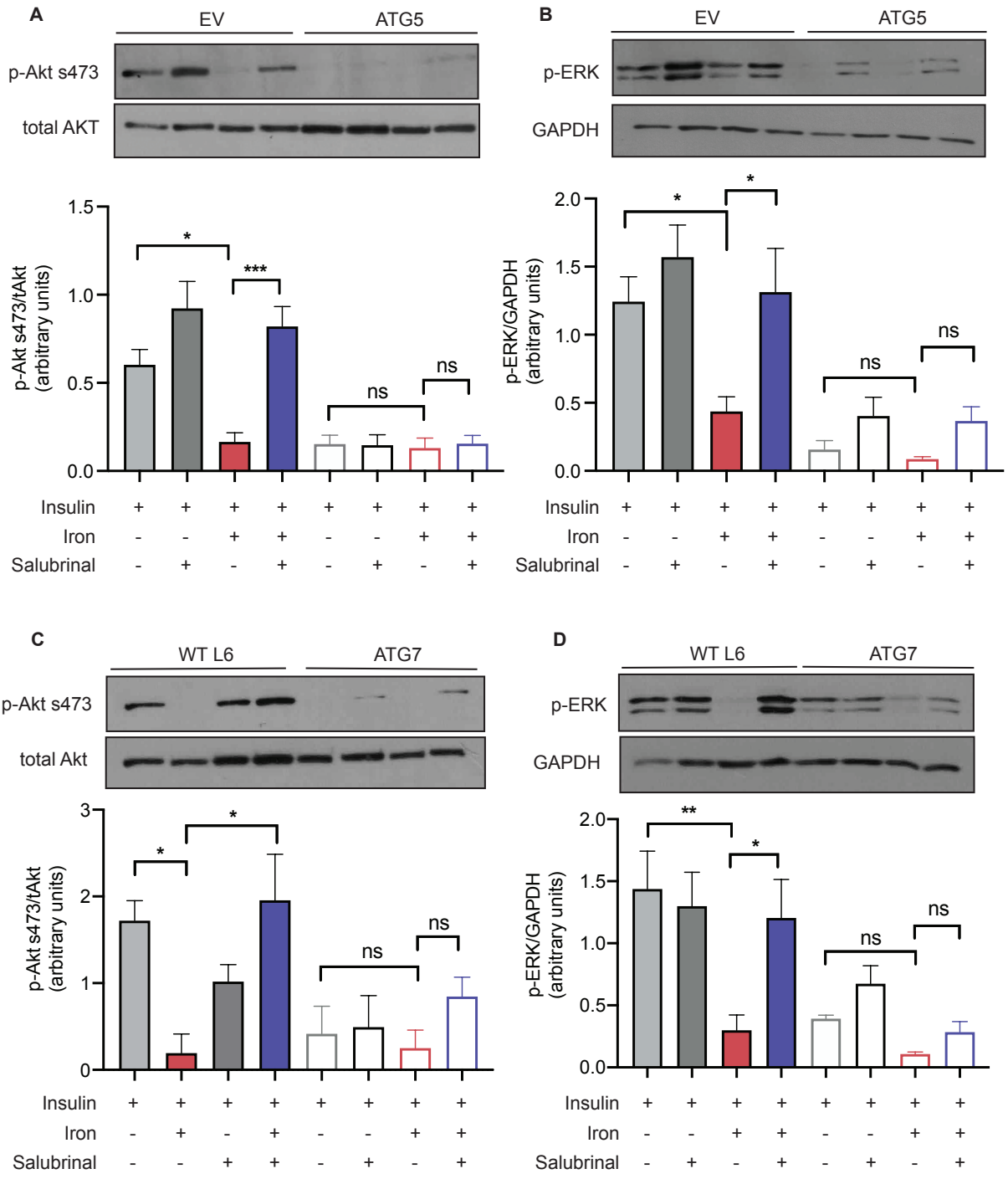
A
EV
ATG5
p-Akt s473
total AKT
p-Akt s473/tAkt (arbitrary units)
1.5
1.0
0.5
0.0
*
***
ns
ns
Insulin + + + + + + + +
Iron - - + + - - + +
Salubrinal - + - + - + - +
B
EV
ATG5
p-ERK
GAPDH
p-ERK/GAPDH (arbitrary units)
2.0
1.5
1.0
0.5
0.0
*
*
ns
ns
Insulin + + + + + + + +
Iron - - + + - - + +
Salubrinal - + - + - + - +
C
WT L6
ATG7
p-Akt s473
total Akt
p-Akt s473/tAkt (arbitrary units)
3
2
1
0
*
*
ns
ns
Insulin + + + + + + + +
Iron - + - + - - + +
Salubrinal - - + + - + - +
D
WT L6
ATG7
p-ERK
GAPDH
p-ERK/GAPDH (arbitrary units)
2.0
1.5
1.0
0.5
0.0
**
*
ns
ns
Insulin + + + + + + + +
Iron - - + + - - + +
Salubrinal - + - + - + - +

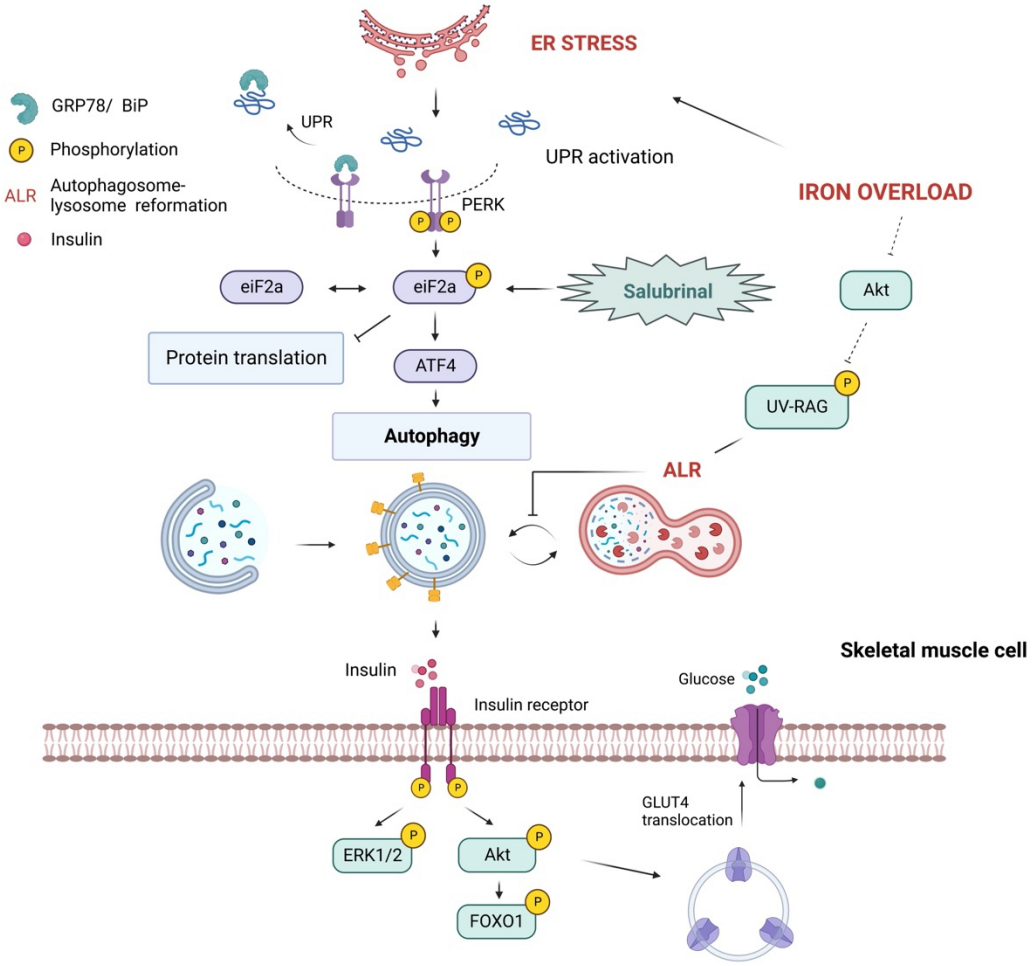

Figure 9. Schematic diagram of ER- stress induced iron overload leading to insulin resistance Iron-overload causes ER stress in L6 skeletal muscle cells and the subsequent UPR activation. Iron-overload also causes impaired autophagic flux through impaired autophagosome lysosome reformation (ALR). This ALR defect leads to insulin resistance in L6 skeletal muscle cells. Salubrinal, an eIF2α phosphatase inhibitor, induces UPR activation, specifically the eIF2α and

ATF4 pathway, resulting in improved autophagic flux and insulin sensitivity, both in the presence and absence of iron.

2.5 Discussion

Iron homeostasis imbalance is still a somewhat underappreciated contributor to various diseases, including cancer, inflammation, neurodegenerative diseases, and most notably cardiometabolic dysfunction [192]. Indeed, a dysmetabolic iron overload syndrome (DIOS) has been defined since elevated iron levels are observed in 15% of metabolic syndrome patients and in half of those with non-alcoholic fatty liver disease (NAFLD) [193,194]. Nevertheless, the precise mechanisms linking iron overload with such adverse metabolic outcomes remain to be fully understood.

Of particular relevance for this study is the impact of iron overload on skeletal muscle. Iron overload can lead to skeletal muscle atrophy, sarcopenia, reduced power and performance, and has been implicated in muscular dystrophy [195-198]. It has been proposed that in addition to direct metabolic effects, iron overload in skeletal muscle may also impact its endocrine function [199]. Collectively, this means that excess iron on skeletal muscle can impact a wide array of pathophysiological outcomes. Previous study has shown that iron overload induced insulin resistance both in mice and cultured skeletal muscle cells [75]. This involved a decrease in Akt mediated repression of TSC2, resulting in a potent repression of RHEB and mTORC1, with consequent loss of autophagosome lysosome reformation (ALR). This identified mTOR-UVRAG dependent lysosomal pool regeneration as a determinant of skeletal muscle insulin sensitivity and demonstrated an important role for autophagic flux in improving insulin sensitivity. Other studies have documented the association of autophagy and insulin sensitivity, with strategies to promote

autophagy flux conferring improved responsiveness [191][200-205]. Thus, inhibition of autophagy is an important means via which iron attenuates insulin sensitivity.

Several previous studies using models from yeast to mammalian cells and tissues have shown, as I did here, that iron could cause endoplasmic reticulum stress [206, 207]. For example, in mouse hippocampal neuronal cells iron induced ER stress leading to mitochondrial fragmentation and neuronal cell death [208]. Lipocalin-2 mediated iron accumulation in pulmonary arterial smooth muscle cells and hypoxia-induced iron accumulation in oligodendrocytes both led to ER stress [209,210]. Induction of ER stress led to insulin resistance in L6 and C2C12 skeletal muscle cells [211,212], murine preadipocytes [213], hepatocytes [214], and was associated with reduced insulin sensitivity in db/db mice [215]. Upregulation of tribbles 3 (TRB3) and inhibition of the skeletal muscle-enriched inositol polyphosphate phosphatase (SKIP) with suppression of insulin receptors' transportation to the cell surface are potential mechanistic pathway linking ER stress and insulin resistance [216-218]. Strategies to counteract cellular ER stress, either endogenous homeostatic mechanisms or therapeutic interventions, are clearly of widespread potential benefit.

To alleviate ER stress and restore optimal homeostasis, an endogenous cellular response is activation of the UPR which can lead to corrective mechanisms including suppressing protein translation, inducing the production of molecular chaperones involved in protein folding and degrading misfolded proteins via routes such as induction of autophagy. A study in 3T3-L1 adipocytes suggested that induction of autophagy by UPR was important for maintenance of insulin sensitivity [219]. One of the three main branches of the UPR involves the eukaryotic translation

initiation factor 2 alpha (eIF2α) [220, 221]. In this study I found that iron induced UPR activation, as observed by an increase in the expression of the GRP78 promoter-dependent fluorescent reporter. My results were corroborated with western blot analysis showing an increase in phosphorylation of eIF2α and increased ATF4. However, although UPR was induced in response to iron, I found that the normal increase in autophagy flux in response to UPR activation was prevented by iron. Thus, via ALR attenuation, iron effectively suppressed a critical endogenous corrective cellular response which is designed to restore insulin sensitivity.

Exercise has been proposed as a potential means of promoting autophagy to alleviate ER stress and increase insulin sensitivity [222]. Effects of exercise are variable, and I contend a more direct and controlled route would be advantageous. eIF2α can be activated using salubrinal, a small molecule protein phosphatase 1C inhibitor which maintains eIF2α phosphorylation. Via enhancing PERK/ eIF2α/ATF4 signaling, salubrinal has been suggested as a potential therapeutic approach for hypoxia-induced retinal microangiopathy, neuroprotection and in cerebral ischemia [223-227]. In my study I found in the L6 cell model that salubrinal stimulated eIF2α-mediated induction of autophagy and that this attenuated the extent of insulin resistance caused by iron. Furthermore, administration of salubrinal to mice before systemic injection of iron could attenuate development of insulin resistance in skeletal muscle. These data validate, using a pharmacological approach, the potential of therapeutically targeting eIF2α to promote improved insulin sensitivity. It should also be noted that $eIF2\alpha^{S/A}$ mice, which exhibit defective eIF2α phosphorylation [228] would offer another powerful tool to further validate the role of UPR and autophagy in the context of insulin resistance.

In summary, I have established that skeletal muscle cells treated with iron or skeletal muscle of mice with iron overload develop ER stress and insulin resistance. By virtue of also suppressing autophagy, iron prevents the ability of endogenous UPR to enhance autophagic flux and restore cellular homeostasis. I found that directly promoting eIF2α-dependent activation of UPR and autophagy with salubrinal prior to iron exposure could attenuate development of insulin resistance. New knowledge from this study identifies the potential use of salubrinal to improve insulin sensitivity in metabolic syndrome patients with iron overload.

CHAPTER 3: STUDY 2

"ALY688 improves insulin sensitivity following iron overload via activation of autophagic flux"

3.1 Abstract

Iron overload (IO) is a common contributing factor to complications in MetS including insulin resistance. Since skeletal muscle is responsible for over three-quarters of whole-body insulin initiated glucose disposal, it is important to understand how skeletal muscle's resistance to insulin develops. Among the contributors to insulin resistance are oxidative stress and impaired autophagy, both of which are closely linked to endoplasmic reticulum (ER) stress. This project probed insulin sensitivity in skeletal muscle cells when subjected to high doses of iron and with a mechanistic focus on ER stress and the unfolded protein response. I found that the adiponectin receptor agonist ALY688 could prevent insulin resistance in L6 skeletal muscle cells following iron overload. This conclusion was based on western blot of pAkt s473 and pERK showing that 24-hour pre-treatment of ALY688 attenuated iron-induced inhibition of insulin signaling. An Akt biosensor system tracing the nuclear fluorescent signal of Foxo1 was also used to analyze the kinetics of insulin sensitivity in real-time, where FoxO1 translocation was observed in cells treated with ALY688 but not iron. Iron overload caused ER stress, a corresponding activation of UPR, but with inhibition of autophagic flux. Autophagic flux was significantly upregulated upon pre-treatment with ALY688. Indeed, the beneficial effects of ALY688 were autophagy-dependent since the ability to protect against iron-induced insulin resistance was not observed in autophagy deficient cell lines. My results show that iron overload induced ER stress and impaired autophagic flux, leading to insulin resistance. These were attenuated when an adiponectin mimetic was used

to induce autophagy. My work suggests the strong need for autophagy inducing therapeutics, which would promote insulin sensitivity and provide more favorable clinical outcomes.

3.2 Introduction

Iron is an essential element that is involved in various biological processes [229,230]. Maintaining balanced iron levels helps to prevent the onset of certain diseases, since too much or too little iron can have detrimental effects on the body. From the pathological perspective, iron overload contributes to leukemia, cirrhosis, heart failure, or endocrine dysfunction [231-234]. Most importantly, iron overload is a risk factor for insulin resistance, which may lead to diabetic conditions, as shown in cases of patients diagnosed with hemochromatosis and thalassemia [235-236].

Insulin resistance occurs when cells do not respond effectively to insulin. It is linked to a variety of diseases and serious health conditions, including type 2 diabetes and heart failure. Despite its importance, the molecular mechanisms of insulin resistance are not fully understood. Among the contributors to insulin resistance are impaired autophagy and oxidative stress, both of which are closely linked to endoplasmic reticulum (ER) stress.

ER stress is a cellular condition that stems from changes in the function of ER, which leads to the unfolded protein response (UPR) as an adaptive mechanism to maintain cell viability and function. Once initiated, the UPR will lead to the activation of three transmembrane proteins that help improve cellular homeostasis by elevating the ER protein-folding capacity, reducing global protein translation, and promoting ER-associated degradation (ERAD). Upon activation, protein kinase RNA-like ER kinase (PERK) will generate a cascade of signal transduction that phosphorylates eukaryotic translation initiation factor (eIF2α), while its downstream initiates transcription factor 4 (ATF4). These transcription factors help the ER maintain its homeostasis states by inhibiting

global translation levels on the one hand, and activating autophagic responses on the other [128], [131-133]. Working in parallel with the PERK sensor is inositol requiring enzyme 1 (IRE1). By employing the unique mRNA splicing mechanisms, this transmembrane protein helps alleviate ER stress. Upon induction, IRE1 excises the intron regions of X-box binding protein 1 (XBP1), resulting in the formation of its spliced form called s-XBP1. This transcription factor improves cellular homeostasis by mediating lipid biosynthetic enzymes and ER-associated degradation constituents. In addition, it enhances the formation of an elaborate ER that is characteristic of active secretory cells [133]. When ER stress persists, however, autophagy becomes the final means to restore cellular balance.

Adiponectin, an adipocyte- derived hormone, is well known to exert insulin sensitizing effects in diabetic patients [237]. These include facilitating glucose levels, lipid metabolism and insulin sensitivity through its anti-inflammatory and antioxidant benefits [105-107]. Adiponectin promoted insulin sensitivity through upregulating hepatic IRS-2 expression via an IL-6 dependent pathway [107]. Adiponectin-KO mice have shown to develop impaired glucose transport, insulin resistance, inflammation, and subsequent diabetes [108-111], while adiponectin replenishment could reverse insulin resistance and metabolic syndrome in models of T2D [112-114]. In addition, previous studies have emphasized the role of adiponectin in stimulating autophagic flux via activation of AMPK pathway that leads to phosphorylation of ULK1 (Ser 555), an initiating factor of autophagy [238-241]. The interplay between iron, ER stress, and autophagy in regulating adiponectin' s insulin sensitizing effects are not fully studied. Due to its correlation with certain metabolic conditions, targeting adiponectin as a prospective therapeutic treatment is of potential benefits.

In this project, I established a cellular model of iron overload in skeletal muscle cells. I combined this together with pre-treatment with or without the adiponectin receptor agonist ALY688. Here, it was hypothesized that ALY688 acts on both the autophagic and unfolded protein response activation pathways to prevent iron overload- induced insulin resistance. An autophagy deficient cell line model based upon the Atg7 gene knock out was also generated to validate the functional significance of autophagy in adiponectin action and prevention of insulin resistance upon iron overload.

3.3 Materials and methods

Cell culture and maintenance of L6 skeletal muscle cells

L6 rat skeletal muscle cell line was grown in alpha-minimum essential medium (AMEM) (Wisent; #210-010) supplemented with 10% fetal bovine serum (FBS) (Wisent; #080-150) and 1% antibiotic/antimycotic (Gibco; #15240062) at 37°C with 95% air and 5% CO_2. Cells were maintained in 75 cm^2 flasks and passed at 70% confluency. For iron treatment, iron (II) sulfate heptahydrate (Sigma-Aldrich; #215422) was prepared by dissolving in sterile distilled water with the stock concentration of 100 mM. ALY688 was from Allysta Pharmaceuticals, with stock concentration being 100 μM. The working concentration for ALY688 is 300nM and the drug is diluted in AMEM supplemented with 0.5% FBS. A cellular model of autophagy inhibition was established by using CRISPR to delete Atg7 in skeletal muscle cells, as previously described.

Western blotting

L6 cells were seeded on 6- well plates until having 80-90% confluency. Cells were subjected to treatments of $FeSO_4$ 250 μM for 24-h followed by insulin 100 nM (Lilly; Humulin-R U-100) for 10 min. Iron-treatment cells were treated with $FeSO_4$ in AMEM 0.5% FBS for 24-h, while control groups were grown in AMEM 0.5% FBS after reaching 70% confluency. For ALY688 groups, cells were pretreated with the drug at the working concentration of 300 nM in AMEM 0.5% FBS for 24-h, followed by with and without another 24-h of iron treatment. After treatment time, proteins were extracted according to protocol mentioned in section 2.3. To analyze insulin signaling markers, 2 primary antibodies were used: phospho-Akt ser473 (Cell Signaling; #9271)

and phospho-ERK thr202/tyr204 (Cell Signaling; #9106L) with the dilutions of 1:1000. The secondary antibody used was an anti-rabbit immunoglobulin G horseradish peroxidase-conjugated antibody (Cell Signaling; #7074) for phospho-Akt s473 and anti-mouse antibody (Cell Signaling; #7076) for phospho- ERK at 1:5000 dilution. Western blot band intensity was quantified using ImageJ software, normalized to total Akt (Cell Signaling; #9272) or glyceraldehyde 3-phosphate dehydrogenase (GAPDH) (Cell Signaling; #2118).

To examine the role of iron and ALY688 in activating UPR, western blotting was performed according to protocol aforementioned (section 2.3). 2 primary antibodies were used in this assay including p-eIF2α (Cell Signaling; #9721) and IRE1-alpha (Ser724) (Novus Biologicals; #NB1002323) with dilutions as described in section 2.3.

To assess the effects of iron and ALY688 treatments on autophagic flux, L6 skeletal muscle cells were seeded on 6 well plates until reaching 80-90% confluency. 4 groups of treatment were performed including control, iron, ALY688 and ALY688 iron. For iron- treated samples, cells were subjected to treatments of $FeSO_4$ 250 μM in AMEM supplemented with 0.5 % FBS for 16 h, while control cells were treated in AMEM 0.5% FBS alone. For ALY688 groups, cells were pretreated with ALY688 300 nM for 24 h prior to with and without iron treatment 16-h. Western blot analysis was performed according to section 2.3. 2 primary antibodies were used in this assay including LC3B (Cell Signaling; #2775) and SQSTM1/p62 (Cell Signaling; #5114).

ATG7 knock out cell lines were used as molecular models to assess the role of autophagy in beneficial effects of ALY688. Wild-type L6 cells were used as controls. Cells were seeded on 6

well plates until having 80-90% confluency. 4 treatment groups were determined including insulin, iron insulin, ALY688 insulin and ALY688 iron insulin. Cells were subjected to treatments of

$FeSO_4$ 250 μM in AMEM 0% FBS for 24-h. For ALY688 groups, cells were pre-treated with ALY688 300 nM for 24 h prior to with and without 24 h iron treatment. All samples were stimulated with insulin 100 nM for 10 min after treatment time. Western blot analysis was performed according to protocol aforementioned with 2 primary antibodies being used were phospho-Akt s473 and phospho-ERK.

Real-time imaging of insulin signaling using an Akt biosensor

L6 cells transfected to stably overexpress an Akt biosensor were generated according to section 2.3 were seeded onto a 96-well plate for treatment. When cells reached 50-60% confluency, they were subjected to 5 groups of treatment including control, insulin, iron insulin, ALY688 insulin and ALY688 iron insulin. For the iron treatment samples, cells were treated with $FeSO_4$ 250 μM overnight. For the ALY688 treatment groups, cells were pretreated with ALY688 300 nM for 24 h prior to with or without overnight iron treatment. All treatments were performed using AMEM 0% FBS media. After incubation time, cells in all treatment groups were washed and starved in 0% FBS AMEM for 90 min, then treated with 100 nM insulin and imaged on EVOS FL Auto 2 for green fluorescence over a span of 30 min to observe fluorescent translocation. Nuclear fluorescence signal was traced from the nucleus to the cytosol in all treatments with number of cells being 10 for each time point and treatment. Automated data quantitation was performed using Celleste software.

Insulin sensitivity measured by glucose uptake assay

L6-GLUT4myc cells were seeded on 96-well plate at 10,000 cells/ well before treatment. Cells were then treated with the following conditions: control, iron, ALY688, ALY688 iron (all stimulated with and without insulin 100nM). Treatment was performed according to protocol in chapter 2.3). After 24 h treatment, 2DG6P detection reagent was added and luminescence was recorded using Varioskan LUX.

ThT staining assay

L6 skeletal muscle cells were seeded at 70% confluency on a µ-slide 4-well chambered polymer coverslip, and the growth medium was then replaced with 0% FBS AMEM (Phenol-red free) for control groups, and with $FeSO_4$ treatment (250 µM) for 4 h for iron groups. ALY688 was pretreated for 24 h followed by with and without iron 4 h treatment. After treatment, Tht solution was prepared in phenol-red free DMEM media 0% FBS and cells were stained for 30 min. After staining time, cells were imaged, and analysis was performed as previously described in chapter 2.3.

Gene expression analysis

Total RNA was extracted with RNEasy Mini Kit and then converted to cDNA using the RevertAid RT Kit. qPCR was performed according to previously mentioned protocol (chapter 2.3). Relative gene expression levels were normalized to 18S rRNA. Primers used in this study are summarized in Table 1.

Statistical analysis

One-way ANOVA test with turkey's multiple comparisons was carried out on GraphPad Prism to determine statistical significance in which p values < 0.05 were considered significant.

3.4 Results

ALY688 pre-treatment prevented iron-induced ER stress in L6 skeletal muscle cells

Iron overload is an important contributor to impaired insulin sensitivity, yet its effects on ER stress is not clearly elucidated in skeletal muscle cells. To investigate this, Tht assay which stains for protein aggregates, a hallmark of ER stress, was employed. In this experiment, skeletal muscle cells were treated with and without $FeSO_4$ 250uM for 4 hours. Thioflavin T dye as a probe was used to monitor misfolded protein accumulation in cells. Cells imaged after 4h- treatment (Fig 10) showed that fluorescence was observed in iron overload conditions, indicating the elevation of ER stress in L6 cells upon iron overload. However, protein aggregation was not enhanced by iron upon pre-treatment with ALY688, indicative of its ability to prevent ER stress upon iron overload.

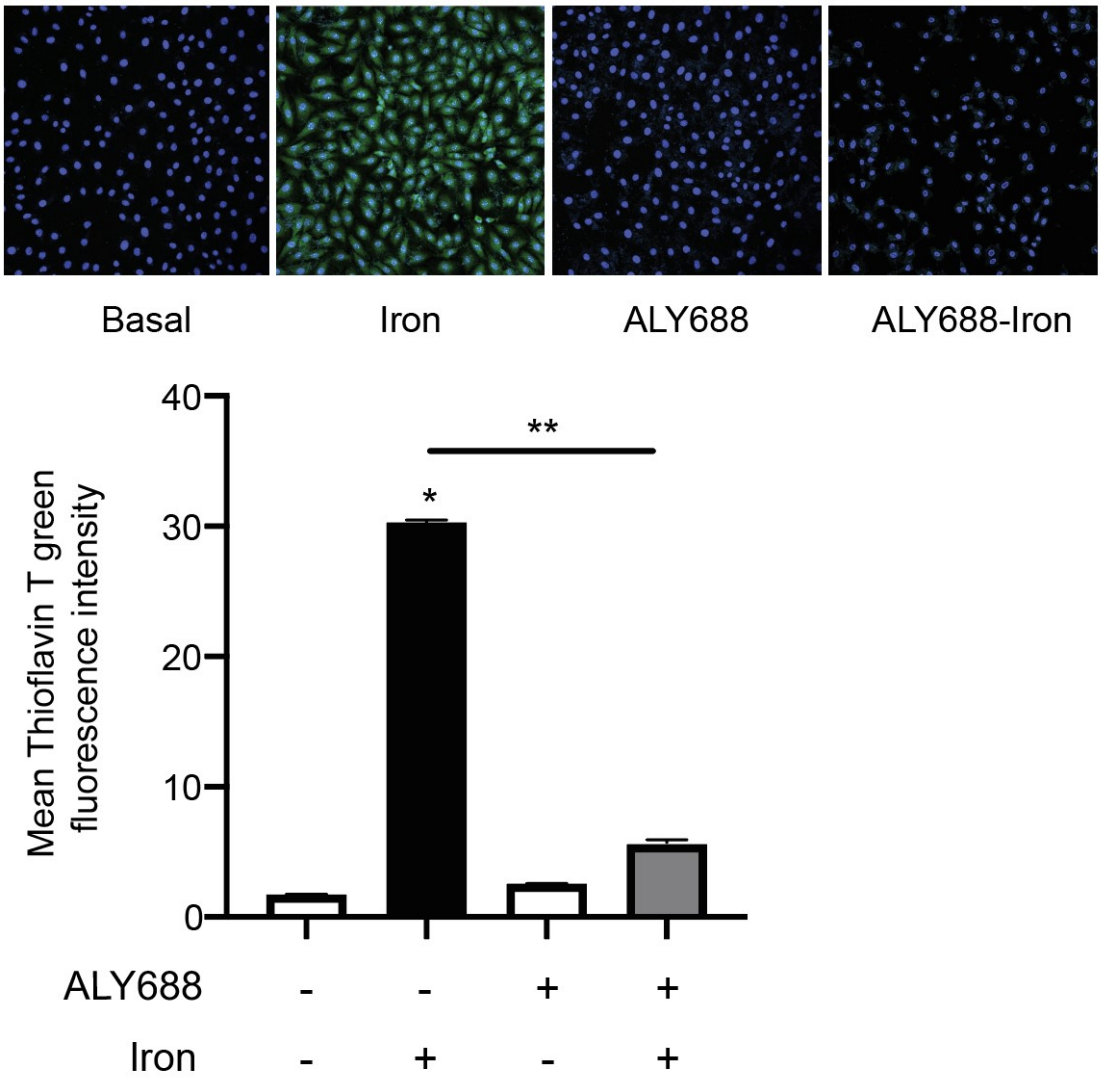

Figure 10: Effect of iron overload and ALY688 on ER stress

Representative confocal images and quantification of Tht assay measuring protein aggregates in skeletal muscle cells after iron treatment ($FeSO_4$, 250 uM, 4 h), with and without ALY688 pre-treatment (300nM, 24 h) compared to control. Values are mean ± s.e.m (n=3) *P < 0.05 **P < 0.005 (one-way ANOVA with multiple comparisons).

UPR activation was induced upon iron overload and ALY688 treatment

To validate the role of ALY688 in mitigating ER stress upon iron overload, analysis of western blotting was carried out. My results demonstrated that ALY688 induced a significant upregulation in phosphorylation of eIF2α and IRE1 (Fig 11 A & B), confirming the activation of UPR pathway. In addition, the downstream target of IRE1, spliced-xbp1 was assessed by quantitating mRNA expression levels. In accordance with my western blotting analysis, qPCR results demonstrated a significant upregulation in response to ALY688 pre-treatment (Fig 11C), both in the presence and absence of iron overload, further confirming induction of the UPR. This result suggested ALY688 exerted its beneficial effects in ER stress response in both branches of the UPR.

Figure 11

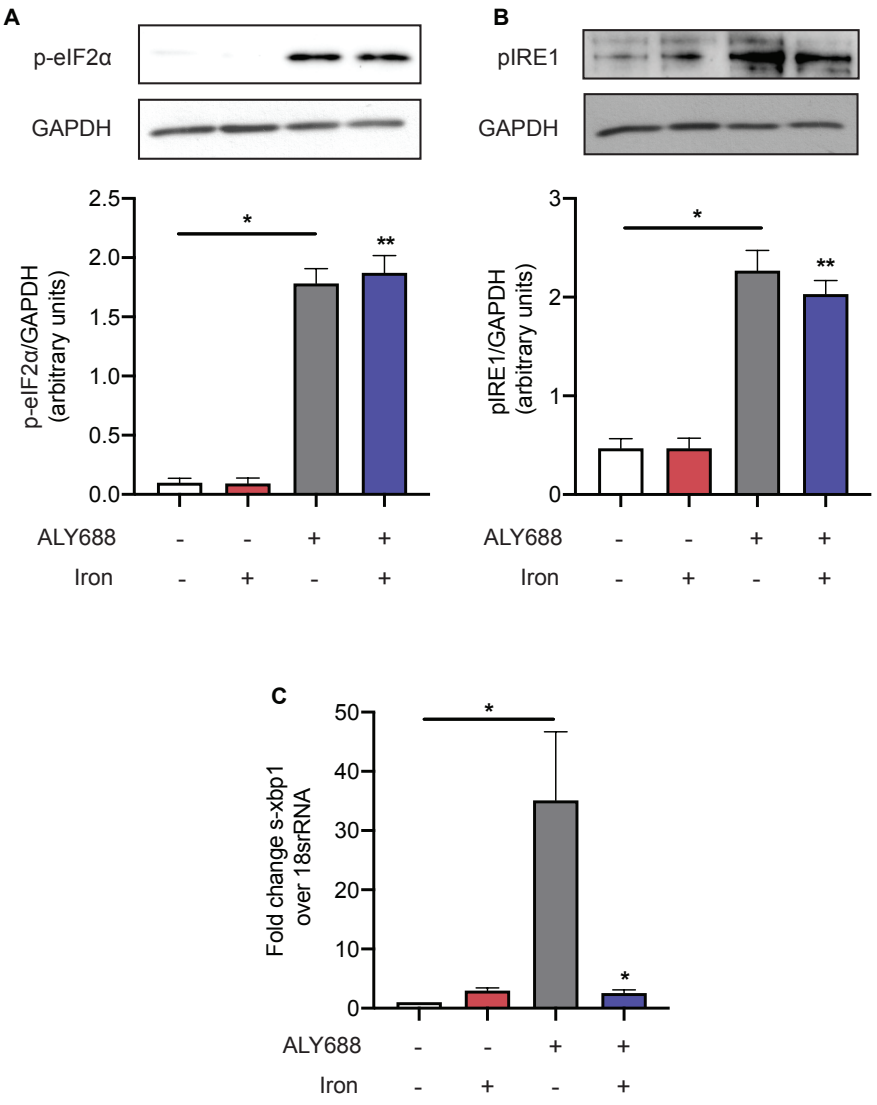
A
p-eIF2α
GAPDH
p-eIF2α/GAPDH (arbitrary units)
2.5
2.0
1.5
1.0
0.5
0.0
*
**
ALY688 - - + +
Iron - + - +
B
pIRE1
GAPDH
pIRE1/GAPDH (arbitrary units)
3
2
1
0
*
**
ALY688 - - + +
Iron - + - +
C
Fold change s->xbp1 over 18srRNA
50
40
30
20
10
0
*
*
ALY688 - - + +
Iron - + - +

Figure 11. Effect of iron overload and ALY688 on UPR activation **A.** Representative Western blot images and quantification of phospho- eIF2α over GAPDH after iron treatment (250 uM, 24 h), with and without ALY688 treatment (300nM, 24 h). Values are mean ± s.e.m (n=3) *P < 0.05 (one-way ANOVA with multiple comparisons). **B.** Representative Western blot images and quantification of p-IRE1 over GAPDH with after iron treatment (250 uM, 24 h), with and without ALY688 pre-treatment (300nM, 24 h). Values are mean ± s.e.m (n=3) *P < 0.05 (one-way ANOVA with multiple comparisons). **C.** Relative gene expression of spliced X-box binding protein 1 (sXBP1) normalized to 18S rRNA expression upon iron treatment (250 uM, 24 h) with and without ALY688 pre-treatment (300nM, 24 h). Values are mean ± s.e.m (n=3) *P < 0.05 (one-way ANOVA with multiple comparisons).

ALY688 pre-treatment prevented iron overload- induced insulin resistance in L6 skeletal muscle cells

ALY688, an inducer of autophagy, was used as the treatment to clarify the relationship between iron overload and insulin resistance through the unfolded protein response pathway. Insulin sensitivity was first assessed by western blot analysis. Results showed that a significant decrease in phosphorylation of ERK and Akt s473 upon iron treatment, demonstrating that insulin response in L6 cells was significantly impaired upon iron overload (Fig 12 A & B), recapitulating the observations from chapter 2 of my thesis. The insulin-sensitizing effect of ALY688 was then examined both in the presence and absence of 24-h iron treatment. Upon ALY688 treatment, L6 cells' insulin response in both phosphorylation of ERK and Akt at serine 473 was elevated, suggesting that ALY688 could prevent insulin sensitivity upon iron overload.

Insulin kinetics was then analyzed by employing the sleeping beauty transposase system to generate Akt biosensor expressing L6 cells. Representative images of cells visually reflected the

difference in the nuclear fluorescent intensity over a span of 20 mins (Fig 12C). Results suggested that Akt activity was significantly activated in cells treated with insulin compared to the control cells. Iron-insulin treated cells also reflected a significant decrease in FoxO1 phosphorylation compared to that of insulin treatment alone, indicating that iron treatment induced insulin resistance in L6 skeletal muscle cells. Upon pre-treatment with ALY688, however, insulin resistance was prevented as seen by a corresponding increase in Akt activity in comparison with iron-insulin treatment. This observation was in accordance with my western blotting analysis (Fig 12D & E). To corroborate my results, glucose uptake was observed. GLUT4- myc cells were treated with the same conditions as in my western blot assay including control, iron, ALY688 and ALY688 with iron (cells were stimulated with and without insulin 100nM). In control conditions, there was a marked increase in glucose uptake in response to insulin stimulation, which meant the assay was reliable. Consequently, a significant reduction in glucose uptake was observed in 24h iron overload- treated cells. In accordance with salubrinal treatment, ALY688 induced an apparent elevation in glucose uptake, indicative of its capacity in promoting L6 cells' insulin response, both in the presence and absence of iron treatment (Fig 12F). Together, these results confirmed the detrimental effects of iron overload on skeletal muscle cells' insulin response and the beneficial role of ALY688 in attenuating insulin resistance.

Figure 12

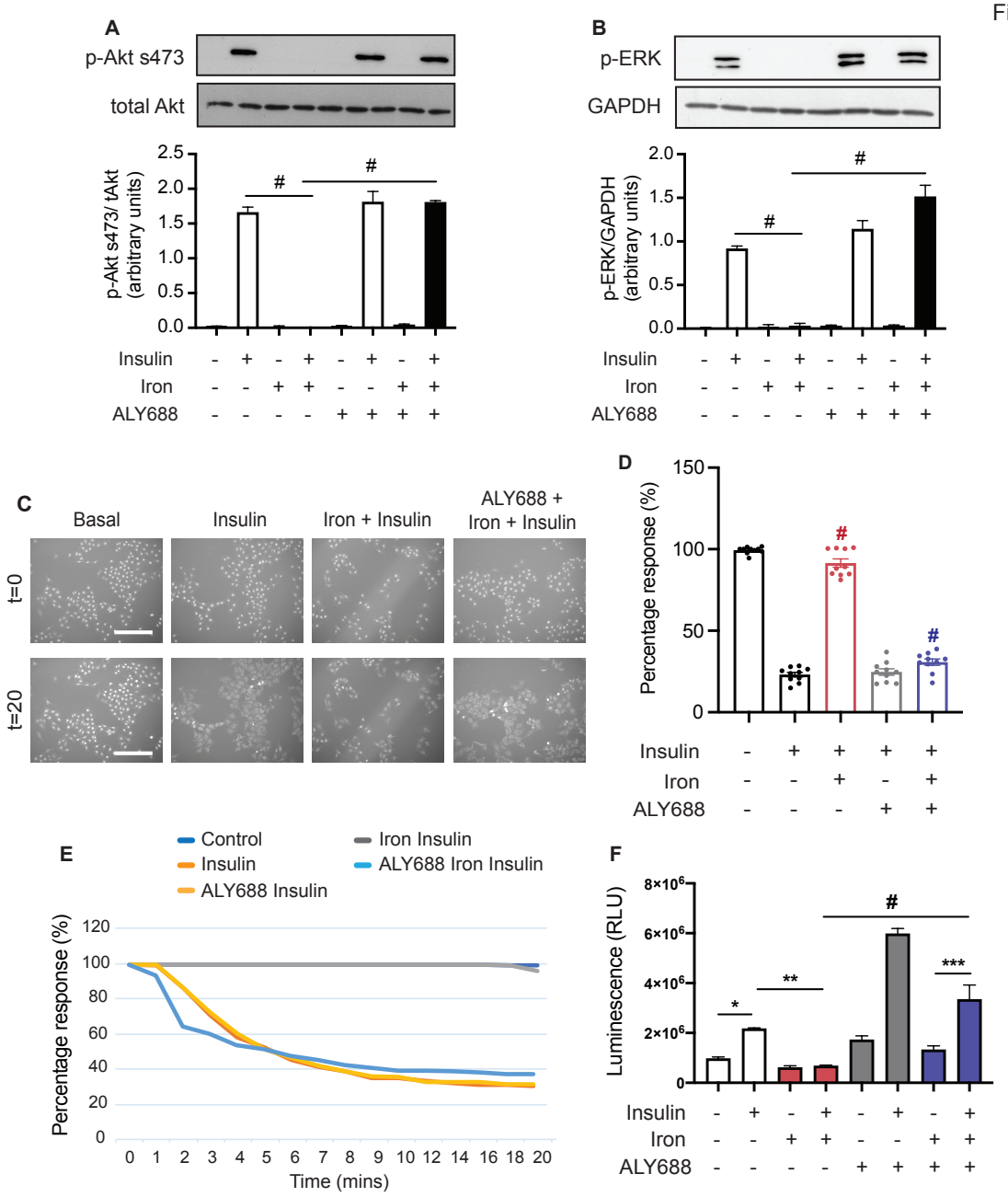
A
p-Akt s473
total Akt
p-Akt s473/ tAkt (arbitrary units)
Insulin
Iron
ALY688
B
p-ERK
GAPDH
p-ERK/GAPDH (arbitrary units)
C
Basal
Insulin
Iron + Insulin
ALY688 + Iron + Insulin
t=0
t=20
D
Percentage response (%)
E
Control
Insulin
ALY688 Insulin
Iron Insulin
ALY688 Iron Insulin
Percentage response (%)
Time (mins)
F
Luminescence (RLU)

Figure 12. Effect of iron overload and ALY688 on insulin sensitivity **A.** Representative Western blot images and quantification of phospho-Akt (S473) over total Akt with insulin stimulation (100 nM, 10 min) after iron treatment (250 uM, 24 h) with and without aly688 pre-treatment (300nM, 24 h). Values are mean ± s.e.m (n=3) #P < 0.0001 (one-way ANOVA with multiple comparisons). **B.** Representative Western blot images and quantification of phospho-ERK over GAPDH with insulin stimulation (100 nM, 10 min) after iron treatment (250 uM, 24 h) with and without ALY688 pre-treatment (300nM, 24 h). Values are mean ± s.e.m (n=3) #P < 0.0001 (one-way ANOVA with multiple comparisons). **C.** Representative microscope images of biosensor cells recorded at timepoints t=0 and t=20 (min) with insulin stimulation (100 nM, 10 min) after iron treatment (250 µM, 24 h) with and without ALY688 pre-treatment (300 nM, 24 h) All experiments were repeated three times. **D.** Percentage response (%) of green fluorescent signal in biosensor cells (n=10) recorded for a time course of 20 min with insulin stimulation (100 nM) after iron treatment (250 µM, 24 h) with and without ALY688 pre-treatment (300 nM, 24 h). Values are mean ± s.e.m #P < 0.0001 (one-way ANOVA with multiple comparisons). **E.** Percentage change of green nuclear fluorescent signal in biosensor cells (n=10) recorded for a time course of 20 min with insulin stimulation (100 nM, 10 min) after iron treatment (250 µM, 24 h) with and without ALY688 pre-treatment (300 nM, 24 h). Percentage change was recorded as mean values. **F.** Glucose uptake of L6 cells with insulin stimulation (100 nM, 20 min) after iron treatment (250 uM, 24 h) with and without ALY688 pre-treatment (300nM, 24 h). Values are mean ± s.e.m. *P < 0.05 **P < 0.005 ***P < 0.0005 #P < 0.0001 (one-way ANOVA with multiple comparisons).

Initiation of autophagy is upregulated in L6 skeletal muscle cells upon iron and ALY688 treatment

Next, various well-established assays were employed to examine different stages of autophagy. The importance of autophagy as a mechanism through which ALY688 could enhance IO induced-insulin resistance was first accessed, by performing qPCR against autophagy-related gene 5 (ATG5), autophagy-related gene 10 (ATG10), autophagy-related gene 12 (ATG12), autophagy related gene 16 (ATG16) and unc-51 like autophagy activating kinase 1 (ULK1). qPCR data showed that ALY688 alone significantly increased the expression of ATG5, ATG12, ATG16 and ULK1 compared to basal, and this effect was also observed in combination with iron overload, indicating upregulation of initiation of autophagy (Fig 13).

Figure 13

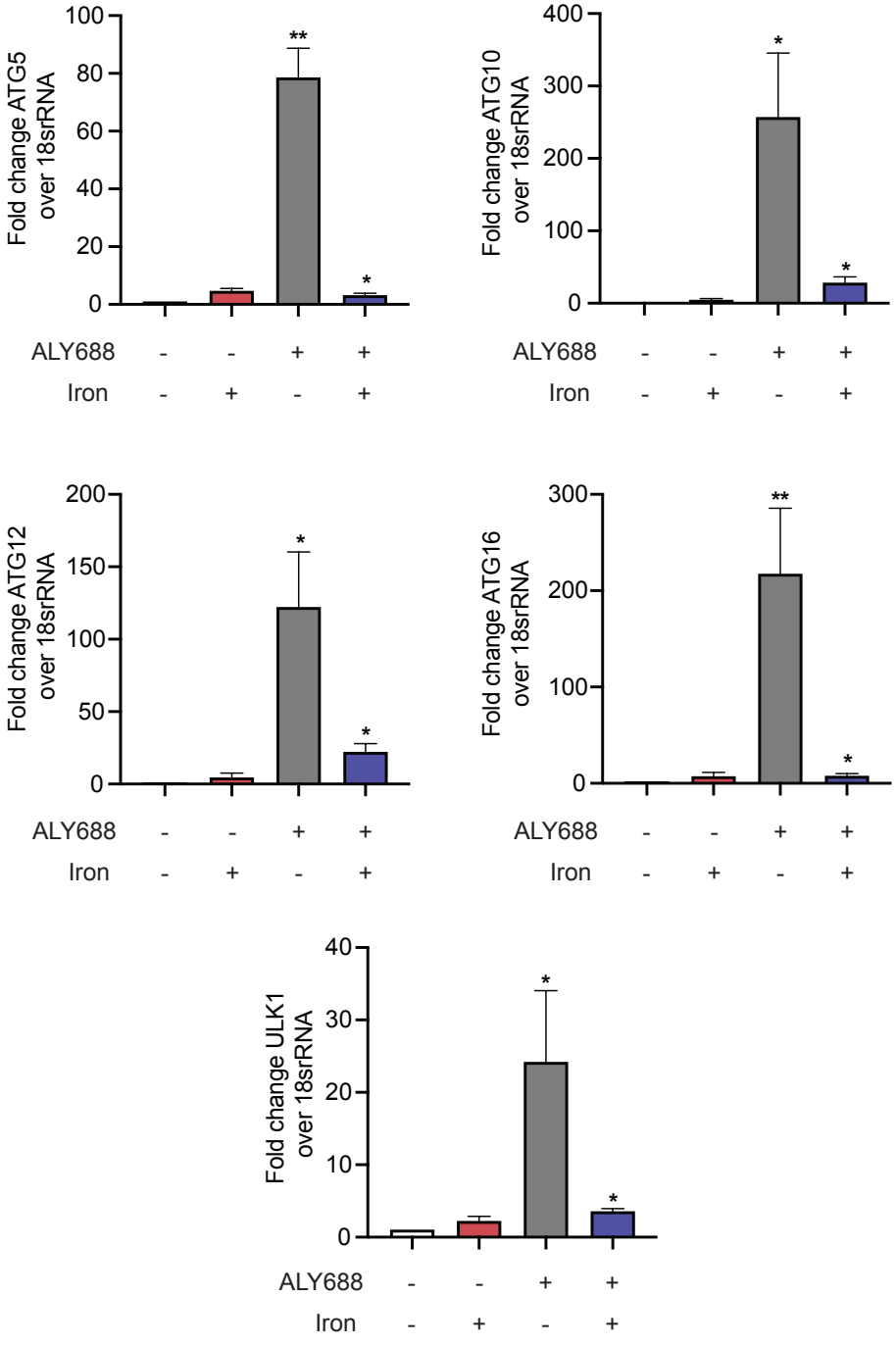
Fold change ATG5 over 18srRNA
100
80
60
40
20
0
**
*
ALY688 - - + +
Iron - + - +
Fold change ATG10 over 18srRNA
400
300
200
100
0
*
*
ALY688 - - + +
Iron - + - +
Fold change ATG12 over 18srRNA
200
150
100
50
0
*
*
ALY688 - - + +
Iron - + - +
Fold change ATG16 over 18srRNA
300
200
100
0
**
*
ALY688 - - + +
Iron - + - +
Fold change ULK1 over 18srRNA
40
30
20
10
0
*
*
ALY688 - - + +
Iron - + - +

Figure 13. Effect of iron and ALY688 on autophagy

Relative gene expressions— autophagy-related gene 5 (ATG5), autophagy-related gene 10 (ATG10), autophagy-related gene 12 (ATG12), autophagy-related gene 16 (ATG16) and unc-51 like autophagy activating kinase 1 (ULK1)- normalized to 18S rRNA expression (250 uM, 24 h) with and without ALY688 pre-treatment (300nM, 24 h). Values are mean ± s.e.m (n=3) *P < 0.05 **P < 0.005 (significance compared to basal) (one-way ANOVA with multiple comparisons).

ALY688 induced autophagosome formation and enhanced autophagic flux

The independent effects of iron and ALY688 on cells' autophagic flux were also investigated by measuring the contents of LC3 and p62 proteins. An increase in LC3-II contents was exhibited in both iron and ALY688 iron- treated cells, signifying formation of autophagosomes, which was in alignment with my qPCR results (Fig 14 A&B). When assessing p62 levels, a significant accumulation of p62 was observed in response to iron treatment, indicating a blockage of autophagic flux. Meanwhile, levels of p62 were consequentially downregulated upon pre-treatment with ALY688 (Fig 14 C), suggesting that ALY688 induced autophagic activity upon iron overload in L6 skeletal muscle cells. This observation suggests the importance of autophagy in mediating insulin response upon iron overload.

Figure 14

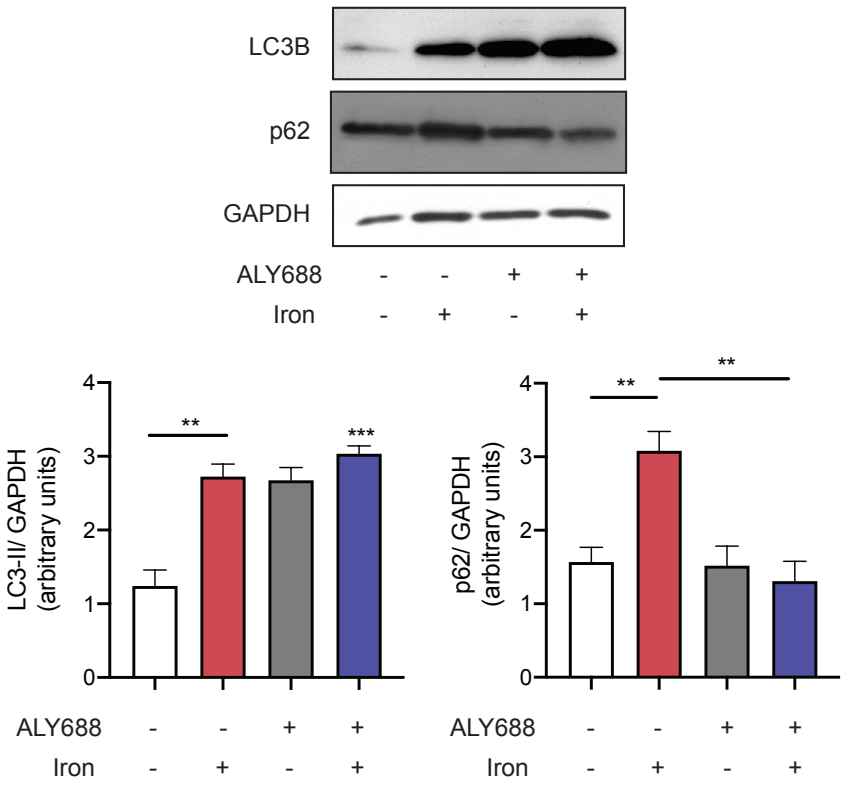
LC3B
p62
GAPDH
ALY688 - - + +
Iron - + - +
LC3-II/ GAPDH (arbitrary units)
0
1
2
3
4
**
***
ALY688 - - + +
Iron - + - +
p62/ GAPDH (arbitrary units)
0
1
2
3
4
**
**
ALY688 - - + +
Iron - + - +

Figure 14. Effect of iron and ALY688 on autophagy

Representative Western blot images and quantification of LC3B-II and p62 over GAPDH in L6 cells after iron treatment (250 uM, 16 h), with and without ALY688 pre-treatment (300nM, 24 h). Values are mean ± s.e.m (n=3) **P < 0.005 ***P < 0.0005 (one-way ANOVA with multiple comparisons).

The insulin- sensitizing effects of ALY688 is autophagy- dependent

To validate whether autophagy is vital for the beneficial effect of ALY688 in alleviating insulin resistance, the loss of function approach was utilized to block the process. To do so, the autophagy deficient of ATG7 knockout cell lines were generated. The wild-type L6 cell line was also used to compare the ability of ALY688 in upregulating insulin sensitivity. Analysis of insulin signaling markers demonstrated that iron overload impaired insulin response in the wild-type cells while ALY688 prevented insulin resistance, in accordance with my established L6 skeletal muscle model. However, this beneficial effect of ALY688 was diminished in autophagy-deficient cells (Fig 15 A & B). Taken together, my results show that targeting autophagy is crucial to alleviate IO-induced ER stress in skeletal muscle cells, which in turn helps attenuate insulin sensitivity. This study also suggests the potential benefit of using ALY688 as a therapeutic target in mediating insulin resistance upon iron overload.

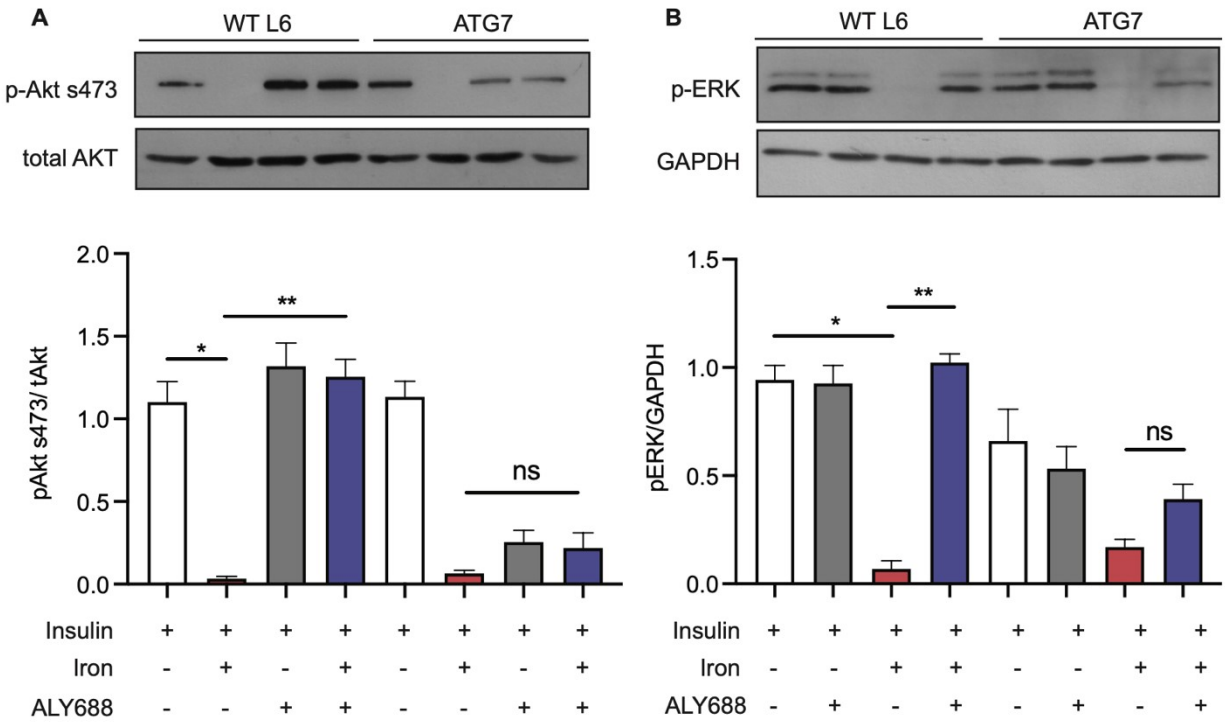

Figure 15. Role of autophagy in beneficial effect of ALY688 **A.** Representative Western blot images and quantification of phospho-Akt (S473) over total Akt in L6 and ATG7 cells with insulin stimulation (100 nM, 10 min) after iron treatment (250 uM, 24 h) with and without ALY688 pre-treatment (300nM, 24 h). Values are mean ± s.e.m (n=3) *P < 0.05 ** P < 0.005 (one-way ANOVA with multiple comparisons). **B.** Representative Western blot images and quantification of phospho-ERK over GAPDH in L6 and ATG7 cells with insulin stimulation (100 nM, 10 min) after iron treatment (250 uM, 24 h) with and without ALY688 pre-treatment (300nM, 24 h). Values are mean ± s.e.m (n=3) *P < 0.05 ** P < 0.005 (one-way ANOVA with multiple comparisons).

3.5 Discussion

Iron overload is closely associated with diabetic conditions. From the clinical perspective, prevalence of diabetes is observed in up to 30% of primary hemochromatosis and thalassemia patients [242-244]. Yet, the crosstalk between iron overload and insulin resistance is not fully understood. In my study, I employed an in vitro model of L6 skeletal muscle cells of iron overload to investigate a novel mechanism underlying IO- induced insulin resistance. I demonstrated that IO compromised skeletal muscle cells' insulin response by initiating ALR defects, which was consistent with my previous works that showed improved autophagy could enhance insulin sensitivity.

My study suggested that iron overload could elicit disrupted insulin signaling via endoplasmic reticulum stress. Mitochondrial ROS production, lipid peroxidation, and ferroptosis are among the means through which acute iron loading impaired ER functions [245-248]. Iron enrichment was also found to affect IRE-1 clustering with consequent ER stress in both yeast and human cells. In a mouse model of alcohol and high-fat diet-induced liver injury, prolonged iron toxicity led to steatohepatitis, fibrosis, impaired autophagy with consequent ER stress, and apoptosis [249]. Iron loading has been proven to cause defects in insulin secretion and progress to type 2 diabetes. For example, in vivo models of mice lacking X-box–binding protein–1 (XBP-1), a transcription factor that modulated the ER stress response exhibited glucose intolerance and insulin resistance via reduction of Akt and IRS-1 phosphorylation [250]. Overexpression of oxygen-regulated protein 150 (ORP150), a molecular chaperone that protected cells from ER stress, significantly improved insulin resistance and ameliorated glucose tolerance in obese mice.

Upon initiation, ER stress signaled a cascade of adaptive responses called the UPR, to maintain cellular homeostasis. Alterations of activating factor 6 (ATF6α) and spliced X-box

binding protein 1 (sXBP1) and phosphorylation of eukaryotic initiation factor 2 (eIF2α) gave rise to dysfunctional β-cells and insulin resistance in mice [251]. However, if prolonged chronically, the protective mechanism of the UPR would confer counteracting effects and progress to the development of various disorders, specifically insulin resistance and obesity. Therefore, I sought to investigate the crosstalk between IO- induced ER stress, UPR and progression to impaired insulin signaling. In this study, I found that iron induced the UPR response, albeit with autophagic flux defects in parallel. This suggested that targeting autophagy had potential advantages in ameliorating insulin signaling.

On another note, UPR activation via the PERK and IRE-1 pathway also induces autophagic activity as a pro-survival pathway to cope with ER stress [252,253]. Adiponectin has been demonstrated as an effective means of boosting autophagy to relieve ER stress and enhance insulin sensitivity. In insulin resistant- associated conditions, elevation in interleukin 6 (IL-6), reduction in leptin and alterations in adiponectin secretion are noted [254-256]. Decreased levels of adiponectin give rise to induction of the mTOR signaling pathway, which in turn induces the inhibition of IRS-1 with consequent disruption in insulin signaling [257]. A study in adipocytes also proposed that the downregulation of adiponectin during ER stress-induced autophagy was critical in developing insulin resistance in murine models [258]. Collectively, strategies to target adiponectin increment have produced beneficial effects in counteracting ER stress- induced insulin resistance. Several researches have indicated that intakes of fish oils and linoleic acid are among the practical approaches to increase plasma adiponectin levels that help regulate insulin signaling [259]. Pioneering studies using animal models have shown, as I did here, that replenishment of adiponectin could significantly mitigate insulin resistance and hypertriglyceridemia [260-262]. These observations were also aligned with models of adiponectin-deficient and adiponectin transgenic mice where adiponectin was shown to be an effective adipokine against obesity and

insulin resistant [263]. In my study, inducing UPR activation and autophagy with adiponectin mimic receptor agonist pre-treatment could alleviate insulin response. Autophagy has been known to effectively clear misfolded proteins [264]. As such, in my autophagy-deficient cell lines, the beneficial effects of ALY688 in boosting insulin response were absent, further confirming that insulin-sensitizing capacity of adiponectin upon IO was autophagy dependent.

In summary, my study showed that iron overload elevated ER stress, impaired autophagy and induced insulin resistance in skeletal muscle cells. I found that pre-treatment with adiponectin receptor ALY688 stimulated autophagic flux response in skeletal muscle cells, which exerted insulin-sensitizing effects upon iron overload. Accordingly, my work further emphasized the important role of autophagy in the cellular crosstalk between IO- induced ER stress and regulation of insulin response in skeletal muscle cells. New insights from this study highlight the significance of adiponectin in enhancing insulin sensitivity through promoting autophagy and preventing ER stress by activating the unfolded protein response.

CHAPTER 4: CONCLUSIONS

4.1 Thesis summary

My thesis has confirmed the significance of iron homeostasis imbalance and its contributions to insulin resistance. Acknowledgment of the causative relationship between IO and insulin secretion defects notwithstanding, it remains unclear exactly how iron elicit insulin resistance. It is commonly believed that IO in skeletal muscle is underappreciated. The mechanisms underlying iron overload- induced insulin resistance are widespread, yet my project has provided novel findings in which iron overload not only impaired autophagy but also induced ER stress. This led to the importance of targeting autophagy as the means to restore both ER stress and insulin sensitivity. Salubrinal is a well-established pharmacological inhibitor of peIF2α phosphatase enzymes [265,266]. Particularly significant to this study is the critical role of salubrinal in improving insulin sensitivity upon iron overload through promoted UPR as well as enhanced autophagic flux. In this study, an in vitro model of L6 cells was first employed, followed by translation of iron overload administration in mice. In both, a compromise of insulin sensitivity was observed, and it appeared that salubrinal could effectively attenuate this defect. More notably, I found that the insulin sensitizing effects of salubrinal were not observed in autophagy-deficient cell lines. Collectively, these observations suggested that autophagy produced protective effects against insulin resistance, and that its precise regulation was the key factor in mediating metabolic disorders. This conclusion led to the follow up of my thesis where I investigated the effects of ALY688 as an autophagy inducer to mitigate insulin resistance. IO-induced insulin resistance has been elucidated to reduce adiponectin expression in adipocytes. In insulin resistant models, a downregulation of adiponectin is closely related to impaired autophagy. My study suggested that pre-treating L6 cells with the adiponectin receptor agonist ALY688 could prevent IO-induced

insulin resistance and ER stress, which was consistent with the significance of adiponectin in T2D patients in clinical settings. The crosstalk between adiponectin signaling and the UPR is elusive.

However, a recent study has demonstrated that phosphorylation of AMPK could directly induce PERK and its signal transduction pathway in acute myeloid leukemia (AML) cells [267]. This finding further corroborated my observation where the UPR was activated upon ALY688 pre-treatment. It is also important to note that ER stress can be stimulated via inducer such as ROS production. Therefore, the antioxidative effect of ALY688 is of potential benefit to prevent ER stress. Moreover, an animal model of iron overload administration followed by ALY688 is another powerful approach to recapitulate my findings in the L6 cellular model.

Overall, the studies described above highlight the significance of autophagy in skeletal muscles in iron overload- associated insulin resistance. It is important to note that despite the difference in magnitude of insulin resistance induced upon iron overload observed in the 2 chapters, the trend remains clear where IO is associated with defective insulin response. IO is coupled with impaired mitochondrial dysfunctions, and my study has confirmed that these defects also lead to other organelles' dysfunctions, including the endoplasmic reticulum. My findings indicated for the first time that salubrinal elicited an eIF2α-autophagy which effectively suppressed ER stress and exhibited insulin sensitizing benefits. Additionally, the second study of my thesis unveiled a critical role of adiponectin as the key mediator in autophagy regulation under impaired metabolic syndrome conditions. Collectively, these findings implicated the potential benefits of using either salubrinal or ALY688 as pharmacological approaches in clinical studies regarding insulin resistance.

4.2 Future works

The first chapter of my thesis has examined the mechanisms through which iron overload induces insulin resistance including ER stress and impaired autophagy. More importantly, it was established that salubrinal promoted phospho- eIF2α-dependent activation of UPR leading to autophagy-mediated attenuation of iron-induced insulin resistance. Further in vivo work can be developed to confirm the effects of salubrinal in enhancing autophagy and insulin sensitivity. This includes western blotting to look at some well-established autophagy markers such as LC3-II or p62 in skeletal muscles. Glucose tolerance tests can be carried out to examine whether salubrinal treatment exerts the insulin sensitizing effects in vivo. It is important to note that eIF2αS/A mice with eIF2α phosphorylation knock-in would offer another powerful tool to validate the role of UPR and autophagy in improving insulin sensitivity following iron overload. This experimental model is currently collaborated where four groups of mice will be analyzed. These include wild type and eIF2αS/A mice injected with and without iron. Following tissue collection, western blotting of insulin signaling autophagic flux markers will be examined. The purpose is to see if the cellular model of salubrinal- inducing peIF2α would be recapitulated in the animal model, which in turn is beneficial for future clinical studies targeting peIF2α as gene therapy. Inducing autophagic flux with ALY688 has proven to be an effective means of ameliorating iron overload-induced insulin resistance. However, further research should be developed to characterize the mechanism through which ALY688 potentially relieves ER stress and induces the UPR response. It is established that ROS production is a strong source of ER stress induction. Given adiponectin's anti-oxidative effects, it will be interesting to look at whether ALY688 can ameliorate ER stress through ROS inhibition. This can be performed by imaging the cells upon stained with the ROS

indicator dye CellROX® red. The overall proteomes and signal transduction pathway produced following ALY688 pre-treatment in the presence and absence of iron overload can be extensively investigated by conducting proteomics analysis. Achieving this will further allow me to look at the specific mechanisms behind ALY688's mitigation of ER stress. Developing a mouse model of systemic iron overload administration with ALY688 pre-treatment is also essential to recapitulate ALY688' s insulin sensitizing effects in vivo. Overall, understanding the pathophysiology of iron overload in inducing insulin resistance at the molecular level will pave the way for development of therapeutic strategies to improve human health.

REFERENCES

[1] Kerie, S., Menberu, M., & Geneto, M. (2019). Metabolic syndrome among residents of MizanAman town, South West Ethiopia, 2017: a cross sectional study. *PLoS One*, *14*(1), e0210969.

[2] Huang, P. L. (2009). A comprehensive definition for metabolic syndrome. *Disease models & mechanisms*, *2*(5-6), 231-237.

[3] Mottillo, S., Filion, K. B., Genest, J., Joseph, L., Pilote, L., Poirier, P., ... & Eisenberg, M. J. (2010). The metabolic syndrome and cardiovascular risk: a systematic review and metaanalysis. *Journal of the American College of Cardiology*, *56*(14), 1113-1132.

[4] Swarup, S., Goyal, A., Grigorova, Y., & Zeltser, R. (2022). Metabolic syndrome. In *StatPearls [internet]*. StatPearls Publishing.

[5] Bonora, E. (2006). The metabolic syndrome and cardiovascular disease. *Annals of medicine*, *38*(1), 64-80.

[6] Wilson, P. W., D'Agostino, R. B., Parise, H., Sullivan, L., & Meigs, J. B. (2005). Metabolic syndrome as a precursor of cardiovascular disease and type 2 diabetes mellitus. *Circulation*, *112*(20), 3066-3072.

[7] da Silva, A. A., do Carmo, J. M., Li, X., Wang, Z., Mouton, A. J., & Hall, J. E. (2020). Role of hyperinsulinemia and insulin resistance in hypertension: metabolic syndrome revisited. *Canadian Journal of Cardiology*, *36*(5), 671-682.

[8] Wallace, D. F. (2016). The regulation of iron absorption and homeostasis. *The Clinical Biochemist Reviews*, *37*(2), 51.

[9] Brissot, P., Ropert, M., Le Lan, C., & Loréal, O. (2012). Non-transferrin bound iron: a key role in iron overload and iron toxicity. *Biochimica et Biophysica Acta (BBA)-General Subjects*, *1820*(3), 403-410.

[10] Tofano, R. J., Pescinni-Salzedas, L. M., Chagas, E. F. B., Detregiachi, C. R. P., Guiguer, E. L., Araujo, A. C., ... & Barbalho, S. M. (2020). Association of metabolic syndrome and hyperferritinemia in patients at cardiovascular risk. *Diabetes, Metabolic Syndrome and Obesity: Targets and Therapy*, *13*, 3239.

[11] Jehn, M., Clark, J. M., & Guallar, E. (2004). Serum ferritin and risk of the metabolic syndrome in US adults. *Diabetes care*, *27*(10), 2422-2428.

[12] Piperno, A., Trombini, P., Gelosa, M., Mauri, V., Pecci, V., Vergani, A., ... & Mancia, G. (2002). Increased serum ferritin is common in men with essential hypertension. *Journal of hypertension*, *20*(8), 1513-1518.

[13] American Diabetes Association. (2010). Diagnosis and classification of diabetes mellitus. *Diabetes care*, *33*(Supplement_1), S62-S69.

[14] Goyal, R., & Jialal, I. (2018). Diabetes mellitus type 2.

[15] Chen, R., Ovbiagele, B., & Feng, W. (2016). Diabetes and stroke: epidemiology, pathophysiology, pharmaceuticals and outcomes. *The American journal of the medical sciences*, *351*(4), 380-386.

[16] Umegaki, H. (2012). Neurodegeneration in diabetes mellitus. *Neurodegenerative diseases*, 258-265.

[17] Leon, B. M., & Maddox, T. M. (2015). Diabetes and cardiovascular disease: epidemiology, biological mechanisms, treatment recommendations and future research. *World journal of diabetes*, *6*(13), 1246.

[18] Abudawood, M. (2019). Diabetes and cancer: a comprehensive review. *Journal of Research in Medical Sciences: The Official Journal of Isfahan University of Medical Sciences*, *24*.

[19] Shin, J. A., Lee, J. H., Lim, S. Y., Ha, H. S., Kwon, H. S., Park, Y. M., ... & Son, H. Y. (2013). Metabolic syndrome as a predictor of type 2 diabetes, and its clinical interpretations and usefulness. *Journal of diabetes investigation*, *4*(4), 334-343.

[20] Bancej, C., Jayabalasingham, B., Wall, R. W., Rao, D. P., Do, M. T., De Groh, M., & Jayaraman, G. C. (2015). Trends and projections of obesity among Canadians. *Health promotion and chronic disease prevention in Canada: research, policy and practice*, *35*(7), 109.

[21] Savini, I., Catani, M. V., Evangelista, D., Gasperi, V., & Avigliano, L. (2013). Obesityassociated oxidative stress: strategies finalized to improve redox state. *International journal of molecular sciences*, *14*(5), 10497-10538.

[22] Romieu, I., Dossus, L., Barquera, S., Blottière, H. M., Franks, P. W., Gunter, M., ... & Willett, W. C. (2017). Energy balance and obesity: what are the main drivers?. *Cancer Causes & Control*, *28*(3), 247-258.

[23] Hill, J. O., Wyatt, H. R., & Peters, J. C. (2012). Energy balance and

obesity. *Circulation*, *126*(1), 126-132.

[24] Baskin, M. L., Ard, J., Franklin, F., & Allison, D. B. (2005). Prevalence of obesity in the United States. *Obesity reviews*, *6*(1), 5-7.

[25] GBD 2015 Obesity Collaborators. (2017). Health effects of overweight and obesity in 195 countries over 25 years. *New England journal of medicine*, *377*(1), 13-27.

[26] Hu, Y., Bhupathiraju, S. N., de Koning, L., & Hu, F. B. (2014). Duration of obesity and overweight and risk of type 2 diabetes among US women. *Obesity*, *22*(10), 2267-2273.

[27] Gray, A., & Threlkeld, R. J. (2015). Nutritional recommendations for individuals with diabetes.

[28] Quianzon, C. C., & Cheikh, I. (2012). History of insulin. *Journal of community hospital internal medicine perspectives*, *2*(2), 18701.

[29] Fu, Z., R Gilbert, E., & Liu, D. (2013). Regulation of insulin synthesis and secretion and pancreatic Beta-cell dysfunction in diabetes. *Current diabetes reviews*, *9*(1), 25-53.

[30] Nasri, H., & Rafieian-Kopaei, M. (2014). Metformin: current knowledge. *Journal of research in medical sciences: the official journal of Isfahan University of Medical Sciences*, *19*(7), 658.

[31] Wilcox, G. (2005). Insulin and insulin resistance. *Clinical biochemist reviews*, *26*(2), 19.

[32] Hou, J. C., Min, L., & Pessin, J. E. (2009). Insulin granule biogenesis, trafficking and exocytosis. *Vitamins & Hormones*, *80*, 473-506.

[33] Lee, J., & Pilch, P. F. (1994). The insulin receptor: structure, function, and signaling. *American Journal of Physiology-Cell Physiology*, *266*(2), C319-C334.

[34] Liu, B. A., Engelmann, B. W., Jablonowski, K., Higginbotham, K., Stergachis, A. B., & Nash, P. D. (2012). SRC Homology 2 Domain Binding Sites in Insulin, IGF-1 and FGF receptor mediated signaling networks reveal an extensive potential interactome. *Cell Communication and Signaling*, *10*(1), 1-23.

[35] Leto, D., & Saltiel, A. R. (2012). Regulation of glucose transport by insulin: traffic control of GLUT4. *Nature reviews Molecular cell biology*, *13*(6), 383-396.

[36] Angin, Y., Beauloye, C., Horman, S., & Bertrand, L. (2016). Regulation of carbohydrate metabolism, lipid metabolism, and protein metabolism by AMPK. *AMP-Activated Protein Kinase*, 23-43.

[37] Shan, Z., Fa, W. H., Tian, C. R., Yuan, C. S., & Jie, N. (2022). Mitophagy and mitochondrial dynamics in type 2 diabetes mellitus treatment. *Aging (Albany NY)*, *14*(6), 2902.

[38] Kuramoto, K., Kim, Y. J., Hong, J. H., & He, C. (2021). The autophagy protein Becn1 improves insulin sensitivity by promoting adiponectin secretion via exocyst binding. *Cell reports*, *35*(8), 109184.

[39] Su, Z., Nie, Y., Huang, X., Zhu, Y., Feng, B., Tang, L., & Zheng, G. (2019). Mitophagy in hepatic insulin resistance: therapeutic potential and concerns. *Frontiers in pharmacology*, *10*, 1193.

[40] Vecchio, I., Tornali, C., Bragazzi, N. L., & Martini, M. (2018). The discovery of insulin: an important milestone in the history of medicine. *Frontiers in endocrinology*, *9*, 613.

[41] Batista, T. M., Haider, N., & Kahn, C. R. (2021). Defining the underlying defect in insulin action in type 2 diabetes. *Diabetologia*, *64*(5), 994-1006.

[42] De Meyts, P. (2016). The insulin receptor and its signal transduction network. *Endotext [Internet]*.

[43] Bashan, N., Kovsan, J., Kachko, I., Ovadia, H., & Rudich, A. (2009). Positive and negative regulation of insulin signaling by reactive oxygen and nitrogen species. *Physiological reviews*.

[44] Arneth, B., Arneth, R., & Shams, M. (2019). Metabolomics of type 1 and type 2 diabetes. *International journal of molecular sciences*, *20*(10), 2467.

[45] Ormazabal, V., Nair, S., Elfeky, O., Aguayo, C., Salomon, C., & Zuñiga, F. A. (2018). Association between insulin resistance and the development of cardiovascular

disease. *Cardiovascular diabetology*, *17*(1), 1-14.

[46] da Silva Rosa, S. C., Nayak, N., Caymo, A. M., & Gordon, J. W. (2020). Mechanisms of muscle insulin resistance and the cross-talk with liver and adipose tissue. *Physiological Reports*, *8*(19), e14607.

[47] Lanuza-Masdeu, J., Arévalo, M. I., Vila, C., Barberà, A., Gomis, R., & Caelles, C. (2013). In vivo JNK activation in pancreatic β-cells leads to glucose intolerance caused by insulin resistance in pancreas. *Diabetes*, *62*(7), 2308-2317.

[48] Hirosumi, J., Tuncman, G., Chang, L., Görgün, C. Z., Uysal, K. T., Maeda, K., ... & Hotamisligil, G. S. (2002). A central role for JNK in obesity and insulin resistance. *Nature*, *420*(6913), 333-336.

[49] Brown, M., Dainty, S., Strudwick, N., Mihai, A. D., Watson, J. N., Dendooven, R., ... & Schröder, M. (2020). Endoplasmic reticulum stress causes insulin resistance by inhibiting delivery of newly synthesized insulin receptors to the cell surface. *Molecular biology of the cell*, *31*(23), 2597-2629.

[50] Sergi, D., Naumovski, N., Heilbronn, L. K., Abeywardena, M., O'Callaghan, N., Lionetti, L., & Luscombe-Marsh, N. (2019). Mitochondrial (dys) function and insulin resistance: from pathophysiological molecular mechanisms to the impact of diet. *Frontiers in physiology*, *10*, 532.

[51] Hurrle, S., & Hsu, W. H. (2017). The etiology of oxidative stress in insulin resistance. *Biomedical journal*, *40*(5), 257-262.

[52] Simcox, J. A., & McClain, D. A. (2013). Iron and diabetes risk. *Cell metabolism*, *17*(3), 329341.

[53] Adams, P. C., & Barton, J. C. (2007). Haemochromatosis. *The Lancet*, *370*(9602), 1855-1860.

[54] Bahar, A., Kashi, Z., Sohrab, M., Kosaryan, M., & Janbabai, G. (2012). Relationship between beta-globin gene carrier state and insulin resistance. *Journal of Diabetes & Metabolic Disorders*, *11*(1), 1-4.

[55] Mackenzie, E. L., Iwasaki, K., & Tsuji, Y. (2008). Intracellular iron transport and storage: from molecular mechanisms to health implications. *Antioxidants & redox signaling*, *10*(6), 9971030.

[56] Zorov, D. B., Juhaszova, M., & Sollott, S. J. (2014). Mitochondrial reactive oxygen species (ROS) and ROS-induced ROS release. *Physiological reviews*, *94*(3), 909-950.

[57] Kaludercic, N., & Di Lisa, F. (2020). Mitochondrial ROS formation in the pathogenesis of diabetic cardiomyopathy. *Frontiers in Cardiovascular Medicine*, *7*, 12.

[58] Houschyar, K. S., Lüdtke, R., Dobos, G. J., Kalus, U., Broecker-Preuss, M., Rampp, T., ... & Michalsen, A. (2012). Effects of phlebotomy-induced reduction of body iron stores on metabolic syndrome: results from a randomized clinical trial. *BMC medicine*, *10*(1), 1-8.

[59] Cooksey, R. C., Jones, D., Gabrielsen, S., Huang, J., Simcox, J. A., Luo, B., ... & McClain, D. A. (2010). Dietary iron restriction or iron chelation protects from diabetes and loss of β-cell function in the obese (ob/ob lep−/−) mouse. *American Journal of Physiology-Endocrinology and Metabolism*, *298*(6), E1236-E1243.

[60] Gabrielsen, J. S., Gao, Y., Simcox, J. A., Huang, J., Thorup, D., Jones, D., ... & McClain, D. A. (2012). Adipocyte iron regulates adiponectin and insulin sensitivity. *The Journal of clinical investigation*, *122*(10), 3529-3540.

[61] Wlazlo, N., Van Greevenbroek, M. M., Ferreira, I., Jansen, E. H., Feskens, E. J., Van Der Kallen, C. J., ... & Stehouwer, C. D. (2013). Iron metabolism is associated with adipocyte insulin

resistance and plasma adiponectin: the Cohort on Diabetes and Atherosclerosis Maastricht (CODAM) study. *Diabetes care*, *36*(2), 309-315.

[62] Chadt, A., Scherneck, S., Joost, H. G., & Al-Hasani, H. (2018). Molecular links between obesity and diabetes:"diabesity". *Endotext [Internet]*.

[63] Zorena, K., Jachimowicz-Duda, O., Ślęzak, D., Robakowska, M., & Mrugacz, M. (2020). Adipokines and obesity. Potential link to metabolic disorders and chronic complications. *International journal of molecular sciences*, *21*(10), 3570.

[64] Zhang, Y., Proenca, R., Maffei, M., Barone, M., Leopold, L., & Friedman, J. M. (1994). Positional cloning of the mouse obese gene and its human homologue. *Nature*, *372*(6505), 425432.

[65] Obradovic, M., Sudar-Milovanovic, E., Soskic, S., Essack, M., Arya, S., Stewart, A. J., ... & Isenovic, E. R. (2021). Leptin and obesity: role and clinical implication. *Frontiers in Endocrinology*, *12*, 585887.

[66] Feinstein, R., Kanety, H., Papa, M. Z., Lunenfeld, B., & Karasik, A. (1993). Tumor necrosis factor-alpha suppresses insulin-induced tyrosine phosphorylation of insulin receptor and its substrates. *Journal of Biological Chemistry*, *268*(35), 26055-26058.

[67] Wellen, K. E., & Hotamisligil, G. S. (2003). Obesity-induced inflammatory changes in adipose tissue. *The Journal of clinical investigation*, *112*(12), 1785-1788.

[68] Eder, K., Baffy, N., Falus, A., & Fulop, A. K. (2009). The major inflammatory mediator interleukin-6 and obesity. *Inflammation Research*, *58*(11), 727-736.

[69] Izquierdo, A. G., Crujeiras, A. B., Casanueva, F. F., & Carreira, M. C. (2019). Leptin, obesity, and leptin resistance: where are we 25 years later?. *Nutrients*, *11*(11), 2704.

[70] Nigro, E., Scudiero, O., Monaco, M. L., Palmieri, A., Mazzarella, G., Costagliola, C., ... & Daniele, A. (2014). New insight into adiponectin role in obesity and obesity-related diseases. *BioMed research international*, *2014*.

[71] Nakamura, K., Fuster, J. J., & Walsh, K. (2014). Adipokines: a link between obesity and cardiovascular disease. *Journal of cardiology*, *63*(4), 250-259.

[72] Guenther, M., James, R., Marks, J., Zhao, S., Szabo, A., & Kidambi, S. (2014). Adiposity distribution influences circulating adiponectin levels. *Translational Research*, *164*(4), 270-277.

[73] Hui, X., Lam, K. S., Vanhoutte, P. M., & Xu, A. (2012). Adiponectin and cardiovascular health: an update. *British journal of pharmacology*, *165*(3), 574-590.

[74] Kim-Mitsuyama, S., Soejima, H., Yasuda, O., Node, K., Jinnouchi, H., Yamamoto, E., ... & Matsui, K. (2019). Total adiponectin is associated with incident cardiovascular and renal events in treated hypertensive patients: subanalysis of the ATTEMPT-CVD randomized trial. *Scientific reports*, *9*(1), 1-9.

[75] Bhatta, A., Yao, L., Xu, Z., Toque, H. A., Chen, J., Atawia, R. T., ... & Caldwell, R. W. (2017). Obesity-induced vascular dysfunction and arterial stiffening requires endothelial cell arginase 1. *Cardiovascular research*, *113*(13), 1664-1676.

[76] Shimada, K., Miyazaki, T., & Daida, H. (2004). Adiponectin and atherosclerotic disease. *Clinica chimica acta*, *344*(1-2), 1-12.

[77] Abdullaha, M., Ali, M., Kour, D., Mudududdla, R., Khajuria, P., Kumar, A., & Bharate, S. B. (2021). Tetramethoxystilbene Inhibits NLRP3 inflammasome assembly via blocking the oligomerization of apoptosis-associated speck-like protein containing caspase recruitment domain: In vitro and in vivo evaluation. *ACS Pharmacology & Translational Science*, *4*(4), 1437-1448.

[78] Abdella, N. A., & Mojiminiyi, O. A. (2018). Clinical applications of adiponectin measurements in type 2 diabetes mellitus: screening, diagnosis, and marker of diabetes control. *Disease markers*, *2018*.

[79] Trujillo, M. E., & Scherer, P. E. (2005). Adiponectin–journey from an adipocyte secretory protein to biomarker of the metabolic syndrome. *Journal of internal medicine*, *257*(2), 167-175.

[80] Hui, X., Lam, K. S., Vanhoutte, P. M., & Xu, A. (2012). Adiponectin and cardiovascular health: an update. *British journal of pharmacology*, *165*(3), 574-590.

[81] Kobayashi, H., Ouchi, N., Kihara, S., Walsh, K., Kumada, M., Abe, Y., ... & Matsuzawa, Y. (2004). Selective suppression of endothelial cell apoptosis by the high molecular weight form of adiponectin. *Circulation research*, *94*(4), e27-e31.

[82] Pajvani, U. B., Hawkins, M., Combs, T. P., Rajala, M. W., Doebber, T., Berger, J. P., ... & Scherer, P. E. (2004). Complex distribution, not absolute amount of adiponectin, correlates with thiazolidinedione-mediated improvement in insulin sensitivity. *Journal of Biological Chemistry*, *279*(13), 12152-12162.

[83] Kupchak, B. R., Garitaonandia, I., Villa, N. Y., Smith, J. L., & Lyons, T. J. (2009). Antagonism of human adiponectin receptors and their membrane progesterone receptor paralogs by TNFα and a ceramidase inhibitor. *Biochemistry*, *48*(24), 5504-5506.

[84] Achari, A. E., & Jain, S. K. (2017). Adiponectin, a therapeutic target for obesity, diabetes, and endothelial dysfunction. *International journal of molecular sciences*, *18*(6), 1321.

[85] Yamauchi, T., Kamon, J., Minokoshi, Y. A., Ito, Y., Waki, H., Uchida, S., ... & Kadowaki, T. (2002). Adiponectin stimulates glucose utilization and fatty-acid oxidation by activating AMPactivated protein kinase. *Nature medicine*, *8*(11), 1288-1295.

[86] Tomita, K., Oike, Y., Teratani, T., Taguchi, T., Noguchi, M., Suzuki, T., ... & Hibi, T. (2008). Hepatic AdipoR2 signaling plays a protective role against progression of nonalcoholic steatohepatitis in mice. *Hepatology*, *48*(2), 458-473.

[87] Yamauchi, T., Nio, Y., Maki, T., Kobayashi, M., Takazawa, T., Iwabu, M., ... & Kadowaki, T. (2007). Targeted disruption of AdipoR1 and AdipoR2 causes abrogation of adiponectin binding and metabolic actions. *Nature medicine*, *13*(3), 332-339.

[88] Mao, X., Kikani, C. K., Riojas, R. A., Langlais, P., Wang, L., Ramos, F. J., ... & Dong, L. Q. (2006). APPL1 binds to adiponectin receptors and mediates adiponectin signalling and function. *Nature cell biology*, *8*(5), 516-523.

[89] Wang, C., Xin, X., Xiang, R., Ramos, F. J., Liu, M., Lee, H. J., ... & Dong, L. Q. (2009). YinYang regulation of adiponectin signaling by APPL isoforms in muscle cells. *Journal of Biological Chemistry*, *284*(46), 31608-31615.

[90] Tyagi, S., Gupta, P., Saini, A. S., Kaushal, C., & Sharma, S. (2011). The peroxisome proliferator-activated receptor: A family of nuclear receptors role in various diseases. *Journal of advanced pharmaceutical technology & research*, *2*(4), 236.

[91] Nissen, S. E., Nicholls, S. J., Wolski, K., Howey, D. C., McErlean, E., Wang, M. D., ... & Russo, J. M. (2007). Effects of a potent and selective PPAR-α agonist in patients with atherogenic dyslipidemia or hypercholesterolemia: two randomized controlled trials. *Jama*, *297*(12), 13621373.

[92] Kim, Y., & Park, C. W. (2019). Mechanisms of adiponectin action: implication of adiponectin receptor agonism in diabetic kidney disease. *International journal of molecular sciences*, *20*(7), 1782.

[93] Zhou, L., Deepa, S. S., Etzler, J. C., Ryu, J., Mao, X., Fang, Q., ... & Dong, L. Q. (2009). Adiponectin activates AMP-activated protein kinase in muscle cells via APPL1/LKB1-dependent and phospholipase C/Ca2+/Ca2+/calmodulin-dependent protein kinase kinase-dependent pathways. *Journal of Biological Chemistry*, *284*(33), 22426-22435.

[94] Saddik, M. A. R. U. F., Gamble, J., Witters, L. A., & Lopaschuk, G. D. (1993). Acetyl-CoA carboxylase regulation of fatty acid oxidation in the heart. *Journal of Biological Chemistry*, *268*(34), 25836-25845.

[95] Niu, W., Huang, C., Nawaz, Z., Levy, M., Somwar, R., Li, D., ... & Klip, A. (2003). Maturation of the regulation of GLUT4 activity by p38 MAPK during L6 cell myogenesis. *Journal of Biological Chemistry*, *278*(20), 17953-17962.

[96] Thors, B., Halldórsson, H., & Thorgeirsson, G. (2011). eNOS activation mediated by AMPK after stimulation of endothelial cells with histamine or thrombin is dependent on LKB1. *Biochimica et Biophysica Acta (BBA)-Molecular Cell Research*, *1813*(2), 322-331.

[97] Nawrocki, A. R., Rajala, M. W., Tomas, E., Pajvani, U. B., Saha, A. K., Trumbauer, M. E., ... & Scherer, P. E. (2006). Mice lacking adiponectin show decreased hepatic insulin sensitivity and reduced responsiveness to peroxisome proliferator-activated receptor γ agonists. *Journal of Biological Chemistry*, *281*(5), 2654-2660.

[98] Achari, A. E., & Jain, S. K. (2017). Adiponectin, a therapeutic target for obesity, diabetes, and endothelial dysfunction. *International journal of molecular sciences*, *18*(6), 1321.

[99] Nguyen, T. M. D. (2020). Adiponectin: role in physiology and pathophysiology. *International journal of preventive medicine*, *11*.

[100] Ouchi, N., Kihara, S., Arita, Y., Maeda, K., Kuriyama, H., Okamoto, Y., ... & Matsuzawa, Y. (1999). Novel modulator for endothelial adhesion molecules: adipocyte-derived plasma protein adiponectin. *Circulation*, *100*(25), 2473-2476.

[101] Kobashi, C., Urakaze, M., Kishida, M., Kibayashi, E., Kobayashi, H., Kihara, S., ... & Kobayashi, M. (2005). Adiponectin inhibits endothelial synthesis of interleukin-8. *Circulation research*, *97*(12), 1245-1252.

[102] Kumada, M., Kihara, S., Ouchi, N., Kobayashi, H., Okamoto, Y., Ohashi, K., ... & Matsuzawa, Y. (2004). Adiponectin specifically increased tissue inhibitor of metalloproteinase-1 through interleukin-10 expression in human macrophages. *Circulation*, *109*(17), 2046-2049.

[103] Magalang, U. J., Rajappan, R., Hunter, M. G., Kutala, V. K., Kuppusamy, P., Wewers, M. D., ... & Parinandi, N. L. (2006). Adiponectin inhibits superoxide generation by human neutrophils. *Antioxidants & redox signaling*, *8*(11-12), 2179-2186.

[104] Yamauchi, T., Kamon, J., Minokoshi, Y. A., Ito, Y., Waki, H., Uchida, S., ... & Kadowaki, T. (2002). Adiponectin stimulates glucose utilization and fatty-acid oxidation by activating AMPactivated protein kinase. *Nature medicine*, *8*(11), 1288-1295.

[105] Fruebis, J., Tsao, T. S., Javorschi, S., Ebbets-Reed, D., Erickson, M. R. S., Yen, F. T., ... & Lodish, H. F. (2001). Proteolytic cleavage product of 30-kDa adipocyte complement-related protein increases fatty acid oxidation in muscle and causes weight loss in mice. *Proceedings of the National Academy of Sciences*, *98*(4), 2005-2010.

[106] Kadowaki, T., Yamauchi, T., Kubota, N., Hara, K., Ueki, K., & Tobe, K. (2006). Adiponectin and adiponectin receptors in insulin resistance, diabetes, and the metabolic syndrome. *The Journal of clinical investigation*, *116*(7), 1784-1792.

[107] Awazawa, M., Ueki, K., Inabe, K., Yamauchi, T., Kubota, N., Kaneko, K., ... & Kadowaki, T. (2011). Adiponectin enhances insulin sensitivity by increasing hepatic IRS-2 expression via a macrophage-derived IL-6-dependent pathway. *Cell metabolism*, *13*(4), 401-412.

[108] Farese, R. V., Sajan, M. P., Yang, H., Li, P., Mastorides, S., Gower, W. R., ... & Leitges, M. (2007). Muscle-specific knockout of PKC-λ impairs glucose transport and induces metabolic and diabetic syndromes. *The Journal of clinical investigation*, *117*(8), 2289-2301.

[109] Asano, T., Watanabe, K., Kubota, N., Gunji, T., Omata, M., Kadowaki, T., & Ohnishi, S. (2009). Adiponectin knockout mice on high fat diet develop fibrosing steatohepatitis. *Journal of gastroenterology and hepatology*, *24*(10), 1669-1676.

[110] Maeda, N., Shimomura, I., Kishida, K., Nishizawa, H., Matsuda, M., Nagaretani, H., ... & Matsuzawa, Y. (2002). Diet-induced insulin resistance in mice lacking adiponectin/ACRP30. *Nature medicine*, *8*(7), 731-737.

[111] Kubota, N., Terauchi, Y., Yamauchi, T., Kubota, T., Moroi, M., Matsui, J., ... & Noda, T. (2002). Disruption of adiponectin causes insulin resistance and neointimal formation. *Journal of Biological Chemistry*, *277*(29), 25863-25866.

[112] Ohashi, K., Kihara, S., Ouchi, N., Kumada, M., Fujita, K., Hiuge, A., ... & Shimomura, I. (2006). Adiponectin replenishment ameliorates obesity-related hypertension. *Hypertension*, *47*(6), 1108-1116.

[113] Kadowaki, T., & Yamauchi, T. (2005). Adiponectin and adiponectin receptors. *Endocrine reviews*, *26*(3), 439-451.

[114] Zhao, L., Fu, Z., Wu, J., Aylor, K. W., Barrett, E. J., Cao, W., & Liu, Z. (2015). Globular adiponectin ameliorates metabolic insulin resistance via AMPK-mediated restoration of microvascular insulin responses. *The Journal of physiology*, *593*(17), 4067-4079.

[115] Aksu, N. M., Aksoy, D. Y., Akkaş, M., Çinar, N., Uçar, F., Yildiz, O. B., & Usman, A. (2020). Adiponectin levels decrease independently of body mass index and diabetes type afterthe normalization of hyperglycemia. *Turkish Journal of Medical Sciences*, *50*(2), 312-315.

[116] Manley, S. J., Olou, A. A., Jack, J. L., Ruckert, M. T., Walsh, R. M., Eades, A. E., ... & VanSaun, M. N. (2022). Synthetic adiponectin-receptor agonist, AdipoRon, induces glycolytic dependence in pancreatic cancer cells. *Cell death & disease*, *13*(2), 1-10.

[117] Da Eira, D., Jani, S., Sung, H., Sweeney, G., & Ceddia, R. B. (2020). Effects of the adiponectin mimetic compound ALY688 on glucose and fat metabolism in visceral and subcutaneous rat adipocytes. *Adipocyte*, *9*(1), 550-562.

[118] Otvos Jr, L. (2019). Potential adiponectin receptor response modifier therapeutics. *Frontiers in endocrinology*, *10*, 539.

[119] Schwarz, D. S., & Blower, M. D. (2016). The endoplasmic reticulum: structure, function and response to cellular signaling. *Cellular and molecular life sciences*, *73*(1), 79-94.

[120] Oakes, S. A., & Papa, F. R. (2015). The role of endoplasmic reticulum stress in human pathology. *Annual review of pathology*, *10*, 173.

[121] García-Jiménez, C., & Goding, C. R. (2019). Starvation and pseudo-starvation as drivers of cancer metastasis through translation reprogramming. *Cell metabolism*, *29*(2), 254-267.

[122] Akman, M., Belisario, D. C., Salaroglio, I. C., Kopecka, J., Donadelli, M., De Smaele, E., & Riganti, C. (2021). Hypoxia, endoplasmic reticulum stress and chemoresistance: dangerous liaisons. *Journal of Experimental & Clinical Cancer Research*, *40*(1), 1-17.

[123] Rajakumar, S., Bhanupriya, N., Ravi, C., & Nachiappan, V. (2016). Endoplasmic reticulum stress and calcium imbalance are involved in cadmium-induced lipid aberrancy in Saccharomyces cerevisiae. *Cell Stress and Chaperones*, *21*(5), 895-906.

[124] Cao, S. S., & Kaufman, R. J. (2014). Endoplasmic reticulum stress and oxidative stress in cell fate decision and human disease. *Antioxidants & redox signaling*, *21*(3), 396-413.

[125] Vembar, S. S., & Brodsky, J. L. (2008). One step at a time: endoplasmic reticulum-associated degradation. *Nature reviews Molecular cell biology*, *9*(12), 944-957.

[126] Qi, L., Tsai, B., & Arvan, P. (2017). New insights into the physiological role of endoplasmic reticulum-associated degradation. *Trends in cell biology*, *27*(6), 430-440.

[127] Lemmer, I. L., Willemsen, N., Hilal, N., & Bartelt, A. (2021). A guide to understanding endoplasmic reticulum stress in metabolic disorders. *Molecular metabolism*, *47*, 101169.

[128] Gardner, B. M., Pincus, D., Gotthardt, K., Gallagher, C. M., & Walter, P. (2013). Endoplasmic reticulum stress sensing in the unfolded protein response. *Cold Spring Harbor perspectives in biology*, *5*(3), a013169.

[129] Mori, K. (2015). The unfolded protein response: the dawn of a new field. *Proceedings of the Japan Academy, Series B*, *91*(9), 469-480.

[130] Szegezdi, E., Logue, S. E., Gorman, A. M., & Samali, A. (2006). Mediators of endoplasmic reticulum stress-induced apoptosis. *EMBO reports*, *7*(9), 880-885.

[131] DuRose, J. B., Scheuner, D., Kaufman, R. J., Rothblum, L. I., & Niwa, M. (2009). Phosphorylation of eukaryotic translation initiation factor 2α coordinates rRNA transcription and translation inhibition during endoplasmic reticulum stress. *Molecular and cellular biology*, *29*(15), 4295-4307.

[132] Blais, J. D., Filipenko, V., Bi, M., Harding, H. P., Ron, D., Koumenis, C., ... & Bell, J. C. (2004). Activating transcription factor 4 is translationally regulated by hypoxic stress. *Molecular and cellular biology*, *24*(17), 7469-7482.

[133] Siwecka, N., Rozpędek-Kamińska, W., Wawrzynkiewicz, A., Pytel, D., Diehl, J. A., & Majsterek, I. (2021). The structure, activation and signaling of IRE1 and its role in determining cell fate. *Biomedicines*, *9*(2), 156.

[134] Nishitoh, H., Matsuzawa, A., Tobiume, K., Saegusa, K., Takeda, K., Inoue, K., ... & Ichijo, H. (2002). ASK1 is essential for endoplasmic reticulum stress-induced neuronal cell death triggered by expanded polyglutamine repeats. *Genes & development*, *16*(11), 1345-1355.

[135] Shen, J., & Prywes, R. (2004). Dependence of site-2 protease cleavage of ATF6 on prior site-1 protease digestion is determined by the size of the luminal domain of ATF6. *Journal of Biological Chemistry*, *279*(41), 43046-43051.

[136] Tam, A. B., Roberts, L. S., Chandra, V., Rivera, I. G., Nomura, D. K., Forbes, D. J., & Niwa, M. (2018). The UPR activator ATF6 responds to proteotoxic and lipotoxic stress by distinct mechanisms. *Developmental cell*, *46*(3), 327-343.

[137] Nakatani, Y., Kaneto, H., Kawamori, D., Yoshiuchi, K., Hatazaki, M., Matsuoka, T. A., ... & Matsuhisa, M. (2005). Involvement of endoplasmic reticulum stress in insulin resistance and diabetes. *Journal of Biological Chemistry*, *280*(1), 847-851.

[138] Labandeira, C. M., Fraga-Bau, A., Ron, D. A., Alvarez-Rodriguez, E., Vicente-Alba, P.,

Lago-Garma, J., & Rodriguez-Perez, A. I. (2022). Parkinson's disease and diabetes mellitus: Common mechanisms and treatment repurposing. *Neural Regeneration Research*, *17*(8), 1652.

[139] Parzych, K. R., & Klionsky, D. J. (2014). An overview of autophagy: morphology, mechanism, and regulation. *Antioxidants & redox signaling*, *20*(3), 460-473.

[140] Lemmer, I. L., Willemsen, N., Hilal, N., & Bartelt, A. (2021). A guide to understanding endoplasmic reticulum stress in metabolic disorders. *Molecular metabolism*, *47*, 101169.

[141] Mizushima, N., Levine, B., Cuervo, A. M., & Klionsky, D. J. (2008). Autophagy fights disease through cellular self-digestion. *nature*, *451*(7182), 1069-1075.

[142] Condello, M., Pellegrini, E., Caraglia, M., & Meschini, S. (2019). Targeting autophagy to overcome human diseases. *International journal of molecular sciences*, *20*(3), 725.

[143] Levine, B., Mizushima, N., & Virgin, H. W. (2011). Autophagy in immunity and inflammation. *Nature*, *469*(7330), 323-335.

[144] Choi, Y., Bowman, J. W., & Jung, J. U. (2018). Autophagy during viral infection—a doubleedged sword. *Nature Reviews Microbiology*, *16*(6), 341-354.

[145] Kirkin, V. (2020). History of the selective autophagy research: how did it begin and where does it stand today?. *Journal of molecular biology*, *432*(1), 3-27.

[146] Levine, B., & Klionsky, D. J. (2017). Autophagy wins the 2016 Nobel Prize in Physiology or Medicine: Breakthroughs in baker's yeast fuel advances in biomedical research. *Proceedings of the National Academy of Sciences*, *114*(2), 201-205.

[147] Grant, P. R., Grant, B. R., Huey, R. B., Johnson, M. T., Knoll, A. H., & Schmitt, J. (2017).

Evolution caused by extreme events. *Philosophical Transactions of the Royal Society B: Biological Sciences*, *372*(1723), 20160146.

[148] Wei, Y., Liu, M., Li, X., Liu, J., & Li, H. (2018). Origin of the autophagosome membrane in mammals. *BioMed research international*, *2018*.

[149] Mari, M., Tooze, S. A., & Reggiori, F. (2011). The puzzling origin of the autophagosomal membrane. *F1000 biology reports*, *3*.

[150] Mancias, J. D., & Kimmelman, A. C. (2016). Mechanisms of selective autophagy in normal physiology and cancer. *Journal of molecular biology*, *428*(9), 1659-1680.

[151] Yim, W. W. Y., & Mizushima, N. (2020). Lysosome biology in autophagy. *Cell discovery*, *6*(1), 1-12.

[152] Vellai, T., Takács-Vellai, K., Sass, M., & Klionsky, D. J. (2009). The regulation of aging: does autophagy underlie longevity?. *Trends in cell biology*, *19*(10), 487-494.

[153] Chen, Z. F., Li, Y. B., Han, J. Y., Wang, J., Yin, J. J., Li, J. B., & Tian, H. (2011). The double-edged effect of autophagy in pancreatic beta cells and diabetes. *Autophagy*, *7*(1), 12-16.

[154] Sheng, Q., Xiao, X., Prasadan, K., Chen, C., Ming, Y., Fusco, J., ... & Gittes, G. K. (2017). Autophagy protects pancreatic beta cell mass and function in the setting of a high-fat and highglucose diet. *Scientific reports*, *7*(1), 1-10.

[155] Scheele, C., Nielsen, A. R., Walden, T. B., Sewell, D. A., Fischer, C. P., Brogan, R. J., ... & Timmons, J. A. (2007). Altered regulation of the PINK1 locus: a link between type 2 diabetes and neurodegeneration?. *The FASEB journal*, *21*(13), 3653-3665.

[156] Nakahira, K., Cloonan, S. M., Mizumura, K., Choi, A. M., & Ryter, S. W. (2014). Autophagy: a crucial moderator of redox balance, inflammation, and apoptosis in lung disease. *Antioxidants & redox signaling*, *20*(3), 474-494.

[157] Pyo, J. O., Yoo, S. M., Ahn, H. H., Nah, J., Hong, S. H., Kam, T. I., ... & Jung, Y. K. (2013). Overexpression of Atg5 in mice activates autophagy and extends lifespan. *Nature communications*, *4*(1), 1-9.

[158] Yang, L., Li, P., Fu, S., Calay, E. S., & Hotamisligil, G. S. (2010). Defective hepatic autophagy in obesity promotes ER stress and causes insulin resistance. *Cell metabolism*, *11*(6), 467-478.

[159] Ding, W. X., Li, M., Chen, X., Ni, H. M., Lin, C. W., Gao, W., ... & Yin, X. M. (2010). Autophagy reduces acute ethanol-induced hepatotoxicity and steatosis in mice. *Gastroenterology*, *139*(5), 1740-1752.

[160] Lin, C. W., Zhang, H., Li, M., Xiong, X., Chen, X., Chen, X., ... & Yin, X. M. (2013). Pharmacological promotion of autophagy alleviates steatosis and injury in alcoholic and nonalcoholic fatty liver conditions in mice. *Journal of hepatology*, *58*(5), 993-999.

[161] Abbaspour, N., Hurrell, R., Kelishadi, R., 2014. Review on iron and its importance for human health. Journal of research in medical sciences: the official journal of Isfahan University of Medical Sciences, 19(2), 164.

[162] Wallace, D. F., 2016. The regulation of iron absorption and homeostasis. The Clinical Biochemist Reviews, 37(2), 51.

[163] Taher, A. T., Saliba, A. N., 2017. Iron overload in thalassemia: different organs at different rates. Hematology 2014, the American Society of Hematology Education Program Book, 2017(1), 265-271.

[164] Gattermann, N., 2018. Iron overload in myelodysplastic syndromes (MDS). International Journal of Hematology, 107(1), 55-63.

[165] ZELTMACHER, K., Bevans, M., 1945. Aplastic anemia and its association with hemochromatosis. Archives of Internal Medicine, 75(6), 395-403.

[166] Vela, D., 2018. Iron metabolism in prostate cancer; from basic science to new therapeutic strategies. Frontiers in oncology, 547.

[167] Cornelissen, A., Guo, L., Sakamoto, A., Virmani, R., Finn, A. V., 2019. New insights into the role of iron in inflammation and atherosclerosis. EBioMedicine, 47, 598-606.

[168] Sipe, J. C., Lee, P., & Beutler, E., 2002. Brain iron metabolism and neurodegenerative disorders. Developmental neuroscience, 24(2-3), 188-196.

[169] Padwal, M. K., Murshid, M., Nirmale, P., Melinkeri, R. R., 2015. Association of serum ferritin levels with metabolic syndrome and insulin resistance. Journal of Clinical and Diagnostic Research: JCDR, 9(9), BC11.

[170] Simcox, J. A., McClain, D. A., 2013. Iron and diabetes risk. Cell metabolism, 17(3), 329341

[171] Ormazabal, V., Nair, S., Elfeky, O., Aguayo, C., Salomon, C., Zuñiga, F. A., 2018. Association between insulin resistance and the development of cardiovascular

disease. Cardiovascular diabetology, 17(1), 1-14.

[172] Kahn, B. B., Flier, J. S., 2000. Obesity and insulin resistance. The Journal of clinical investigation, 106(4), 473-481.

[173] Båvenholm, P. N., Kuhl, J., Pigon, J., Saha, A. K., Ruderman, N. B., Efendic, S., 2003. Insulin resistance in type 2 diabetes: association with truncal obesity, impaired fitness, and atypical malonyl coenzyme A regulation. The Journal of Clinical Endocrinology & Metabolism, 88(1), 82-87.

[174] Riehle, C., Abel, E. D., 2016. Insulin signaling and heart failure. Circulation research, 118(7), 1151-1169.

[175] Jahng, J. W. S., Alsaadi, R. M., Palanivel, R., Song, E., Hipolito, V. E. B., Sung, H. K., et al., 2019. Iron overload inhibits late stage autophagic flux leading to insulin resistance. EMBO reports, 20(10), e47911.

[176] Sung, H. K., Song, E., Jahng, J. W. S., Pantopoulos, K., & Sweeney, G., 2019. Iron induces insulin resistance in cardiomyocytes via regulation of oxidative stress. Scientific reports, 9(1), 1-

13.

[177] Kim, J. A., Wei, Y., Sowers, J. R., 2008. Role of mitochondrial dysfunction in insulin resistance. Circulation research, 102(4), 401-414.

[178] Mizushima, N., 2007. Autophagy: process and function. Genes & development, 21(22), 2861-2873.

[179] Fritzen, A. M., Madsen, A. B., Kleinert, M., Treebak, J. T., Lundsgaard, A. M., Jensen, T. E., et al., 2016. Regulation of autophagy in human skeletal muscle: effects of exercise, exercise training and insulin stimulation. The Journal of physiology, 594(3), 745-761.

[180] Schwarz, D. S., Blower, M. D., 2016. The endoplasmic reticulum: structure, function and response to cellular signaling. Cellular and molecular life sciences, 73(1), 79-94.

[181] Hotamisligil, G. S., 2010. Endoplasmic reticulum stress and the inflammatory basis of metabolic disease. Cell, 140(6), 900-917.

[182] Preissler, S., Rato, C., Yan, Y., Perera, L. A., Czako, A., Ron, D., 2020. Calcium depletion challenges endoplasmic reticulum proteostasis by destabilising BiP-substrate complexes. Elife, 9, e62601.

[183] Lee, S. Y., Lee, M. S., Cherla, R. P., Tesh, V. L., 2008. Shiga toxin 1 induces apoptosis through the endoplasmic reticulum stress response in human monocytic cells. Cellular microbiology, 10(3), 770-780.

[184] Cao, S. S., Kaufman, R. J., 2014. Endoplasmic reticulum stress and oxidative stress in cell fate decision and human disease. Antioxidants & redox signaling, 21(3), 396-413.

[185] Hetz, C., 2012. The unfolded protein response: controlling cell fate decisions under ER stress and beyond. Nature reviews Molecular cell biology, 13(2), 89-102.

[186] Read, A., Schröder, M., 2021. The unfolded protein response: An overview. Biology, 10(5), 384.

[187] Vembar, S. S., Brodsky, J. L., 2008. One step at a time: endoplasmic reticulum-associated degradation. Nature reviews Molecular cell biology, 9(12), 944-957.

[188] Liu, Z., Lv, Y., Zhao, N., Guan, G., Wang, J., 2015. Protein kinase R-like ER kinase and its role in endoplasmic reticulum stress-decided cell fate. Cell death & disease, 6(7), e1822-e1822.

[189] Rozpedek, W., Pytel, D., Mucha, B., Leszczynska, H., Diehl, J. A., Majsterek, I., 2016. The role of the PERK/eIF2α/ATF4/CHOP signaling pathway in tumor progression during endoplasmic reticulum stress. Current molecular medicine, 16(6), 533-544.

[190] Adams, C. J., Kopp, M. C., Larburu, N., Nowak, P. R., Ali, M. M., 2019. Structure and molecular mechanism of ER stress signaling by the unfolded protein response signal activator IRE1. Frontiers in Molecular Biosciences, 6, 11.

[191] Ahlstrom, P., Rai, E., Chakma, S., Cho, H. H., Rengasamy, P., Sweeney, G., 2017. Adiponectin improves insulin sensitivity via activation of autophagic flux. Journal of molecular endocrinology, 59(4), 339-350.

[192] Fillebeen, C., Lam, N. H., Chow, S., Botta, A., Sweeney, G., Pantopoulos, K., 2020.

Regulatory connections between iron and glucose metabolism. International Journal of Molecular Sciences, 21(20), 7773.

[193] Sachinidis, A., Doumas, M., Imprialos, K., Stavropoulos, K., Katsimardou, A., Athyros, V. G., 2020. Dysmetabolic iron overload in metabolic syndrome. Current pharmaceutical design, 26(10), 1019-1024.

[194] Rametta, R., Fracanzani, A. L., Fargion, S., Dongiovanni, P., 2020. Dysmetabolic hyperferritinemia and dysmetabolic iron overload syndrome (DIOS): two related conditions or different entities?. Current Pharmaceutical Design, 26(10), 1025-1035.

[195] Martin, D., Nay, K., Robin, F., Rebillard, A., Orfila, L., Martin, B., et al., 2022. Oxidative and glycolytic skeletal muscles deploy protective mechanisms to avoid atrophy under pathophysiological iron overload. Journal of cachexia, sarcopenia and muscle, 13(2), 1250-1261.

[196] Alves, F. M., Kysenius, K., Caldow, M. K., Hardee, J. P., Chung, J. D., Trieu, J., et al., 2022. Iron overload and impaired iron handling contribute to the dystrophic pathology in models of Duchenne muscular dystrophy. Journal of Cachexia, Sarcopenia and Muscle.

[197] Zhou, D., Zhang, Y., Mamtawla, G., Wan, S., Gao, X., Zhang, L., Wang, X., 2020. Iron overload is related to muscle wasting in patients with cachexia of gastric cancer: using quantitative proteome analysis. Medical Oncology, 37(12), 1-11.

[198] Luszczyk, M., Kaczorowska-Hac, B., Milosz, E., Adamkiewicz-Drozynska, E., Ziemann, E., Laskowski, R., Antosiewicz, J., 2017. Reduction of skeletal muscle power in adolescent males carrying H63D mutation in the HFE gene. BioMed Research International, 2017.

[199] Halon-Golabek, M., Borkowska, A., Herman-Antosiewicz, A., Antosiewicz, J., 2019. Iron metabolism of the skeletal muscle and neurodegeneration. Frontiers in Neuroscience, 165.

[200] Cui, D., Drake, J. C., Wilson, R. J., Shute, R. J., Lewellen, B., Zhang, M., et al., 2020. A novel voluntary weightlifting model in mice promotes muscle adaptation and insulin sensitivity with simultaneous enhancement of autophagy and mTOR pathway. The FASEB Journal, 34(6), 7330-7344.

[201] Li, B., Wu, X., Chen, H., Zhuang, C., Zhang, Z., Yao, S., et al., 2018. miR199a-5p inhibits hepatic insulin sensitivity via suppression of ATG14-mediated autophagy. Cell death &

disease, 9(3), 1-15.

[202] Wang, Y., Hu, Y., Sun, C., Zhuo, S., He, Z., Wang, H., et al., 2016. Down-regulation of Risa improves insulin sensitivity by enhancing autophagy. The FASEB Journal, 30(9), 3133-3145.

[203] Shi, L., Zhang, T., Zhou, Y., Zeng, X., Ran, L., Zhang, Q., et al., 2015. Dihydromyricetin improves skeletal muscle insulin sensitivity by inducing autophagy via the AMPK-PGC-1α-Sirt3 signaling pathway. Endocrine, 50(2), 378-389.

[204] Zhang, Y., Ye, M., Chen, L. J., Li, M., Tang, Z., Wang, C., 2015. Role of the ubiquitinproteasome system and autophagy in regulation of insulin sensitivity in serum-starved 3T3-L1 adipocytes. Endocrine Journal, EJ15-0030.

[205] Liu, Y., Palanivel, R., Rai, E., Park, M., Scheid, M. P., Sweeney, G., 2015. Adiponectin stimulates autophagy and reduces oxidative stress to enhance insulin sensitivity during high-fat diet feeding in mice. Diabetes, 64(1), 36-48.

[206] Wu, L., Ding, Q., Wang, X., Li, P., Fan, N., Zhou, Y., et al., 2019. Visualization of dynamic changes in labile iron (II) pools in endoplasmic reticulum stress-mediated drug-induced liver injury. Analytical chemistry, 92(1), 1245-1251.

[207] Cohen, N., Breker, M., Bakunts, A., Pesek, K., Chas, A., Argemí, J., et al., 2017. Iron affects Ire1 clustering propensity and the amplitude of endoplasmic reticulum stress signaling. Journal of cell science, 130(19), 3222-3233.

[208] Lee, D. G., Kam, M. K., Kim, K. M., Kim, H. S., Kwon, O. S., Lee, H. S., at al., 2018. Peroxiredoxin 5 prevents iron overload-induced neuronal death by inhibiting mitochondrial fragmentation and endoplasmic reticulum stress in mouse hippocampal HT-22 cells. The International Journal of Biochemistry & Cell Biology, 102, 10-19.

[209] Wang, G., Liu, S., Wang, L., Meng, L., Cui, C., Zhang, H., Wei, Y., 2017. Lipocalin-2 promotes endoplasmic reticulum stress and proliferation by augmenting intracellular iron in human pulmonary arterial smooth muscle cells. International Journal of Biological Sciences, 13(2), 135.

[210] Rathnasamy, G., Murugan, M., Ling, E. A., Kaur, C, 2016. Hypoxia-induced iron accumulation in oligodendrocytes mediates apoptosis by eliciting endoplasmic reticulum stress. Molecular neurobiology, 53(7), 4713-4727.

[211] Eo, H., Valentine, R. J., 2021. Imoxin inhibits tunicamycin-induced endoplasmic reticulum stress and restores insulin signaling in C2C12 myotubes. American Journal of Physiology-Cell Physiology, 321(2), C221-C229.

[212] Srinivasan, V., Tatu, U., Mohan, V., Balasubramanyam, M., 2009. Molecular convergence of hexosamine biosynthetic pathway and ER stress leading to insulin resistance in L6 skeletal muscle cells. Molecular and cellular biochemistry, 328(1), 217-224.

[213] Park, T. J., Park, S. Y., Lee, H. J., Abd El-Aty, A. M., Jeong, J. H., Jung, T. W., 2022. αketoisocaproic acid promotes ER stress through impairment of autophagy, thereby provoking lipid accumulation and insulin resistance in murine preadipocytes. Biochemical and Biophysical Research Communications, 603, 109-115.

[214] Tong, X., Zhang, Q., Wang, L., Ji, Y., Zhang, L., Xie, L., et al., 2018. RNF186 impairs insulin sensitivity by inducing ER stress in mouse primary hepatocytes. Cellular Signalling, 52, 155-162.

[215] Zhou, T., Cheng, Y., Yan, W., Shi, X., Xu, X., Zhou, J., et al., 2018. TSPA as a novel ATF6α translocation inducer efficiently ameliorates insulin sensitivity restoration and glucose homeostasis in db/db mice. Biochemical and biophysical research communications, 499(4), 948953.

[216] Koh, H. J., Toyoda, T., Didesch, M. M., Lee, M. Y., Sleeman, M. W., Kulkarni, R. N., et al., 2013. Tribbles 3 mediates endoplasmic reticulum stress-induced insulin resistance in skeletal muscle. Nature communications, 4(1), 1-11.

[217] Ijuin, T., Hosooka, T., Takenawa, T., 2016. Phosphatidylinositol 3, 4, 5-trisphosphate phosphatase SKIP links endoplasmic reticulum stress in skeletal muscle to insulin resistance. Molecular and cellular biology, 36(1), 108-118.

[218] Brown, M., Dainty, S., Strudwick, N., Mihai, A. D., Watson, J. N., Dendooven, R., et al, 2020. Endoplasmic reticulum stress causes insulin resistance by inhibiting delivery of newly synthesized insulin receptors to the cell surface. Molecular biology of the cell, 31(23), 2597-2629.

[219] Zhang, Y., Ye, M., Chen, L. J., Li, M., Tang, Z., Wang, C., 2015. Role of the ubiquitinproteasome system and autophagy in regulation of insulin sensitivity in serum-starved 3T3-L1 adipocytes. Endocrine Journal, EJ15-0030.

[220] Proud, C. G., 2005. eIF2 and the control of cell physiology. In Seminars in cell & developmental biology (Vol. 16, No. 1, p. 3-12). Academic Press.

[221] Komar, A. A., Merrick, W. C., 2020. A Retrospective on EIF2A—and Not the Alpha Subunit of EIF2. International Journal of Molecular Sciences, 21(6), 2054.

[222] Cheng, F., Dun, Y., Cheng, J., Ripley-Gonzalez, J. W., Jiang, W., You, B., Liu, S., 2022. Exercise activates autophagy and regulates endoplasmic reticulum stress in muscle of high-fat diet mice to alleviate insulin resistance. Biochemical and Biophysical Research Communications, 601, 45-51.

[223] Zhang, J., Wang, Y., Ju, M., Song, J., Zheng, Y., Lin, S., et al., 2020. Neuroprotective effect of the inhibitor salubrinal after cardiac arrest in a rodent model. Oxidative Medicine and Cellular Longevity, 2020.

[224] Anuncibay-Soto, B., Pérez-Rodriguez, D., Santos-Galdiano, M., Font-Belmonte, E., Ugidos, I. F., Gonzalez-Rodriguez, P., at al., 2018. Salubrinal and robenacoxib treatment after global cerebral ischemia. Exploring the interactions between ER stress and inflammation. Biochemical Pharmacology, 151, 26-37.

[225] Hu, Y., Lu, X., Xu, Y., Lu, L., Yu, S., Cheng, Q., et al., 2017. Salubrinal attenuated retinal neovascularization by inhibiting CHOP-HIF1α-VEGF pathways. Oncotarget, 8(44), 77219.

[226] Barreda-Manso, M. A., Yanguas-Casás, N., Nieto-Sampedro, M., Romero-Ramírez, L., 2017. Neuroprotection and blood–brain barrier restoration by salubrinal after a cortical stab injury. Journal of Cellular Physiology, 232(6), 1501-1510.

[227] Anuncibay-Soto, B., Pérez-Rodríguez, D., Santos-Galdiano, M., Font, E., RegueiroPurriños, M., Fernández-López, A., 2016. Post-ischemic salubrinal treatment results in a neuroprotective role in global cerebral ischemia. Journal of Neurochemistry, 138(2), 295-306.

[228] Darini, C., Ghaddar, N., Chabot, C., Assaker, G., Sabri, S., Koromilas, A. E., 2019. An integrated stress response via PKR suppresses HER2+ cancers and improves trastuzumab therapy. Nature communications, 10(1), 1-14.

[229] Abbaspour, N., Hurrell, R., & Kelishadi, R. (2014). Review on iron and its importance for human health. *Journal of research in medical sciences: the official journal of Isfahan University of Medical Sciences*, *19*(2), 164.

[230] Paul, B. T., Manz, D. H., Torti, F. M., & Torti, S. V. (2017). Mitochondria and Iron: current questions. *Expert review of hematology*, *10*(1), 65-79.

[231] Yassin, M. A., Soliman, A., De Sanctis, V., Hmissi, S. M., Abdulla, M. A., Ekeibed, Y., ... & Hussein, R. (2018). The impact of iron overload in patients with acute leukemia and

myelodysplastic syndrome on hepatic and endocrine functions. *Acta Bio Medica: Atenei Parmensis*, *89*(Suppl 3), 18.

[232] Ganne-Carrie, N., Christidis, C., Chastang, C., Ziol, M., Chapel, F., Imbert-Bismut, F., ... & Beaugrand, M. (2000). Liver iron is predictive of death in alcoholic cirrhosis: a multivariate study of 229 consecutive patients with alcoholic and/or hepatitis C virus cirrhosis: a prospective follow up study. *Gut*, *46*(2), 277-282.

[233] Gujja, P., Rosing, D. R., Tripodi, D. J., & Shizukuda, Y. (2010). Iron overload cardiomyopathy: better understanding of an increasing disorder. *Journal of the American College of Cardiology*, *56*(13), 1001-1012.

[234] Taher, A. T., Musallam, K. M., & Inati, A. (2009). Iron overload: consequences, assessment, and monitoring. *Hemoglobin*, *33*(sup1), S46-S57.

[235] Utzschneider, K. M., & Kowdley, K. V. (2010). Hereditary hemochromatosis and diabetes mellitus: implications for clinical practice. *Nature Reviews Endocrinology*, *6*(1), 26-33.

[236] Lin, J. H., Walter, P., & Yen, T. B. (2008). Endoplasmic reticulum stress in disease pathogenesis. *Annual review of pathology*, *3*, 399.

[237] Yamauchi, T., Kamon, J., Waki, H., Terauchi, Y., Kubota, N., Hara, K., ... & Kadowaki, T. (2001). The fat-derived hormone adiponectin reverses insulin resistance associated with both lipoatrophy and obesity. *Nature medicine*, *7*(8), 941-946.

[238] Chung, S. J., Nagaraju, G. P., Nagalingam, A., Muniraj, N., Kuppusamy, P., Walker, A., ... & Sharma, D. (2017). ADIPOQ/adiponectin induces cytotoxic autophagy in breast cancer cells through STK11/LKB1-mediated activation of the AMPK-ULK1 axis. *Autophagy*, *13*(8), 13861403.

[239] Kubota, N., Yano, W., Kubota, T., Yamauchi, T., Itoh, S., Kumagai, H., ... & Kadowaki, T. (2007). Adiponectin stimulates AMP-activated protein kinase in the hypothalamus and increases food intake. *Cell metabolism*, *6*(1), 55-68.

[240] Huypens, P., Moens, K., Heimberg, H., Ling, Z., Pipeleers, D., & Van de Casteele, M. (2005). Adiponectin-mediated stimulation of AMP-activated protein kinase (AMPK) in pancreatic beta cells. *Life Sciences*, *77*(11), 1273-1282.

[241] Yamauchi, T., Iwabu, M., Okada-Iwabu, M., Ueki, K., & Kadowaki, T. (2010, September). Adiponectin and AdipoR1 regulate PGC-1alpha and mitochondria by Ca2+ signalling and AMPK/SIRT1 like exercise. In *Diabetologia* (Vol. 53, pp. S47-S48). 233 SPRING ST, NEW YORK, NY 10013 USA: SPRINGER.

[242] Jiang, R., Manson, J. E., Meigs, J. B., Ma, J., Rifai, N., & Hu, F. B. (2004). Body iron stores in relation to risk of type 2 diabetes in apparently healthy women. *Jama*, *291*(6), 711-717.

[243] Raju, K., & Venkataramappa, S. M. (2018). Primary hemochromatosis presenting as type 2 diabetes mellitus: a case report with review of literature. *International Journal of Applied and Basic Medical Research*, *8*(1), 57.

[244] Liu, J., Li, Q., Yang, Y., & Ma, L. (2020). Iron metabolism and type 2 diabetes mellitus: A meta-analysis and systematic review. *Journal of diabetes investigation*, *11*(4), 946-955.

[245] Zhang, S., Xin, W., Anderson, G. J., Li, R., Gao, L., Chen, S., ... & Liu, S. (2022). Doubleedge sword roles of iron in driving energy production versus instigating ferroptosis. *Cell death & disease*, *13*(1), 1-13.

[246] Mancardi, D., Mezzanotte, M., Arrigo, E., Barinotti, A., & Roetto, A. (2021). Iron overload, oxidative stress, and ferroptosis in the failing heart and liver. *Antioxidants*, *10*(12), 1864.

[247] Chen, X., Yu, C., Kang, R., & Tang, D. (2020). Iron metabolism in ferroptosis. *Frontiers in cell and developmental biology*, *8*, 590226.

[248] Cohen, N., Breker, M., Bakunts, A., Pesek, K., Chas, A., Argemí, J., ... & Schuldiner, M. (2017). Iron affects Ire1 clustering propensity and the amplitude of endoplasmic reticulum stress signaling. *Journal of cell science*, *130*(19), 3222-3233.

[249] Tan, T. C., Crawford, D. H., Jaskowski, L. A., Subramaniam, V. N., Clouston, A. D., Crane, D. I., ... & Fletcher, L. M. (2013). Excess iron modulates endoplasmic reticulum stress-associated pathways in a mouse model of alcohol and high-fat diet-induced liver injury. *Laboratory investigation*, *93*(12), 1295-1312.

[250] Akiyama, M., Liew, C. W., Lu, S., Hu, J., Martinez, R., Hambro, B., ... & Kulkarni, R. N. (2013). X-box binding protein 1 is essential for insulin regulation of pancreatic α-cell function. *Diabetes*, *62*(7), 2439-2449.

[251] Engin, F., Nguyen, T., Yermalovich, A., & Hotamisligil, G. S. (2014). Aberrant islet unfolded protein response in type 2 diabetes. *Scientific reports*, *4*(1), 1-6.

[252] Corazzari, M., Gagliardi, M., Fimia, G. M., & Piacentini, M. (2017). Endoplasmic reticulum stress, unfolded protein response, and cancer cell fate. *Frontiers in oncology*, *7*, 78.

[253] C Bell, M., E Meier, S., L Ingram, A., & F Abisambra, J. (2016). PERK-opathies: an endoplasmic reticulum stress mechanism underlying neurodegeneration. *Current Alzheimer Research*, *13*(2), 150-163.

[254] Schultz, O., Oberhauser, F., Saech, J., Rubbert-Roth, A., Hahn, M., Krone, W., & Laudes, M. (2010). Effects of inhibition of interleukin-6 signalling on insulin sensitivity and lipoprotein (a) levels in human subjects with rheumatoid diseases. *PloS one*, *5*(12), e14328.

[255] Paz-Filho, G., Mastronardi, C., Wong, M. L., & Licinio, J. (2012). Leptin therapy, insulin sensitivity, and glucose homeostasis. *Indian journal of endocrinology and metabolism*, *16*(Suppl 3), S549.

[256] Lian, K., Du, C., Liu, Y., Zhu, D., Yan, W., Zhang, H., ... & Tao, L. (2015). Impaired adiponectin signaling contributes to disturbed catabolism of branched-chain amino acids in diabetic mice. *Diabetes*, *64*(1), 49-59.

[257] Kim, D. S., Jeong, S. K., Kim, H. R., Kim, D. S., Chae, S. W., & Chae, H. J. (2007). Effects of triglyceride on ER stress and insulin resistance. *Biochemical and biophysical research communications*, *363*(1), 140-145.

[258] Pfaffenbach, K. T., Gentile, C. L., Nivala, A. M., Wang, D., Wei, Y., & Pagliassotti, M. J. (2010). Linking endoplasmic reticulum stress to cell death in hepatocytes: roles of C/EBP homologous protein and chemical chaperones in palmitate-mediated cell death. *American Journal of Physiology-Endocrinology and Metabolism*, *298*(5), E1027-E1035.

[259] Lalia, A. Z., & Lanza, I. R. (2016). Insulin-sensitizing effects of omega-3 fatty acids: lost in translation?. *Nutrients*, *8*(6), 329.

[260] Yamauchi, T., & Kadowaki, T. (2013). Adiponectin receptor as a key player in healthy longevity and obesity-related diseases. *Cell metabolism*, *17*(2), 185-196.

[261] Qiao, L., Zou, C., van der Westhuyzen, D. R., & Shao, J. (2008). Adiponectin reduces plasma triglyceride by increasing VLDL triglyceride catabolism. *Diabetes*, *57*(7), 1824-1833.

[262] Choi, H. M., Doss, H. M., & Kim, K. S. (2020). Multifaceted physiological roles of adiponectin in inflammation and diseases. *International journal of molecular sciences*, *21*(4), 1219.

[263] Kadowaki, T., Yamauchi, T., Kubota, N., Hara, K., Ueki, K., & Tobe, K. (2006). Adiponectin and adiponectin receptors in insulin resistance, diabetes, and the metabolic syndrome. *The Journal of clinical investigation*, *116*(7), 1784-1792.

[264] Lin, F., & Qin, Z. H. (2013). Degradation of misfolded proteins by autophagy: is it a strategy for Huntington's disease treatment?. *Journal of Huntington's disease*, *2*(2), 149-157.

[265] Balakrishnan, B., Siddiqi, A., Mella, J., Lupo, A., Li, E., Hollien, J., ... & Lai, K. (2019). Salubrinal enhances eIF2α phosphorylation and improves fertility in a mouse model of classic galactosemia. *Biochimica et Biophysica Acta (BBA)-Molecular Basis of Disease*, *1865*(11), 165516.

[266] Matsuoka, M., & Komoike, Y. (2015). Experimental evidence shows salubrinal, an eIF2α dephosphorylation inhibitor, reduces xenotoxicant-induced cellular damage. *International journal of molecular sciences*, *16*(7), 16275-16287.

[267] Grenier, A., Poulain, L., Mondesir, J., Jacquel, A., Bosc, C., Stuani, L., ... & Tamburini, J. (2022). AMPK-PERK axis represses oxidative metabolism and enhances apoptotic priming of mitochondria in acute myeloid leukemia. *Cell Reports*, *38*(1), 110197.

APPENDIX

Below are two manuscripts to which I have contributed data during the course of my MSc studies. These were conducted as part of projects with two of Dr Sweeney's collaborators: Dr Schertzer (McMaster University) and Dr Abdul-Sater (York University).

I. Statins activate the NLRP3 inflammasome and inhibit glycolysis the Hippo pathway to promote myopathy

Robin N, Barra NG, Li E, Foley KP, Patoli D, Duggan BM, Rebalka IA, Nguyen K, Sweeney G, Hawke, TJ, Py B, Schertzer JD

In preparation for *Cell Metabolism*

II. Copper-treated Fabric Attenuates Inflammation in Macrophages

Safoura Zangiabadi, Khalil P. Chamoun, Khang Nguyen, Gary Sweeney and Ali A. Abdul-Sater

In preparation for *PLOS One*

Statement of Contributions

I would like to acknowledge Dr. Sung's contributions to confocal microscope assays (Figure 4 A&B), including the Tht and GRP78 reporter assays, as described in section 2.3. I would also like to acknowledge PhD students Carina Tang and Sungji Cho's collaboration with the mice injection part (Figure 7) of my thesis. Their contributions include iron and salubrinal injections for mice model, as described in section 2.3.